UNIVERSITY OF CALIFORNIA,
IRVINE

Development of the Plug-in Electric Vehicle Charging Infrastructure via Smart-Charging Algorithms

DISSERTATION

submitted in partial satisfaction of the requirements
for the degree of

DOCTOR OF PHILOSOPHY

in Mechanical and Aerospace Engineering

by

Edgar De Jesus Ramos Muñoz

Dissertation Committee:
Professor Faryar Jabbari
Professor Gregory Washington
Professor G. Scott Samuelsen

2019

DEDICATION

To my family, friends, and mentors

TABLE OF CONTENTS

LIST OF FIGURES

LIST OF TABLES

ACKNOWLEDGMENTS

I would like to thank my advisor, Prof. Faryar Jabbari, for his guidance and support throughout my graduate career. He has always been a great mentor and has always had my best interest in mind. His teachings have helped me grow immensely as a researcher, writer, and educator.

I would also like to thank Dean Gregory Washington and Prof. Scott Samuelsen for serving on my dissertation committee. The conversations we had during our collaborative meetings have provided a great deal of insight to my research.

I would like to thank everyone that has helped guide me throughout my academic career. Thank you, Andres Flores, for getting me to tag along to the English placement test for Los Medanos College. Thank you, Chris Sanchez, for getting me to consider graduate school more seriously. Thank you to Prof. Kurt Crowder, Prof. Jeanne Bonner, Prof. Erich Holtmann, and Prof. Kwadwo Poku for giving me the fundamentals I needed after transferring. Thank you, Prof. Kameshwar Poolla, for inspiring me to be the best educator that I can be. Thank you, Prof. Liwei Lin, for being honest and straightforward when giving me advice about graduate school. Thank you, Prof. J. Karl Hedrick, for encouraging me to get a PhD.

I would also like to thank the MESA Program at Los Medanos College, the Competitive Edge Program at UC Irvine, and the GAANN Fellowship; which have been instrumental to my success.

Most importantly, I would like to thank my family and friends for supporting me throughout all my academic endeavors. In particular, my parents, for always encouraging me to pursue my dreams.

CURRICULUM VITAE

EDGAR DE JESUS RAMOS MUÑOZ

Research Interests: Electric Vehicle Technology; Optimization Methods; Energy Management; Renewable Energy; Algorithm Design; Engineering Education

EDUCATION

Doctor of Philosophy, Mechanical and Aerospace Engineering 2019
University of California, Irvine
Advisor: Prof. Faryar Jabbari

Master of Science, Mechanical and Aerospace Engineering 2016
University of California, Irvine

Bachelor of Science, Mechanical Engineering 2013
University of California, Berkeley

Transfer Coursework, Mechanical Engineering 2011
Los Medanos College

FELLOWSHIPS, HONORS, AND AWARDS

Graduate Assistance in Areas of National Need Fellowship 2018-2019
U.S. Department of Education

Ford Foundation Predoctoral Fellowship: Honorable Mention 2017
Ford Foundation

Graduate Assistance in Areas of National Need Fellowship 2016-2017
U.S. Department of Education

Graduate Assistance in Areas of National Need Fellowship 2015-2016
U.S. Department of Education

Graduate Assistance in Areas of National Need Fellowship 2014-2015
U.S. Department of Education

Competitive Edge Summer Research Fellowship 2014
University of California, Irvine

MESA/NSF S-STEM Scholarship 2011-2013
National Science Foundation

Los Medanos College Associated Students Scholarship 2011-2012
Los Medanos College

PUBLICATIONS

E. Ramos Munoz, G. Razeghi, L. Zhang, & F. Jabbari, *Electric vehicle charging algorithms for coordination of the grid and distribution transformer levels*, Energy. 113 (2016) 930-942

E. Ramos Munoz & F. Jabbari, *Smart charging for a workplace parking structure* **(Submitted)**

E. Ramos Munoz & F. Jabbari, *Centralized smart-charging strategies for octopus chargers* **(In Preparation)**

PRESENTATIONS AND INVITED LECTURES

E. Ramos Munoz, "Development of the Plug-in Electric Vehicle Charging Infrastructure via Smart-Charging Algorithms," Research presentation for Embedded and Cyber-Physical Systems course, University of California, Irvine, May 2018

E. Ramos Munoz, "Coordinating Plug-In Electric Vehicle Charging with the Electric Grid and Local Residential Transformers," Competitive Edge 2014 Research Symposium, University of California, Irvine, Aug 2014

POSTER PRESENTATIONS

F. Mayorga, **E. Ramos Munoz**, & F. Jabbari, "Studying the Feasibility of Owning and Operating A Battery Electric Vehicle with Workplace-Only Charging," SACNAS National Diversity in STEM Conference, Honolulu, Hawaii, **(Forthcoming, October 2019)**

TEACHING EXPERIENCE

Teaching Associate (Instructor): Dynamics Fall 2019
University of California, Irvine

Teaching Assistant: Dynamics Summer 2019
University of California, Irvine Summer 2018
Winter 2018
Fall 2017
Summer 2016
Summer 2015

Teaching Assistant: Engineering Analysis I Fall 2018
University of California, Irvine

Teaching Assistant: Control Systems for Cyber-Physical Systems Spring 2018
University of California, Irvine

Math Tutor and Teaching Assistant 2010-2011
Los Medanos College

MESA Tutor: Physics and Chemistry 2010-2011
Los Medanos College

PROFESSIONAL TRAINING AND WORKSHOPS

Mentoring Excellence Program
University of California, Irvine, 2017
Mentoring program that prepares graduates students for mentoring diverse groups of students in academia. Topics include: **The lifecycle of the mentoring relationship, effective interpersonal communication, conflict resolution, and mentoring across differences.**

2019 Asia Pacific University Student Research Workshop
National Chiao Tung University, Taiwan, 2019
Collaborated with students from various universities and academic backgrounds to develop smart-city solutions to real-world problems.

ACADEMIC, PROFESSIONAL, AND COMMUNITY MEMBERSHIPS

Mechanical and Aerospace Engineering Graduate Student Association (MAE-GSA) 2017-Present
Position: Incoming Student Ambassador

Diverse Educational Community and Doctoral Experience (DECADE) 2014-Present
Position: General Member

Students Advocating for Immigrant Rights and Equity 2015-2017
Positions: Cosigner/Treasurer (2015-2016), General Member

Chican@/Latin@ Graduate Student Collective 2016-2017
Position: General Member

ACADEMIC, PROFESSIONAL, AND COMMUNITY SERVICE

Peer Mentor, Competitive Edge Summer Research Program 2019
Organization: Competitive Edge 2017
University of California, Irvine

Panelist, "Graduate Student Experience" 2019
Organizations: CSU Long Beach BUILD and DECADE
University of California, Irvine

Panelist, "Transfer Student Q&A" 2019
Organizations: Compton College and UCI Office of Access & Inclusion
University of California, Irvine

Mentor, Undergraduate Research Project 2018-Present
Project #1: Evaluating Electricity Costs from Electric Vehicle Charging
Project #2: Evaluating the Feasibility of Workplace-Only Charging
University of California, Irvine

Mentor, Undergraduate Research Project 2019-Present
Project: Evaluating Transformer Aging Due to Electric Vehicle Charging
University of California, Irvine

Presentation, "Community College, University, and Financial Aid" 2018
Organization: Valley High School Automotive Academy
Valley High School, Santa Ana, CA

Presentation, "Graduate School Workshop" Fall 2018
Organization: Society of Hispanic Professional Engineers (SHPE) Winter 2018
University of California, Irvine

Peer Writing Reviewer, Competitive Edge Summer Research Program 2017
Organization: Competitive Edge
University of California, Irvine

Panelist, "First-Generation Graduate Student Experience" 2017
Organization: Ready-Set-SOAR Graduate School Conference
University of California, Irvine

Panelist, "Know-How Sessions: Graduate Applications 101" 2016
Organizations: DECADE and Chican@/Latin@ Graduate Student Collective
University of California, Irvine

Panelist, "Underwater Dreams: Film Viewing and Discussion" 2015
Organization: Students Advocating for Immigrant Rights and Equity
University of California, Irvine

SKILLS

Programming: MATLAB, Simulink, and Arduino IDE

Computer-Aided Design (CAD): SolidWorks, Creo Parametric, and Autodesk 3DS MAX Design

Manufacturing/Machining: Mill, Lathe, and Drill Press

Spoken Languages: Fluent in English and Spanish

ABSTRACT OF THE DISSERTATION

Development of the Plug-in Electric Vehicle Charging Infrastructure
via Smart-Charging Algorithms

By

Edgar De Jesus Ramos Muñoz

Doctor of Philosophy in Mechanical and Aerospace Engineering

University of California, Irvine, 2019

Professor Faryar Jabbari, Chair

Electricity generation and the transportation sector make up a large portion of greenhouse gas emissions in the United States. Meeting ambitious reductions in greenhouse gasses requires large scale adoption of plug-in electric vehicles (PEVs) and has led to several policies and laws aimed at incentivizing PEV sales. An inadequate charging infrastructure, however, could be a major obstacle for a large-scale adoption of PEVs. Large electrical demands from PEVs could negatively affect circuitry, increase electricity costs, and exacerbate stress to local electrical components during times of high electricity usage. These issues, however, can be addressed by deploying smart-charging strategies.

This work is focused on the development of smart-charging protocols for workplace battery electric vehicle (BEV) charging. Three comprehensive smart-charging protocols with different applications are proposed. Each protocol is developed with varying degrees of focus on

communication requirements and privacy concerns. The BEV-based Optimization Protocol is a decentralized, non-iterative strategy that allows BEVs to individually schedule their charging schedules. The Octopus Charger-based MILP Protocol allows octopus chargers (i.e., charging stations with multiple cables) to independently schedule charging for their assigned BEVs. The Real-Time Octopus Charger-based MILP Protocol allows octopus chargers to schedule BEV charging in real time, without prior information from BEVs. By using the appropriate cost signal and assignment algorithms, the proposed protocols can manage a parking structure demand load while reducing the number of installed charging stations.

Driving patterns from the National Household Travel Survey were used to perform simulations, to verify and quantify the effectiveness of each protocol. The proposed protocols resulted in improved peak load reductions for all simulated smart-charging scenarios, when compared with uncontrolled charging. By using octopus chargers, all protocols were able to reduce the number of charging stations needed at parking structures, while meeting the charging requests of all BEVs. Time-Of-Use rate plans from Southern California Edison were used to estimate monthly electricity costs for the simulated parking structures. The smart-charging protocols resulted in reduced electricity costs for most cases studied, when compared to uncontrolled charging.

1 Introduction

1.1 Overview and Goal

The need to reduce greenhouse gas emissions and fossil fuel consumption has increased the popularity of plug-in electric vehicles (PEVs) [1]. In 2017, the transportation sector and electricity generation made up 29% and 28% of greenhouse gas emissions, respectively, in the United States [2]. In [3], it was shown that meeting ambitious reductions in greenhouse gasses, such as those planned for California, requires large numbers of PEVs. An inadequate charging infrastructure, however, could be a major obstacle for the large scale adoption of plug-in electric vehicles (PEVs) [4]. Increases in PEV charging infrastructure results in increases of electric vehicle (EV) sales [5]. In this work, however, it is shown that single-cable charging stations go unused for large portions of time (when PEVs are connected, but not charging). This often causes frustration for drivers that want to charge, but do not have access to an available charging station [6]. By charging multiple PEVs with a single charging station, utilization rates can be improved. Thus, resulting in more cost-effective infrastructure investments.

While the overall market share of electric vehicles (EVs) is currently small, recent years have seen a significant increase in sales [7], partly due to the emergence of high range and affordable vehicles. Significant increases in EV production/sales are imminent, with beneficial impacts on fossil fuel consumption and greenhouse gas emissions. Non-uniform concentrations of EV sales and increasing power levels, however, can cause difficulties for electricity delivery systems at the regional and/or residential levels [8]. Large electrical demands from plug-in electric vehicles (PEVs) could negatively affect circuitry, increase electricity costs, and

exacerbate stress to local electrical components during critical times (e.g., high usage durations on hot days). These issues can be addressed by deploying smart-charging strategies.

In [9], it is found that the second most opportune time for PEV charging is at work (behind home charging). Installation of charging stations at workplace parking structures can provide charging opportunities for long-range commuters and battery electric vehicle (BEV) owners without access to home chargers (i.e., apartment dwellers). Furthermore, the curtailment of renewable resources (at high penetration levels) can be alleviated by shifting PHEV charging that occurs during typical working hours [10]. Thus, smart-charging strategies can be developed to lower infrastructure and operational costs to parking structure owners/operators, while also increasing the utilization of renewable resources.

The goal of this project is to study and quantify the benefits of smart charging for BEVs at workplace parking structures. This is accomplished by developing comprehensive smart-charging protocols with varying applications. The protocols proposed in this work are all developed with the goal of reducing infrastructure and operational costs for both the BEV drivers and workplace parking structure operator. Simulations are then performed to verify the effectiveness of each of the proposed protocols.

1.2 Literature Review

1.2.1 Grid-Level Smart Charging

Management of electricity demand loads (e.g., load leveling or load shifting) via smart-charging techniques is increasingly seen as a critical component for the safety and reliability of the grid. Scheduling PEV charging properly, can reduce the daily cycling of power plants and the operational cost of the electric utility [11]. The issue of coordinating charging, for large

populations of PEVs, with power networks has been studied by several research groups. Most smart-charging strategies fall into two categories: centralized charging and decentralized charging [12]. In [13], a modelling method for centralized charging is presented. The method reduces the computational burden of the optimization algorithm, which does not increase with the number of PEVs. Due to concerns about privacy and communication requirements, however, decentralized strategies are generally preferred for real-world applications.

In [14] and [15], a decentralized iterative strategy is proposed to solve the valley filling problem for homogeneous PEVs (all PEVs have the same charging horizon, charging needs, and charging rates). This strategy requires all PEVs to participate in the iterative process, which results in significant communications demands. In [16], another decentralized iterative approach is proposed, which removes the necessity for homogeneous PEVs. A stochastic decentralized strategy is proposed in [12] which charges PEVs at their maximum rate. In [17], a decentralized charging strategy that schedules a PEV's charging profile for an entire day (at various locations) is proposed. The strategy uses electricity prices to minimize operating costs for the driver. In [18], a decentralized vehicle-to-grid (V2G) charging strategy is proposed. The strategy allows individual PEVs to calculate an optimal charging/discharging profile for the entire day by using a cost signal. Under a simplifying assumption, the charging strategies proposed in [17] and [18] assume that each PEV starts and ends with the same battery state of charge (i.e., charged and discharged energy are equal).

In [19], a simple decentralized charging strategy with a non-iterative approach is presented. The strategy charges PEVs at their maximum charging rates and can achieve valley filling, when desired. The strategy can be modified to follow specific grid level demand profiles,

to accommodate the integration of renewable power generation. The modest communication and computational requirements of this strategy make it suitable for real-world applications.

In [8], it was shown that uncoordinated charging (and some forms of coordinated charging) could cause distribution transformers to operate under undesirable conditions. The strategy in [19] was modified, in [8], to develop several strategies to mitigate the burden created by high concentrations of plug-in electric vehicles, at the grid and local levels. It was shown through the analysis of hot spot temperature and equivalent aging factor that the strategies proposed in [8] reduce the chances of transformer failure with the addition of plug-in electric vehicle loads, even for an under-designed transformer. A draft of the manuscript for [8] can be found in the appendix.

The focus of this work is on the development of smart-charging protocols that reduce infrastructure and operational costs for workplace parking structures. We start with the charging strategy from [19], and modify it to incorporate the constraints that arise when scheduling workplace charging (as opposed to overnight charging at home).

1.2.2 Workplace Smart Charging

Generally, PEV charging can be categorized into two types: destination charging and urgent charging [20]. Destination charging involves charging at locations where a PEV driver will be parked (i.e. home, workplace, supermarket, etc.). Urgent charging involves charging on the road due to a low state of charge (SOC). In [21], it is found that 28-38% of typical travel results in a state of charge that is low enough to qualify for Level 3 charging. In most cases, however, charging needs for BEV drivers can be satisfied with Level 1 or Level 2 charging [22]. The focus of this work is on BEV drivers that find Level 2 charging more suitable.

After overnight charging, the second most opportune time for BEV charging is at work [9]. Workplace charging can provide charging opportunities for drivers with long commutes and drivers without access to home chargers (e.g., apartment dwellers). Furthermore, shifting PHEV charging to periods of high renewable generation can alleviate the curtailment of renewable resources (at high penetration levels) [10], [23]. For solar power generation, this typically occurs during daily working hours. Thus, smart-charging strategies can be developed to lower operational and infrastructure costs to parking structures, while also increasing the utilization of renewable resources.

Smart-charging strategies for parking lots/structures have been developed by various research groups. In [24] a centralized scheduling system for EV charging at parking lots is proposed. The optimization-based approach uses a two-layered framework to handle the effects of random deviations from typical driving patterns. Iterative methods are proposed in [25] and [26] to manage PEV charging in parking structures, via computational intelligence. In [25] binary particle swarm optimization is used to schedule V2G charging/discharging to maximize PEV owners' profits. Particle swarm optimization and estimation of distribution algorithms are used in [26] to manage PEV charging at a municipal parking lot. In [27] an algorithm that provides continuous (all-at-once) charging for PEVs is developed to reduce load variation. In [28] fuzzy optimization techniques are used to propose a model that maximizes a parking structure operator's profits while satisfying PEVs drivers' charging needs. The model proposed in [28] is designed to take uncertainties of PEV characteristics, PEV mobility, and the market into consideration. Note that the grid level smart-charging strategies discussed in the previous section can be applied to parking structures with relative ease.

1.2.3 Octopus Charger Model

Range anxiety is described as the fear that a BEV will run out of battery charge before arriving at a destination where it can be recharged. Charger anxiety is described as the concern that chargers will not be available at destination charging locations. Access to electric vehicle chargers can mitigate the negative effects of range anxiety and charger anxiety. In [5] it is found that increases in charging station deployment result in increases of EV sales. In [29] a survey found that 71.7% of participants placed a high degree of importance on having recharging facilities at work or near businesses they frequent, when considering a future PHEV purchase.

Significant investments in charging infrastructure would, however, be required if single-cable charging stations remain the standard. Furthermore, charging needs for most drivers can be met with Level 1 charging [22]. Thus, utilization rates for Level 1 and Level 2 workplace chargers could be quite low for some drivers. Using driving pattern data from the National Household Travel Survey (NHTS), it is found that for 1.92, 3.6, 6.6, and 10 kW charging, PEVs only use chargers 11.14%, 6.28%, 3.48%, and 2.30% of the time during a 24-hour period, respectively. This translates to about 33.02%, 18.86%, 10.51%, and 6.97% of the time that they are parked (see Section 4.2 for details). This suggests that the charging times for a PEV can be shifted around (via smart-charging strategies) to reduce load variation. These low usage rates, however, also suggest that single-cable charging stations go unused during a PEV's idle time (when it is connected, but not charging).

In [30], "octopus chargers" are proposed as a cost-effective solution for charger anxiety. Octopus chargers are designed to contain several cables, such that a single octopus charger can charge multiple PEVs. The concept of connecting multiple BEVs to a single charging station has also been explored in [20]. In that work, Zhang et al. proposed a two-stage stochastic

programming model for planning parking structures equipped with multiple-cable charging stations. The model uses mixed integer linear programming (MILP) to take the influence of coordinated charging into consideration. The proposed model substantially reduced the required investment and the subsequent annual costs for a charging facility.

2 Goals, Objectives, and Approach

2.1 Goal

The goal of this project is to study and quantify the benefits of smart charging for BEVs at workplace parking structures. This is accomplished by developing comprehensive smart-charging protocols for different applications. The protocols proposed in this work are developed with the goal of reducing infrastructure and operational costs for workplace parking structure owners/operators.

2.2 Objectives

In order to achieve this goal, various smart-charging protocols for workplace charging are developed. All smart-charging protocols proposed in this work fulfill the following global objectives:

1. Protocols reduce operational/electricity costs by managing the parking structure demand load.
2. Protocols reduce infrastructure investments by charging multiple BEVs with a single charging station.
3. Protocols charge BEVs at their maximum charging rate.
4. Protocols incorporate constraints of workplace charging (multiple dwelling periods).
5. Protocols do not affect BEVs' charging goals (compared to uncontrolled charging).

2.3 Approach / Summary

In order to accomplish the goal above, several smart-charging protocols were developed, for various applications. Each protocol was developed with varying degrees of focus on communication requirements and/or privacy concerns. The following tasks were established for this work.

Task 1: Develop realistic simulations to analyze and quantify the benefits of each smart-charging strategy.

This task is aimed at developing realistic simulations to compare the smart-charging strategies proposed in this work (see Section 4). Driving patterns from the 2017 National Household Travel Survey (NHTS) [31] were used to generate suitable travel data for simulated BEVs. Several parameters were used to filter the data from the NHTS, which resulted in travel data for 53,951 vehicles. The resulting travel data was used to simulate BEVs in workplace parking structures, under various charging scenarios. Specifications for the 2017 Nissan Leaf were used for all simulated BEVs.

Measured data was used to obtain a building load for the simulated parking structures. Measured data from a photovoltaic (PV) system was used to study the effects of solar power when using smart-charging methods. Time-Of-Use rate plans from Southern California Edison were used to estimate monthly electricity cost for the simulated parking structures in this work.

Task 2: Develop a decentralized smart-charging protocol that maintains privacy.

In this task, a comprehensive BEV-based protocol for workplace charging is proposed. This protocol is referred to as the **BEV-based Optimization Protocol** and is presented in Section 5 of this work. The protocol first uses an ordering strategy, based on each vehicle's load

shifting flexibility, to develop a queue. Next, a decentralized smart-charging strategy is used that allows BEVs to generate their own charging profile via linear programming. By using the appropriate cost signal, the proposed smart-charging strategy can generate a parking structure demand load with desirable characteristics. Finally, an assignment algorithm is used to assign BEVs to octopus chargers.

By allowing BEVs to individually generate their charging profiles, drivers can avoid sharing their driving patterns with the parking structure operator. The only information conveyed to the parking structure operator is the charging profiles generated by the BEVs (to aggregate to the predicted load) and their charging flexibility. The BEVs' charging profiles or charging flexibility do not necessarily give away the BEV's dwell/driving patterns, thus, this decentralized approach maintains a measure of user privacy.

For this protocol, the parking structure operator must gather the charging flexibility of all participating BEVs in the morning (before the first BEV arrives). The operator then generates a queue and executes the appropriate smart-charging strategy. This approach requires somewhat more complex communication between the BEVs and the parking structure operator but provides significant improvements.

Task 3: Develop a smart-charging protocol that allows octopus chargers to generate charging profiles for their assigned BEVs.

In this task, a comprehensive Octopus Charger-based protocol is proposed. This protocol is referred to as the **Octopus Charger-based MILP Protocol** and is presented in Section 6. The parking structure operator first assigns BEVs to octopus chargers based on their charging flexibility. Once assigned, BEVs share their expected driving patterns for the day (along with

basic BEV specifications) to their assigned octopus chargers. A queue is then generated to dictate the order in which octopus chargers generate charging profiles for their assigned BEVs. Once an octopus charger is ready, it uses mixed integer linear programming (MILP) techniques to generate charging profiles for its assigned BEVs. By using the appropriate cost signal, the proposed smart-charging strategy can generate a parking structure demand load with desirable characteristics.

In this protocol, octopus chargers use their assigned BEVs' driving data to generate charging profiles. Thus, privacy is not maintained for the participating BEVs. If privacy is not a high priority and drivers are willing to share their driving patterns, then this protocol can be used to reduce the number of octopus charger needed in a parking structure. Furthermore, driving patterns for entire fleets of buses or delivery trucks are generally known. Applying this protocol can reduce electricity costs and charging infrastructure investments for public transportation and delivery companies.

As in Task 2, it is necessary to execute the protocol in the morning (before the first BEV arrives). Again, this approach requires somewhat more complex interaction between the BEVs and the octopus chargers but provides significant improvements.

Task 4: Develop a smart-charging protocol that allows octopus chargers to generate charging profiles in real time.

In this task, a comprehensive Octopus Charger-based protocol, that generates charging profiles in real time, is proposed. This protocol is referred to as the **Real-Time Octopus Charger-based MILP Protocol** and is presented in Section 7. As each BEV arrives to the parking structure, it is assigned to an octopus charger, without any prior information about the

BEV. The BEV's expected driving patterns for the day become available to the octopus charger as soon as it connects. The octopus charger then generates a charging profile for the BEV and updates the charging profiles of any BEVs that were already connected (if necessary). The process is repeated with the next BEV to arrive, until all BEV charging profiles have been generated. By using the appropriate cost signal, the proposed smart-charging strategy can generate a parking structure demand load with desirable characteristics.

Since drivers must share their expected driving patterns with their assigned octopus chargers, user privacy is not maintained. This protocol, however, eliminates a significant portion of the communication requirements from the BEV-based Optimization Protocol and the Octopus Charger-based MILP Protocol. Once the driver parks, they can simply input their expected driving patterns via the octopus charger's user interface.

3 Terminology

The symbols used in this paper are as follows.

Table 1 Description of symbols used in this work

B	Cost associated with binary decision variable $l_n(t_i)$
b_n	Energy requested and obtained by BEV n (in kWh)
$BC_{n,0}$	Battery charge of BEV n at the beginning of the day (in kWh)
$BC_{n,des}$	Desired battery charge for BEV n at the end of the workday (in kWh)
$BC_{n,cap}$	Battery capacity of BEV n (in kWh)
$BC_{n,ub,j}$	Upper bound on charge BEV n can have at the end of dwelling time $T_{n,j}$ (in kWh)
$C_{load}(t_i)$	Broadcast cost signal from parking structure demand load for each timeslot t_i
$C_n(t_i)$	Cost signal used by octopus charger for BEV n during timeslot t_i
D_n	Total number of dwelling times for each BEV n
F_n	Flexibility Ratio of BEV n
F_n^{-1}	Inverse Flexibility Ratio of BEV n
I	Total number of timeslots for octopus charger-based optimization
J	Total charging cost
$l_n(t_i)$	Binary decision variable or BEV n during timeslot t_i
n	BEV number
N	Total number of BEVs
p_n	Charging power for BEV n (in kW)
P_{oct}	Maximum output power of octopus charger (in kW)
$r_n(t_i)$	Maximum charging energy for each BEV n, at each timeslot t_i (in kWh)
$R(t_i)$	Maximum charging energy that can be provided by an octopus charger at each timeslot t_i (in kWh)
t_i	Timeslot i
$T_{n,j}$	Dwell time j of BEV n

$t_{i,j}$	$t_{i,j} = \{t_i \in T_{n,j}\}$ (i.e., timeslot occurring during dwell time $T_{n,j}$)
$\hat{t}_{i,j}$	$\hat{t}_{i,j} = \{t_i \in \bigcup_k T_{n,k} \quad for\ k = 1, \dots, j\}$ (i.e., timeslot occurring during dwell times $T_{n,1}$ through $T_{n,j}$)
$\Delta t_n(t_i)$	Length of timeslot t_i for BEV n
$x_n(t_i)$	Charging energy for each BEV n, at each timeslot t_i (in kWh)
$y_{n,j}$	Energy used by each BEV, n, from driving done before each dwell time, $T_{n,j}$ (in kWh)
η	BEV charging efficiency

The abbreviations used in this paper are as follows

Table 2 Description of abbreviations used in this paper

BEV	Battery Electric Vehicle
EV	Electric Vehicle
MILP	Mixed Integer Linear Programming
NHTS	National Household Travel Survey
PEV	Plug-in Electric Vehicle
PHEV	Plug-in Hybrid Electric Vehicle
SCE	Southern California Edison
SOC	State of Charge
TOU	Time-of-Use
UCI	University of California, Irvine
V2G	Vehicle-to-Grid

4 Parameters, data, and related assumptions

4.1 Driving Schedules

Large portions of this work assume that the daily driving patterns (or a conservative estimate) of all BEVs are known. This assumption is based on the emergence and advancement of location and calendar information on smart phones (e.g., location reminders). Furthermore, this assumption is generally true when considering delivery and bus companies (where the schedules for the entire fleet are generally known).

4.2 BEV Data

The 2017 National Household Travel Survey (NHTS) [31] was used to obtain vehicle travel data for the following simulations. Since workplace data was needed, different parameters were used to filter the entirety of the NHTS travel data. Travel data with the following characteristics was filtered out.

a) Driving data for participants who did not go to work.

b) Driving data that started or ended at work (because proper dwell times cannot be obtained).

c) Driving data for participants who used their personal vehicle for less than half of their travels (because participants relied heavily on other methods of transportation).

d) Driving data where the participant's personal vehicle was not used to get to work, back home, or both.

e) Driving data with total dwell time lengths of less than 4 hours.

f) Driving data with individual trips longer than 100 miles (battery range of a 2017 Nissan Leaf).

g) Participants with driving data that would not be feasible with a BEV (i.e., the BEV would run out of battery at some point).

h) Driving data where the participant left work on the first day and returned on the second day.

Dwell times were maintained if a participant left work, but did not drive their personal vehicle (i.e., if the participant went for a walk). This processing resulted in travel data for 53,951 vehicles in the United States and 9,274 vehicles in California.

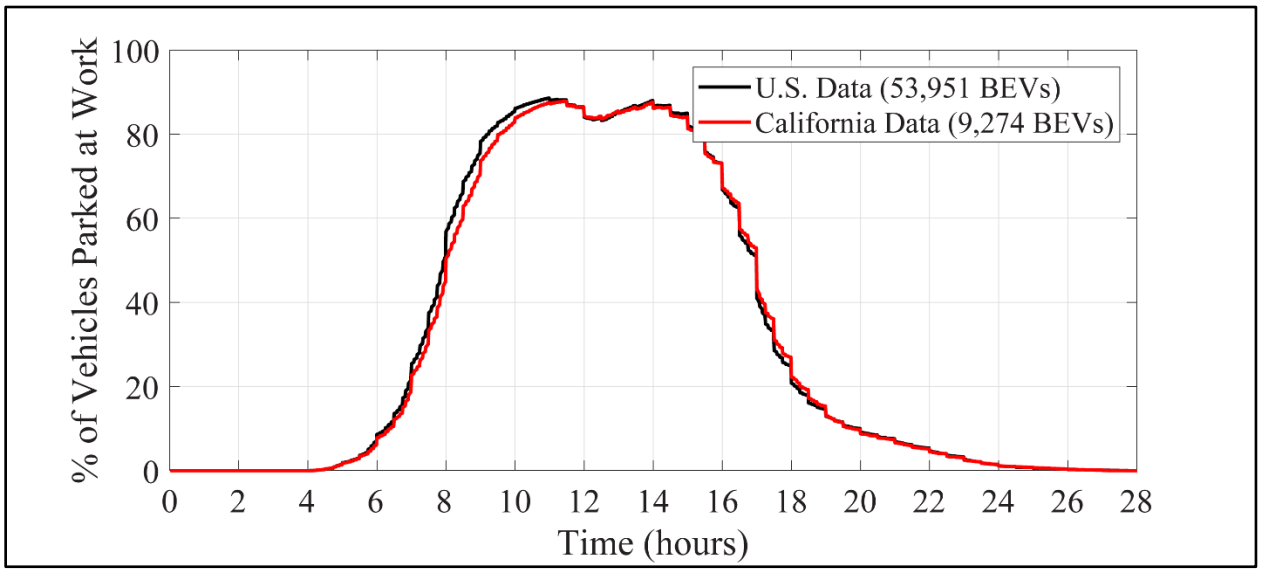

Figure 1 Workplace charging availability for drivers/vehicles in the filtered data sets for the United States and California

The resulting driving data was used to calculate the availability of driver vehicles at the parking structure. Figure 1 shows the percentage of vehicles that are parked at work throughout the day. At least 25% of vehicles in the data set were parked at work between 7:00 am and 5:56

pm. A small dip is seen in the curve around noon, during lunch time. A small percentage of vehicles were also found to be at work past midnight.

Various commute lengths for both data sets were calculated. The commute lengths were for driving done before work, driving after work, and driving done during the entire workday. Figure 2 shows the cumulative percentage of drivers with commute lengths greater than or equal to the given miles (on the x-axis). Both figures show that there are negligible differences between the data sets obtained for the United States and California. The data set for the United States will be used to generate the BEV data used in all simulations performed.

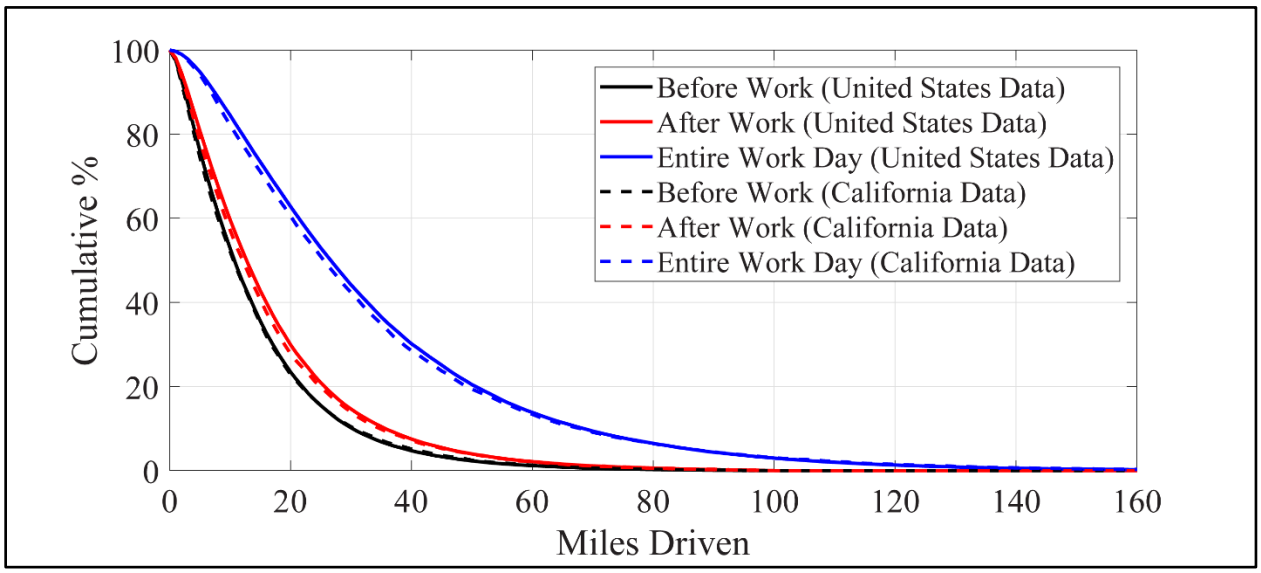

Figure 2 Cumulative percentage of drivers with commute lengths greater than or equal to the given values (for driving done before work, after work, and the entire day)

A charging efficiency (η) of 0.9 was assumed for all BEVs. It was also assumed that all BEVs were fully charged when they left home. Specifications for the 2017 Nissan Leaf were used for all BEVs. These specifications are as follows:

i. 0.3 kWh/mi fuel economy

ii. 30 kWh battery

iii. 3.6 kW charging rate

Using the NHTS travel data with filters (a)-(h), the utilization rates for traditional (single-cable) charging stations were calculated for BEVs attempting to get a full charge at work. For constant 1.92, 3.6, 6.6, and 10 kW charging, BEVs would only use traditional charging stations 11.14%, 6.28%, 3.48%, and 2.30% of the time during a 24-hour period, respectively. This corresponds to 33.02%, 18.86%, 10.51%, and 6.97% of the time they are parked, respectively.

4.3 Baseload Data

Measured data from the Canon B building in the UC Irvine Research Park was used to obtain a building load for the simulations performed. The building load was measured on July 22nd, 2008. Measured data from the photovoltaic (PV) system at the Multipurpose Science and Technology Building at UC Irvine (UCI) was used to study the effects of solar power when using smart-charging methods. The power generated by the PV system was measured on a sunny day on November 18th, 2010. The building load and the PV load were interpolated using the spline method of the "interp1" function of MATLAB, to obtain loads with minute-by-minute resolution. The two baseloads used in this work are presented in Figure 3. Since a small percentage of drivers stay at work past midnight, 48-hour baseloads are needed. The two 24-hour baseloads (seen in Figure 3) are repeated to generate the 48-hour baseloads used in all simulations.

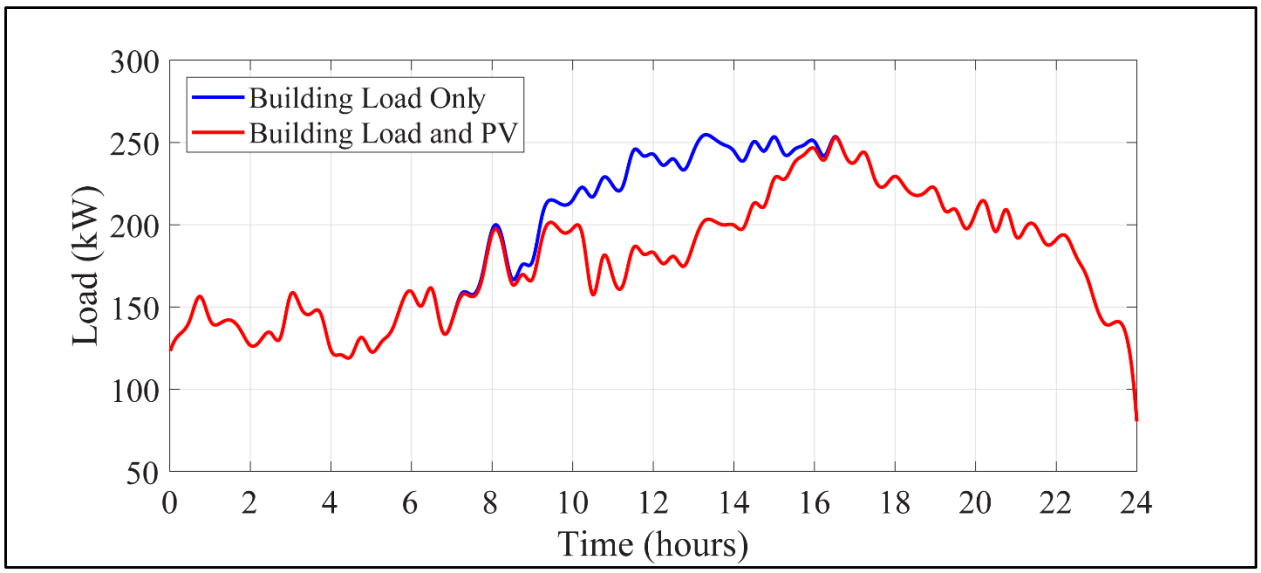

Figure 3 Interpolated baseload data for 24 hours

4.4 Simulation Parameters

Each charging strategy was tested on 50 different simulated parking structures. All parking structures were simulated with 100 and 500 participating BEVs. A different sample of randomly selected BEVs, from the filtered NHTS data, were used for each parking structure. The BEVs included in parking structure #X for 100 BEVs are a random subset of the 500 BEVs used in parking structure #X.

Simulations were performed for situations when drivers attempted to get a full charge and for when they attempted to get less than that. The four cases simulated are as follows. Values higher than the battery capacity of the BEV were reduced to the battery capacity.

1. BEVs attempt to charge enough for all driving required after work.
2. BEVs attempt to charge enough for twice the driving required after work (i.e., a factor of safety (FoS) of 2 for all driving required after work).

3. BEVs attempt to charge enough for five times the driving required after work (i.e., a factor of safety (FoS) of 5 for all driving required after work).

4. BEVs attempt to charge to a 100% SOC.

4.5 Electricity Costs

Time-Of-Use (TOU) is a pricing structure that charges different rates for electricity depending on the season, time of the day, and rate schedule [32]. The Southern California Edison (SCE) TOU pricing scheme includes two seasons: summer and winter. The summer season is June-September, while winter season is October-May. SCE refers to its three pricing periods for businesses as On-Peak, Mid-Peak, and Off-Peak. With On-Peak having the highest energy price and Off-Peak having the lowest. Traditionally, the On-Peak hours have been 12 pm to 6 pm. New On-Peak hours (4 pm to 9 pm), however, have been recently approved by the CPUC for 2019. These new TOU rates allow customers to lower electricity costs by using renewable energy when it is naturally available [33]. Renewable energy, however, can be very uncertain, which adds to the need for flexible smart charging.

Table 3 contains the SCE summer periods for the traditional TOU pricing structure (as of October 1st, 2018) and the new TOU pricing structure (as of April 12th, 2019). In general, electricity usage is more expensive during On-Peak hours.

Table 3 Time-of-Use periods for weekdays during the summer season

	Off-Peak	Mid-Peak	On-Peak
2018	11 pm – 8 am	8 am–12 pm & 6 pm-11 pm	12 pm – 6 pm
2019	12 am – 4 pm & 9 pm – 12 am	N/A	4 pm – 9 pm

Table 4 contains the cost of energy for four TOU rate plans. TOU-GS-2 and TOU-GS-3 correspond to rate plans available to customers with peak demand loads between 20-200 kW and 200-500 kW, respectively. The B plans correspond to the 2018 rate plans, while the D plans correspond to the 2019 rate plans. Note that TOU periods and prices can vary significantly across regions.

Table 4 Energy charge (per kWh) for weekdays during the summer season

	Off-Peak	Mid-Peak	On-Peak
TOU-GS-2-B	$0.05763/kWh	$0.08031/kWh	$0.12271/kWh
TOU-GS-3-B	$0.05834/kWh	$0.07950/kWh	$0.12168/kWh
TOU-GS-2-D	$0.07764/kWh	N/A	$0.11434/kWh
TOU-GS-3-D	$0.07488/kWh	N/A	$0.10904/kWh

Along with the TOU energy pricing, many businesses can also incur monthly per kW demand charges. A facilities related demand charge is calculated based off the highest load incurred at any time. In addition, time related demand charges are calculated based on the highest load incurred during particular TOU periods. Table 5 contains the demand charges for the rate plans above. Note that even modest increases (1-10 kW) can significantly increase the monthly demand charges for a customer.

Table 5 Demand charge (per kW) for weekdays during the summer season only

	All Hours	Mid-Peak	On-Peak
TOU-GS-2-B	$15.89/kW	$3.83/kW	$19.61/kW
TOU-GS-3-B	$18.29/kW	$3.88/kW	$19.73/kW
TOU-GS-2-D	$10.75/kW	N/A	$27.27/kW
TOU-GS-3-D	$11.72/kW	N/A	$27.24/kW

For simplicity and consistency, electricity costs for all parking structures were calculated with the corresponding TOU-GS-3 summer rate schedule, except for 100 BEV parking structures without a baseload. It can be seen, in Figure 5-A, that the maximum load for this case is well below 200 kW. Thus, the corresponding TOU-GS-2 summer rate schedule is used to calculate the electricity costs for 100 BEV parking structures without a baseload.

Note: It can be seen that some strategies result in demand loads above 500 kW (see Figure 5-B). These demand loads would lead to the use of TOU-8 rate schedules (which are designed for demand loads above 500 kW). For the sake of consistency between charging strategies, however, the TOU-GS-3 rate schedules will be used in these cases as well. Note that the use of the TOU-8 rate schedules would result in higher costs for the Uncontrolled Charging cases.

Monthly electricity costs for the simulated parking structures were also calculated with the A and E versions of the rate schedules above (i.e., TOU-GS-3-A and TOU-GS-3-E). These rate schedules resulted in higher monthly costs in most cases when compared to the rate schedules used in this work. Thus, monthly costs for the A and E versions of the above rate schedules are omitted from this work.

5 BEV-based Optimization Protocol

5.1 Introduction

The second most opportune time for BEV charging (behind home charging) is at work [9]. Installation of charging stations at workplace parking structures can provide charging opportunities for long-range commuters and battery electric vehicle (BEV) owners without access to home chargers (i.e., apartment dwellers). BEV manufacturers have invested in workplace charging by donating charging stations to qualifying businesses and property owners [34]. Furthermore, the curtailment of renewable resources (at high penetration levels) can be alleviated by shifting PHEV charging that occurs during typical working hours [10].

Access to EV chargers, at work and public locations, can mitigate the negative effects of range anxiety and charger anxiety [30]. Significant investments in charging infrastructure would, however, be required if single-cable charging stations remain the standard. In Section 4.2, it is shown that single-cable charging stations go unused for large portions of time (when BEVs are connected, but not charging). By charging multiple BEVs with a single charging station, utilization rates can be improved. Thus, resulting in more cost-effective infrastructure investments.

In [17], a decentralized charging strategy that schedules a PEV's charging profile for an entire day (at various locations) is proposed. The strategy uses electricity prices to minimize operating costs for the driver. In [18], a decentralized vehicle-to-grid (V2G) charging strategy is proposed. The strategy allows individual PEVs to calculate an optimal charging/discharging profile for the entire day by using a cost signal. Under a simplifying assumption, the charging

strategies proposed in [17] and [18] assume that each PEV starts and ends with the same battery state of charge (i.e., charged and discharged energy are equal).

In [19], a simple decentralized charging strategy with a non-iterative approach is presented. The strategy charges PEVs at their maximum charging rates and can achieve valley filling, when desired. The strategy can be modified to follow specific grid level demand profiles, to accommodate the integration of renewable power generation. The modest communication and computational requirements of this strategy make it suitable for real-world applications.

The focus of this work is on the development of smart-charging protocols that reduce infrastructure and operational costs for workplace parking structures. We start with the charging strategy from [19], and modify it to incorporate the constraints that arise when scheduling workplace charging (as opposed to overnight charging at home).

In this chapter, a comprehensive BEV-based optimization protocol for workplace charging is proposed. The protocol is developed with the goal of reducing infrastructure and operational costs for a workplace parking structure, while meeting BEV drivers' charging needs. This work is focused on BEVs but applies to PEVs in general. The following are the main contributions of this work. **1)** A smart-charging strategy, that incorporates the constraints of workplace charging, is proposed (see Section 5.3.2). The decentralized, non-iterative strategy manages the parking structure demand load by allowing BEVs to individually generate their own charging profile via linear programming methods. By using the appropriate cost signal, the proposed smart-charging strategy can generate a parking structure demand load with desirable characteristics. The assumption/constraint that each BEV starts and ends with the same battery SOC (needed in [17] and [18]) is removed, so that BEV drivers can explicitly select the SOC they are comfortable with at the end of the workday. **2)** An ordering strategy is proposed, to

further improve the effectiveness of the proposed smart-charging strategy (see Section 5.4.2). **3)** An assignment strategy that allows multiple BEVs to be charged by a single charging station is proposed (See Section 5.5.1) to reduce the total number of charging stations needed at a parking structure.

5.2 Overview of BEV-based Optimization Protocol

The parking structure protocol presented here is similar to the protocols used in [19] and [8]. For this protocol, a queue is initially generated to dictate the order in which BEVs obtain their charging profiles. The queue can be chronological (See Section 5.4.1), or set up through an ordering procedure (See Section 5.4.2). Once a BEV is ready to generate a charging profile, it receives a "cost signal" for the next 48 hours. This cost signal is not a true cost, but a suitably adjusted aggregation of the parking structure demand load and the previously scheduled BEV charging profiles (see Section 5.6.2 and Section 5.6.3). The BEV uses linear programming techniques to independently generate its charging profile based on the broadcast cost signal (See Section 5.3.2). The BEV then sends its charging profile to the parking structure operator, where it is aggregated for an updated cost signal. The process is repeated with next BEV in the queue, until all BEVs have independently generated their charging profiles.

Once the parking structure operator has aggregated all charging profiles, BEVs are assigned to the charging station(s) they will be connected to during their dwelling period(s) (see Section 5.5.1). The application of "octopus chargers" is discussed in Section 5.5.1.2.

5.3 Charging Strategies

5.3.1 Uncontrolled Charging

Uncontrolled Charging is currently the most common method of charging BEVs. Each BEV attempts to charge during each dwelling period at the parking garage. It will continue to charge until it obtains a full battery, reaches a specified battery state of charge (SOC), or disconnects from the charging station (because it leaves the parking structure).

5.3.2 Smart Charging

The procedure and characteristics of this smart-charging strategy are similar to those in [19] and [8] (see Section 5.2). This non-iterative protocol ensures maximum charging power during a BEV's scheduled charging times, while achieving an overall demand profile with desirable characteristics. The simplest objective is so-called **Valley Filling** (see Section 5.6.2), used to reduce peaks and variability in the demand load. Alternatively, as in [19], a modified version of Valley Filling can steer demand away from (or toward) specific times. Thus, allowing the parking structure operator to maximize the use of renewable energy and/or avoid high time-related electricity charges (see Section 5.6.3).

If a BEV is parked for the entire duration of the workday, then the problem formulation from [19] can be used (see Equations (2)-(5) in this work). The key difficulty is that, unlike overnight residential charging, some workers may leave the parking structure for various reasons (i.e., lunch, meetings, errands, etc.). To accommodate for these restrictions, a variety of inequality constraints must be added (see Equations (6)-(8)).

5.3.2.1 Problem Statement: Smart-Charging

In this work, it is assumed that all participating BEVs are plugged into a charging station while they are parked at work, unless stated otherwise (as in Section 5.5.1.1). The continuous periods when a BEV is in the parking structure will be referred to as "dwell times", as trips away from the parking structure can interrupt the stay. $T_{n,j}$ represents the j^{th} dwell time of the n^{th} BEV. The total number of dwell times for the n^{th} BEV is given by D_n. The energy used by the n^{th} BEV before the j^{th} dwell time (due to driving) is given by $y_{n,j}$. Since a BEV can park in different parking spaces during different dwell times, it can connect to different charging stations throughout the day.

The timeslots for the entire workday are given by t_i. Timeslots that occur during dwell time $T_{n,j}$ are given by $t_{i,j}$ (i.e., $t_i \in T_{n,j}$). The length of each timeslot, $\Delta t_n(t_i)$, is given as a fraction of the timeslot resolution. The timeslot resolution used in the simulations in this work will be one hour. Consider a BEV with a dwelling time of 6.25 continuous hours: $\Delta t_n(t_i)$ would equal one for the first six timeslots and 0.25 for the final timeslot. Thus, the total length of each dwell time, $T_{n,j}$, is given by $\sum_i \Delta t_n(t_{i,j})$.

The charging power during timeslot t_i and the grid-to-vehicle charging efficiency are p_n and η, respectively. The initial charge of the n^{th} BEV when it departs from home (before any driving is done) is given by $BC_{n,0}$. In order to ensure that feasible charging profiles are generated, an upper bound must be placed on the charge each BEV's battery can have at the end of each dwell time: $BC_{n,ub,j}$. The value of $BC_{n,ub,j}$ is dictated by the charging power, the energy used before each dwelling time, the length of each dwelling time, and the battery capacity. For example, suppose a BEV has 2 kWh of charge when it arrives at work (i.e., $BC_{n,0} - y_{n,1} = 2$). If

the first dwell time is only long enough to get 3.6 kWh of charge, then $BC_{n,ub,1}$ is 5.6 kWh. On the other hand, if the length of the first dwelling time is long enough, then $BC_{n,ub,1}$ will be limited by the capacity of the BEV's battery, $BC_{n,cap}$. Equation (1) gives the values for $BC_{n,ub,j}$ at the end of all dwell times, $T_{n,j}$. The values for $BC_{n,ub,j}$ are obtained in ascending order, with $BC_{n,ub,0}$ equal to $BC_{n,0}$. The values of $BC_{n,ub,j}$ are used to set up the constraints in Equations (5) and (6) below.

$$BC_{n,ub,j} = min\left\{BC_{n,ub,j-1} - y_{n,j} + \sum_{i} \Delta t_n(t_{i,j}) p_n \eta \ , \ BC_{n,cap} \right\} \quad (1)$$

Single Continuous Dwell Time

Equation (2) gives the objective function for the optimization problem. The decision variables, $x_n(t_i)$, are defined as the energy requested by the n^{th} BEV during timeslot, t_i. The cost signal during timeslot t_i is given by $C_{load}(t_i)$. See Section 5.6.2 and Section 5.6.3 for details on the cost signals used for smart charging. The same conditions of uniqueness of the cost signal from [19] must be maintained as well, i.e. $C_{load}(t_i) \neq C_{load}(t_k)$ for $t_i \neq t_k$.

$$J = \sum_{i} C_{load}(t_i) \times x_n(t_i) \quad (2)$$

The upper and lower bounds for each individual decision variable, $x_n(t_i)$, are given in Equation (3). The lower bound for $x_n(t_i)$ is zero and the upper bound is the product of the charging power p_n and the length of each timeslot, $\Delta t_n(t_i)$.

$$0 \ \leq \ x_n(t_i) \ \leq \ r_n(t_i) \quad (3)$$

$$r_n(t_i) = p_n \times \Delta t_n(t_i) \tag{4}$$

The total amount of energy that the n^{th} BEV can request is given by b_n, in (5). Equation (5) is given in its general form (for cases with both single dwell times and multiple dwell times). Since $D_n = 1$ for the single dwell time case, the summations in Equation (5) reduce to $\sum_{k=1}^{D_n} \frac{y_{n,k}}{\eta} = \frac{y_{n,1}}{\eta}$. The amount of charge desired by the driver of the n^{th} BEV, at the end of the workday, is given by $BC_{n,des}$ (which must be less than or equal to the BEV's battery capacity, $BC_{n,cap}$). Note that the value of b_n is not affected by the smart-charging strategy. It depends entirely on the BEV's driving patterns and characteristics, but it can be limited by BC_{n,ub,D_n}. Thus, $BC_{n,des}$ may not always be feasible. If the desired charge is feasible then then the value of b_n is dictated by the first term of the minimization function in (5). If not, then b_n is dictated by the second term. If the desired charge is already available without charging, the minimization function will be non-positive (resulting in a b_n value of zero). As an example, consider a BEV with $BC_{n,0} = 30\ kWh$ and $BC_{n,des} = 5\ kWh$. If $\sum_{k=1}^{D_n} \frac{y_{n,k}}{\eta} < 25\ kWh$, then the first term of the minimization function is negative, and no charging is required.

$$\begin{aligned} b_n &= \sum_i x_n(t_i) \\ &= max\left\{0, min\left\{\frac{-\left(BC_{n,0} - BC_{n,des}\right)}{\eta} + \sum_{k=1}^{D_n} \frac{y_{n,k}}{\eta}, \right.\right. \\ &\quad \left.\left. \frac{-\left(BC_{n,0} - BC_{n,ub,D_n}\right)}{\eta} + \sum_{k=1}^{D_n} \frac{y_{n,k}}{\eta} \right\}\right\} \end{aligned} \tag{5}$$

Multiple Dwell Times

Additional inequality constraints must be added to (2)-(5) for BEVs with multiple dwell times. To prevent solutions that are not feasible (due to battery capacity), certain limits must be placed on the amount of charging that can occur during particular dwell times. We define $\hat{t}_{i,j}$ as a timeslot (t_i) that occurs during dwell times $T_{n,1}$ through $T_{n,j}$ (i.e., $t_i \in \bigcup_k T_{n,k}$ for $k = 1, \dots, j$). Thus, $\sum_i \Delta t_n(\hat{t}_{i,j})$ gives the total length of dwelling times $T_{n,1}$ through $T_{n,j}$.

Consider a BEV with $BC_{n,cap} = 30\ kWh$ and $BC_{n,0} = 28\ kWh$. The BEV uses $y_{n,1} = 2\ kWh$ and $y_{n,2} = 6\ kWh$ before the first and second dwell times, respectively. If the dwell times are long enough (i.e., $BC_{n,ub,1} = BC_{n,ub,2} = 30\ kWh$), then charging during the first dwell time is limited to $b_{ine,1} = 4\ kWh$ (see Equation (7)). Charging during the entirety of the first two dwell times is limited to $b_{ine,2} = 10kWh$. If the values of $BC_{n,ub,1}$ and/or $BC_{n,ub,2}$ are less than 30 kWh, then the length of the dwell times further limits the amount of charging possible (see Equation (1)). This results in lower values for $b_{ine,1}$ and/or $b_{ine,2}$. These constraints are obtained for $j = 1, 2, \dots, D_n - 1$ via (6), where the value for $b_{ine,j}$ is given by (7). The inequality constraints from (6) limit charging during, dwell times, such that neither the battery capacity nor the time constraints are violated. Note that the summation, on the left-hand side, sums the charging energy during all of timeslots $\hat{t}_{i,j}$ (i.e., during all timeslots that occur during dwell times $T_{n,1}$ through $T_{n,j}$).

$$\sum_i x_n(\hat{t}_{i,j}) \leq b_{ine,j} \quad for\ j = 1, 2, \dots, D_n - 1 \tag{6}$$

$$b_{ine,j} = \frac{-\left(BC_{n,0} - BC_{n,ub,j}\right)}{\eta} + \sum_{k=1}^{j} \frac{y_{n,k}}{\eta} \tag{7}$$

A second inequality constraint must be added in order to prevent the BEV battery from running out of charge while driving between dwell times. Consider a BEV with the following parameters: $BC_{n,0} = 13\ kWh$, $y_{n,1} = 10\ kWh$, $y_{n,2} = 5\ kWh$, and $y_{n,k} = 3\ kWh$. At least 2 kWh of charging must occur in the first dwell time to prevent the BEV from running out of charge during the second trip. Similarly, at least 5 kWh of charging must occur during the first two dwell times to prevent the BEV from running out of charge during the third trip. These values are given by the first term in the minimization function of Equation (8). This constraint must respect the constraints set by Equation (6) and Equation (5). Thus, $b_{ine,j}$ and b_n are included in the minimization function. If the output of the minimization function is negative, then the constraint is not needed and charging during these dwell times must simply be nonnegative (given by the zero in the maximization function). This constraint must be obtained for $j = 1,2 \ldots, D_n - 1$ with Equation (8). Note that if the first entry in the minimization function is greater than the other two entries, then the amount of charge needed to prevent the BEV from running out of battery is not feasible. These constraints are entirely dependent on the BEV's specifications and driving patterns and not affected by smart charging.

$$\sum_{i} x_n(\hat{t}_{i,j}) \geq max\left\{0, min\left\{-\frac{BC_{n,0}}{\eta} + \sum_{k=1}^{j+1} \frac{y_{n,k}}{\eta}\ ,\ b_{ine,j}\ ,\ b_n\right\}\right\} \quad for\ j = 1, 2, \ldots, D_n - 1 \tag{8}$$

If a BEV has one dwell time, then there are no additional inequality constraints, and the problem reduces from (2)-(8) to (2)-(5). Each BEV independently solves the optimization problem above in a decentralized protocol.

This is a linear program, and a variety of fast and robust algorithms exist to obtain the unique solution. The information needed to solve the problem is comprised of the owners driving patterns (t_i, $\Delta t_n(t_i)$, D_n, $BC_{n,des}$, $y_{n,j}$, etc.), specifications/characteristics known to the BEV ($BC_{n,0}$, $BC_{n,cap}$, p_n, etc.), and the updated cost signal ($C_{load}(t_i)$). The only information conveyed to the parking structure operator is the charging profiles generated by the BEVs (to aggregate to the predicted load). The BEVs' charging profiles do not necessarily give away the BEV's dwell/driving patterns, thus, this decentralized approach maintains a measure of user privacy.

This problem formulation can be compared to the smart-charging strategy proposed in [17] and the vehicle-to-grid strategy proposed [18]. Under a simplifying assumption, [17] and [18] assume that each BEV starts and ends with the same battery state of charge. The formulation presented in this work removes this assumption/constraint. Thus, the BEV drivers can explicitly choose the amount of energy that they are comfortable with at the end of the workday. This formulation also reduces the number of additional inequality constraints from ${D_n}^2$ and 48 (in [17] and [18] respectively) to $2(D_n - 1)$.

While the value of D_n may be small for typical office workers, this formulation would drastically reduce the number of additional inequality constraints needed for BEV drivers with large D_n values (i.e., taxis, buses, delivery trucks, etc.).

5.4 Ordering Strategies

In the smart-charging strategies above, the cost signal seen by each BEV is an aggregation of the parking structure demand load and all previously generated BEV charging profiles. Thus, the charging profile of each BEV depends on the charging profiles generated by all previous BEVs. Hence, the order in which BEVs obtain their charging profiles affects the final parking structure demand load. Various ordering strategies can be used to develop the sequence in which BEVs obtain their charging profiles (with the smart-charging strategy above). The two ordering strategies studied in this work are described in the following sections.

5.4.1 Ordering via Arrival Time

This queue is dictated by the order of each BEV's initial arrival to the parking structure. If a driver will be using a single-cable charging station, they can input their expected driving patterns into their BEV's computer/interface when they park. The BEV then communicates with the parking structure operator (potentially via the charging station) to generate its charging profile. This is a naturally occurring queue and requires the least amount of communication between the BEVs and the parking structure operator.

5.4.2 Ordering via Flexibility Ratio

BEVs with long dwell times and low charging needs are less constrained when it comes to shifting their charging profile. This characteristic can be quantified by a term referred to as the Flexibility Ratio (F_n). The numerator in (9) gives the total length of the BEV's dwell times. The denominator gives the time it would take the BEV to meet its desired charging demands ($BC_{n,des}$) at its maximum charge rate.

$$F_n = \frac{\sum_i \Delta t_n(t_i)}{\left(\frac{-\left(BC_{n,0} - BC_{n,des}\right)}{\eta} + \sum_{k=1}^{D_n} \frac{y_{n,k}}{\eta}\right)/p_n} \tag{9}$$

The queue is generated in order of ascending Flexibility Ratios. Since BEVs with low Flexibility Ratios are less likely to shift their loads, this sorting strategy allows them to generate their profiles first. This allows the BEVs with more load shifting capabilities to fill the valleys/gaps generated by the BEVs in the front of the queue.

The parking structure operator must gather the Flexibility Ratios of all participating BEVs and generate the queue in the morning (before the first BEV arrives). Each driver inputs their expected driving patterns the night before or in the early morning via the BEV's interface or a smartphone app. Once the queue is generated, the parking structure operator communicates with the BEVs to perform the smart-charging strategy. This approach requires somewhat more complex interactions between the BEVs and the parking structure operator but provides significant improvements.

Naturally, a variety of alternatives exists. For example, a subset of BEVs upload the information far enough in advance to allow creation of a queue based on their flexibility ratio, while others provide the information only at the arrival (to the structure). For simplicity, we focus on the cases where BEVs are ordered entirely by arrival time or entirely by Flexibility Ratio. Note that charging station assignment must also be performed before the first BEV arrives (see Section 5.5.1).

Note that neither approach affects the level of privacy set forth in [19] and [8]. The only additional information requested by the parking structure operator is the BEVs' Flexibility

Ratios. The Flexibility Ratios are used to generate the queue, but the structure of the decentralized smart-charging strategy remains the same.

5.5 Station Assignment

BEVs participating in the smart-charging strategy from Section 5.3.2 can be charged by providing a traditional single-cable charging station for each BEV. This would, however, require a large investment. Based on driving patterns extracted from the National Household Travel Survey (NHTS), single-cable charging stations go unused for a large portion of the time that BEVs are parked (see Section 4.2). An algorithm to assign multiple BEVs to a single charging station is proposed in the following.

5.5.1 Modified Interval Partitioning Assignment

A well-known scheduling problem is the Interval Partitioning Problem [35]. The goal of the Interval Partitioning Problem (IPP) is to schedule a set of requests with as few identical resources as possible. A classic application of the IPP is finding the minimum number of classrooms needed to schedule a set of lectures. The **depth** of a set of lectures is defined as the maximum number of lectures that overlap at the same time. The number of classrooms needed will be greater than or equal to the depth. A simple, optimal, and well-known algorithm to solve this problem exists, see [35].

The algorithm can be modified to assign multiple BEVs to charging stations, such that the total number of stations is minimized. The identical resources in the algorithm, that play the role of classrooms mentioned above, are charging stations which are denoted as “bins”. Each bin can charge one BEV (at its maximum charging rate) at a time. A bin can have multiple BEVs assigned to it, if the assigned charging profiles do not overlap.

Since each dwell time represents a separate entry into the parking structure, BEVs can park in different spaces at different dwell times. Thus, charging requests during different dwell times for the same BEV can be treated as separate requests (and thus separate BEVs). The charging profile for each dwell time plays the role of the lectures in the Interval Partitioning algorithm, and each becomes a request to be scheduled.

The lectures in the Interval Partitioning algorithm are continuous, thus, compatibility is checked by simply comparing the start and end times of the lectures. BEV profiles generated by the smart-charging strategy proposed here may not be continuous, however. BEV charging profiles could contain intermittent charging due to the valley filling aspects of the strategy in Section 5.3.2. Gaps caused by intermittent charging could fit charging profiles from other BEVs. To take these gaps into consideration, the main algorithm can be modified.

The algorithm orders all the charging profiles by the time when charging starts. Following the sequence, each charging profile is checked for compatibility with the available bins (i.e., charging stations). The algorithm is modified by checking bins with the smallest number of assignments first. If a compatible bin (i.e., charging station) is found, then the charging profile is assigned to that bin. If no compatible bins are found, then a new bin is created for the charging profile.

The first modification is the order in which bins are checked, which increases the chance of assigning charging profiles to bins (charging stations) with few assignments. The other modification is the compatibility check; i.e., ensuring that the charging profiles do not overlap (since only one BEV can be charged at a time). This check can be performed by a simple and fast dot product if the dwell time charging profiles and the profiles assigned to bins are saved as vectors (i.e., compatible if the dot product is zero).

The modified assignment algorithm is presented below. The time when charging begins for dwell time charging profile j is defined as s_j. D is defined as the total number of dwell times for all participating BEVs (i.e., $D = \sum_{n=1}^{N} D_n$). The total number of dwell times assigned to each bin, k, is given by V_k.

Sort the charging profiles by starting time such that $s_1 \leq s_2 \leq \cdots \leq s_D$
$d = 1$ is the number of allocated bins
for $j = 1$ *to* D
  Sort allocated bins by number of assigned charging profiles such that $V_1 \leq V_2 \leq \cdots \leq V_d$
  for $k = 1$ *to* d
    if (charging profile of dwell time j is compatible with bin k)
      assign dwell time j to bin k
      end k for loop
    end
  end
  if (charging profile of dwell time j was not assigned)
    allocate a new bin $d + 1$
    assign dwell time j to bin $d + 1$
    $d = d + 1$
  end
end

The continuity of lectures allows the Interval Partitioning algorithm to generate optimal solutions. The intermittent nature of the charging profiles means that the modified algorithm does not maintain optimality. It is possible generate an optimal assignment with the Interval Partitioning algorithm if each continuous charging duration is treated as a separate request. This

would, however, require a large number of movements by BEVs in a Valet system (see Section 5.5.1.1) and would preclude the octopus charger approach (see Section 5.5.1.2).

5.5.1.1 Valet System

Valet systems, where BEVs are connected/disconnected to/from charging stations when they are scheduled to charge, have been suggested as a possible solution for the lack of charging stations available [21]. Valet systems could be executed manually by employees (hired by the parking structure owner) or by the BEV owners themselves. The BEV charging profiles and the bin assignment developed above could be used to dictate the schedule of a valet system. Executing a manual valet system would, however, be either costly or highly inconvenient. Similarly, an autonomous valet system would alleviate the need for drivers to execute the valet schedule. Autonomous BEVs can be programmed to automatically connect to their assigned charging station when the valet schedule dictates. This, however, requires careful collision avoidance protocols and charging stations that automatically connect to BEVs.

5.5.1.2 Octopus Charger Assignment

The concept of "octopus chargers" is proposed in [30] as a possible solution for charger anxiety. Octopus chargers are charging stations built with more cables than will be simultaneously used. For example, an octopus charger could have four cables, but only one active cable (i.e., only one BEV can be charged at a time). Thus, a group of BEVs, assigned to a bin in the algorithm above, can be assigned to an octopus charger with a single active cable (see Figure 4), as long as they do not have overlapping charging profiles, which the simple check mentioned above ensures.

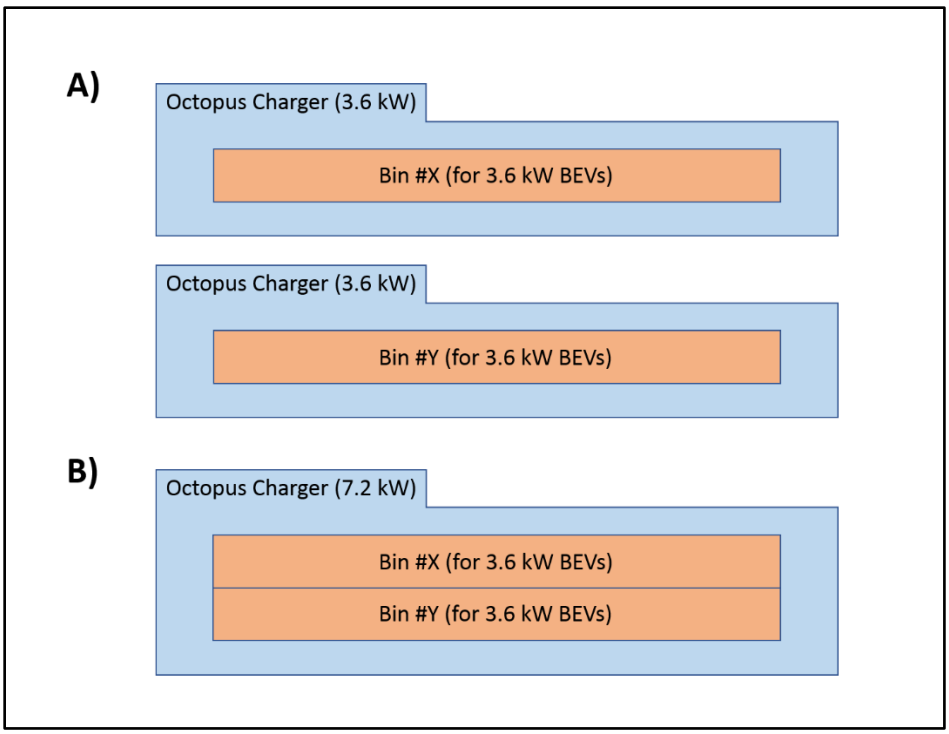

Figure 4 Example of two separate bins assigned to A) two separate octopus chargers with a single active cable or B) one octopus charger with two active cables

Of course, an octopus charger with n active cables could accommodate n bins. If the maximum charging rate of the BEVs assigned to each bin is p, then n bins can be assigned to an octopus charger with a maximum output rate of at least $P_{oct} = np$. See Figure 4-B for an example where $p = 3.6\ kW$ and $n = 2$.

The assignment of multiple bins to an octopus charger with multiple active cables could result in octopus chargers with many cables. An assignment algorithm, such as Sorted-Balance however, could be used to try to balance the number of cables needed by each octopus charger [35]. Sorted-Balance is a well-known approximation algorithm used to solve the Load Balancing Problem. The Sorted-Balance algorithm orders the bins from highest number of cables to lowest.

The bins are then sequentially assigned the octopus charger with the smallest number of cables. See Section 6.3.1 for more details on the Sorted-Balance algorithm.

5.6 Simulation Results

As mentioned above, 48-hour cost signals were used in all simulations to generate 48-hour demand loads. In order to calculate electricity costs, the 48-hour demand loads were converted into 24-hour loads. Any BEV charging that occurred past the 24-hour mark was moved to the early hours of the first day (i.e., charging at 2 am of the second day was moved to 2 am of the first day). All BEVs in the following results charge at the rate of 3.6 kW (see Section 4.2). No BEVs in these simulations obtained a SOC below 0% at any point, because of filter g) in Section 4.2.

5.6.1 Uncontrolled Charging

Representative results from parking structure #2 (out of 50 simulated parking structures) are presented in the following sections. Results for Uncontrolled Charging are shown in Figure 5-A and Figure 5-B, for parking structure simulations with 100 BEVs and 500 BEVs, respectively. The peak loads when BEVs attempt to get a full charge reach values of 126 and 597.6 kW, for 100 BEVs and 500 BEVs respectively. The average values of the maximum load experienced by various 500 BEV simulations are given in Section 5.7. Very little charge is requested by the BEVs when they only get enough charge for the driving required after work (i.e., FoS = 1), due to the assumption that the BEV was fully charged overnight. The loads for 100 BEVs and 500 BEVs have similar shapes/trends, with most of the charging occurring between the early morning and noon. Note that Uncontrolled Charging is not affected by the

baseload. Thus, the results for Uncontrolled Charging with a baseload would simply be the summation of the baseload (see Figure 3) and the corresponding load from Figure 5.

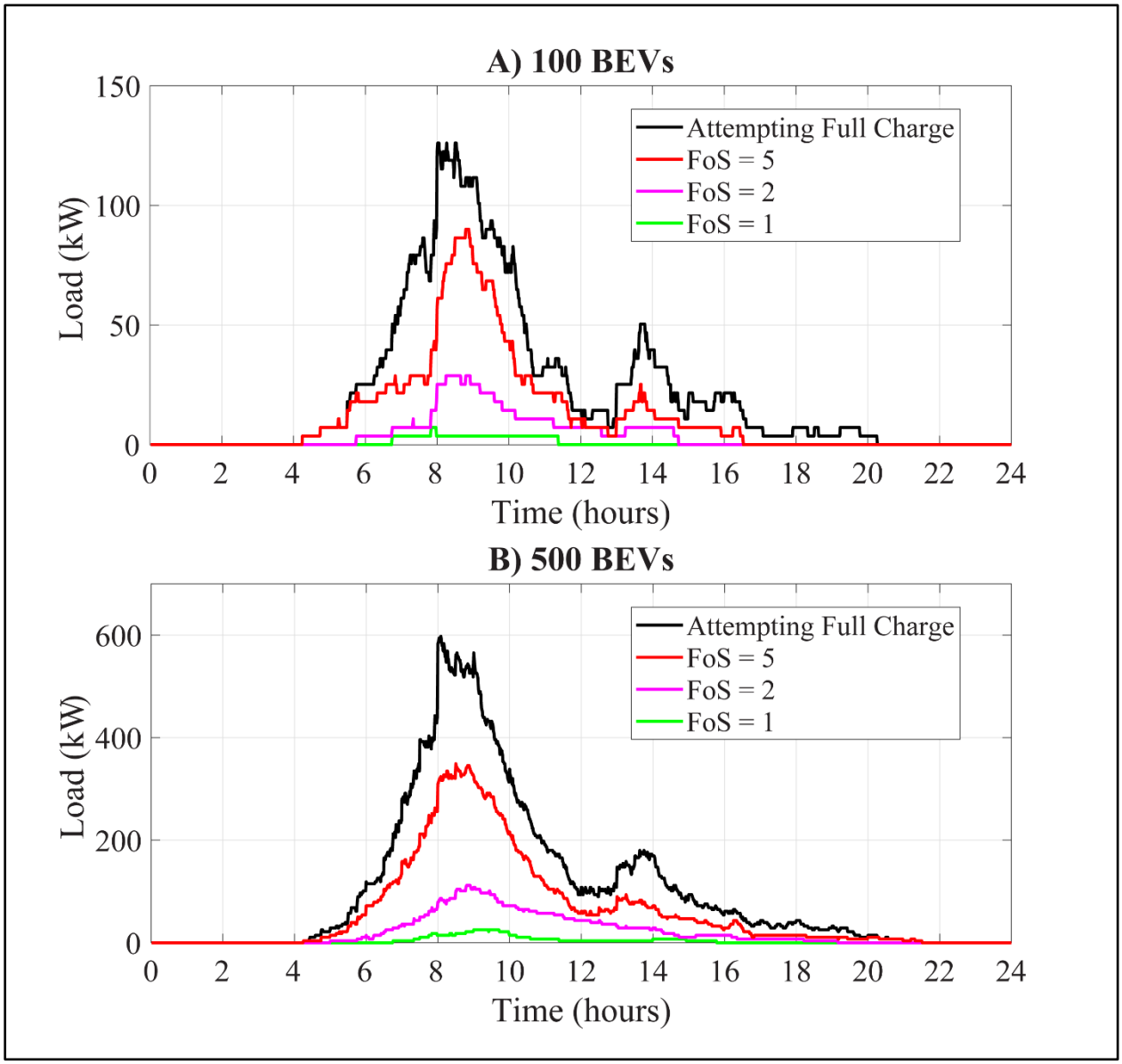

Figure 5 Uncontrolled Charging demand profiles for A) 100 and B) 500 BEV parking structures with no baseload

5.6.2 Smart Charging: Valley Filling

The smart-charging strategy in Section 5.3.2 can be used to perform Valley Filling when the cost signal is an aggregation of the scheduled BEV charging profiles. Results for the Valley Filling strategy for a 500 BEV parking structure with various baseloads are given in Figure 6. The peaks in the demand loads are much smaller than those seen with Uncontrolled Charging in Figure 5. The demand profiles are very flat during times with moderate numbers of parked BEVs (see Figure 1). Ordering via Flexibility Ratio results in lower peak loads, for all three cases. The maximum peaks when ordering via arrival time and Flexibility Ratio are 230 and 184 kW in Figure 6a, respectively.

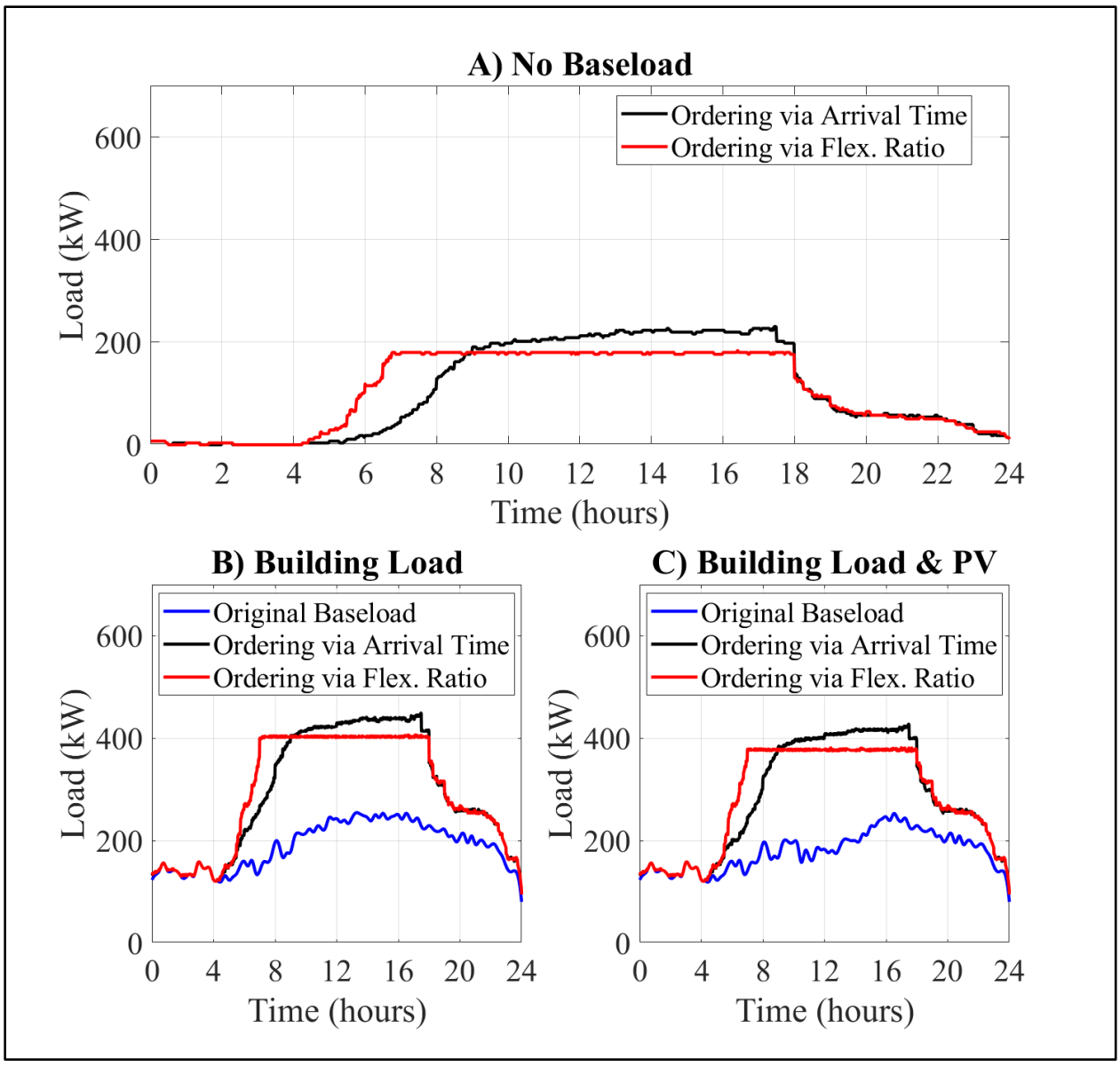

Figure 6 Valley Filling demand profiles for simulated parking structures with 500 BEVs attempting to get a full charge

5.6.3 Smart Charging: Augmented Cost Signal

The Valley Filling strategy above reduces peaks throughout the day via smart charging. In some cases, however, it may be beneficial to avoid charging during certain periods of the day. This could be due to high electricity prices, limitations in the local charging infrastructure, or the

need to reduce the load during scheduled maintenance. With minor modifications to the cost signal, the smart-charging strategy in Section 5.3.2 can steer demand away from (or towards) specific hours. The baseload used for Valley Filling is artificially increased during certain times to generate an augmented baseload (and, thus, augmented cost signal). The artificially high cost signal, thus, discourages BEVs from charging during those times.

A simple application of this strategy is avoiding charging during the more expensive On-Peak hours of Time-Of-Use (TOU) electricity rate plans [32]. See Section 4.5 for more details. Thus, the cost signal used by BEVs is artificially increased during On-Peak hours in order to reduce electricity costs for the parking structure. The cost signal was artificially increased by 1,000 kW for all simulations using an augmented cost signal.

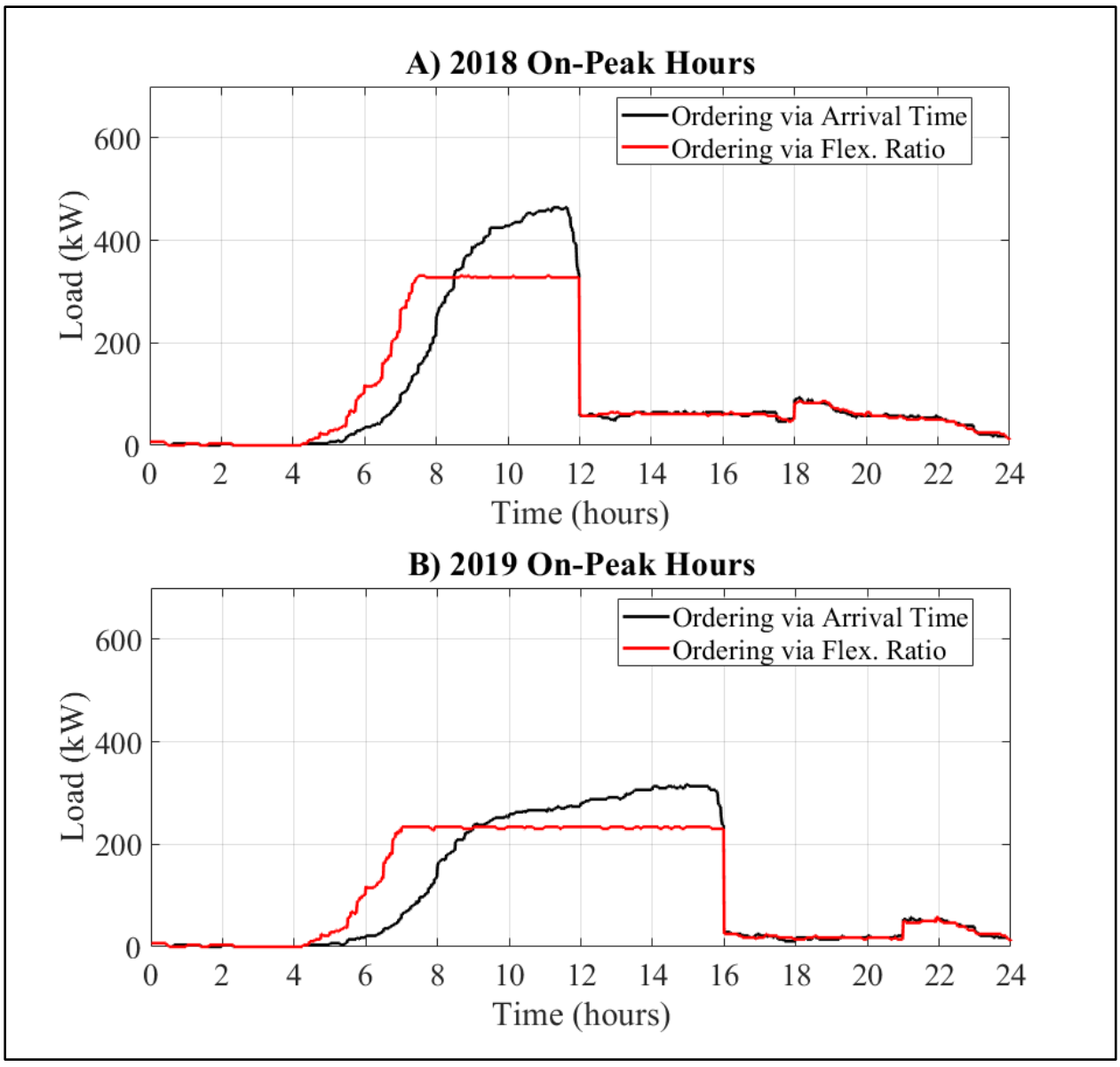

Figure 7 Augmented Cost Signal demand profiles with A) 2018 and B) 2019 On-Peak Hours for simulated parking structures with 500 BEVs attempting to get a full charge and no baseload

Results for the Augmented Cost Signal strategy with 2018 (12pm - 6pm) and 2019 (4pm - 9pm) On-Peak hours are shown in Figure 7. The load during On-Peak times has been lowered

in both cases. Similar to Valley Filling, ordering via Flexibility Ratio produces the lowest maximum peaks during On-Peak times and non-On-Peak times.

The Augmented Cost Signal strategy avoids charging during the 2019 On-Peak hours more effectively than with the 2018 On-Peak hours. The 2019 On-Peak hours also produce better peak reductions during non-On-Peak hours. Both occurrences are because 2019 On-Peak hours (4 pm – 9 pm) occur during the decline of BEV availability at work.

5.7 Effects on Parking Structure Demand Load

The maximum 24-hour loads experienced by 500 BEV parking structures are presented in Figure 8-A. The error bars in this figure represent the maximum and minimum values from all 50 simulated parking structures. Smart-charging reduces the maximum 24-hour load in all cases when compared with Uncontrolled Charging, demonstrating the peak reduction capabilities of smart charging in all scenarios. Valley Filling resulted in the lowest peaks, due to its load reduction capabilities. Ordering via Flexibility Ratio resulted in further peak reductions (when compared to ordering via arrival time). Specifically, ordering the 2018 Augmented Cost Signal strategy by Flexibility Ratio (with no baseload) results in peaks that are 69.4% of those when ordered by arrival time. Note that the maximum 24-hour load and the maximum On-Peak load experienced by both baseloads (without any BEV charging) are all about 254 kW (see Figure 3).

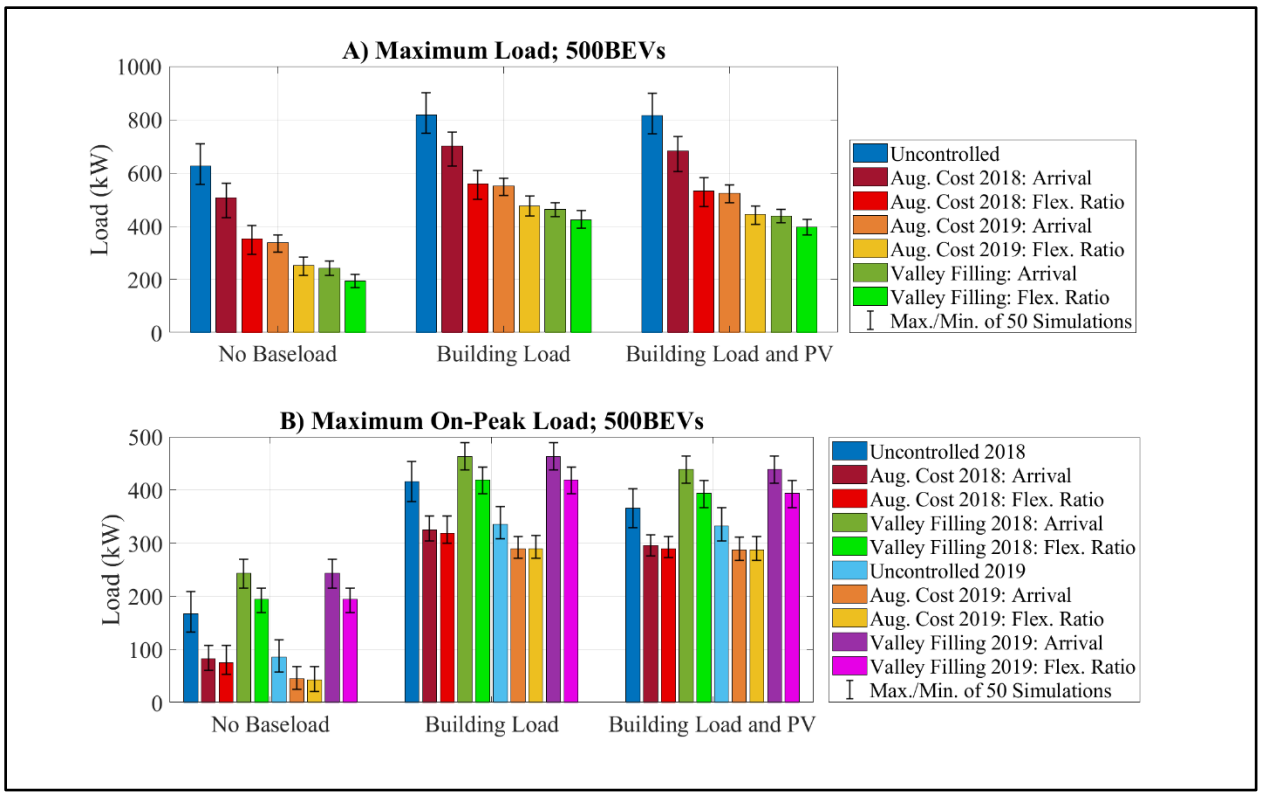

Figure 8 A) Maximum 24-hour load and B) Maximum On-Peak load for 50 simulated parking structures with 500 BEVs attempting to get a full charge

The maximum On-Peak loads experienced by 500 BEV parking structures are shown in Figure 8-B. The maximum On-Peak loads for Uncontrolled Charging are lower with 2019 On-Peak hours, because of the decline of BEV availability during On-Peak hours. The Augmented Cost Signal strategy reduces the maximum On-Peak load by about half when there is no baseload (compared to Uncontrolled Charging). Again, ordering via Flexibility Ratio reduces the maximum On-Peak loads further, for most cases. The ordering strategy makes little difference for the 2019 Augmented Cost Signal strategy (i.e., the dark orange and light orange bars). This is because charging cannot be shifted away from On-Peak hours for a subset of BEVs with low Flexibility Ratios. The flattening nature of the (non-augmented) Valley Filling strategy shifts

charging to On-Peak hours and, thus, increases the maximum On-Peak loads (see Section 5.6.2). The maximum On-Peak loads for Valley Filling in Figure 8-B are almost identical to the maximum 24-hour loads in Figure 8-A. Note that the demand charges incurred by a parking structure depend on the maximum 24-hour load and the maximum On-Peak load (see Table 5).

5.8 Effects on Electricity Costs

The monthly cost of electricity was calculated for each parking structure demand load. For simplicity, the demand load for each simulation was assumed to be the same for each weekday of the month. It was also assumed that the month contained 20 weekdays and that there was no charging or electricity usage during the weekends. The fixed monthly charge associated with each rate schedule was also included in the calculated costs.

For simplicity and consistency, electricity costs for all parking structures were calculated with the corresponding TOU-GS-3 summer rate schedule, except for 100 BEV parking structures without a baseload. It can be seen, in Figure 5-A, that the maximum load for this case is well below 200 kW. Thus, the corresponding TOU-GS-2 summer rate schedule is used to calculate the electricity costs for 100 BEV parking structures without a baseload.

The monthly electricity costs for the simulated parking structures are shown in Figure 9. The error bars in this figure represent the maximum and minimum values from all 50 simulated parking structures. The 2019 rate schedules result in lower electricity costs for Uncontrolled Charging when compared with the 2018 rate schedules. This is attributed to the fact that significantly less charging occurs during 4 – 9 pm with Uncontrolled Charging, when compared to 12 – 6 pm.

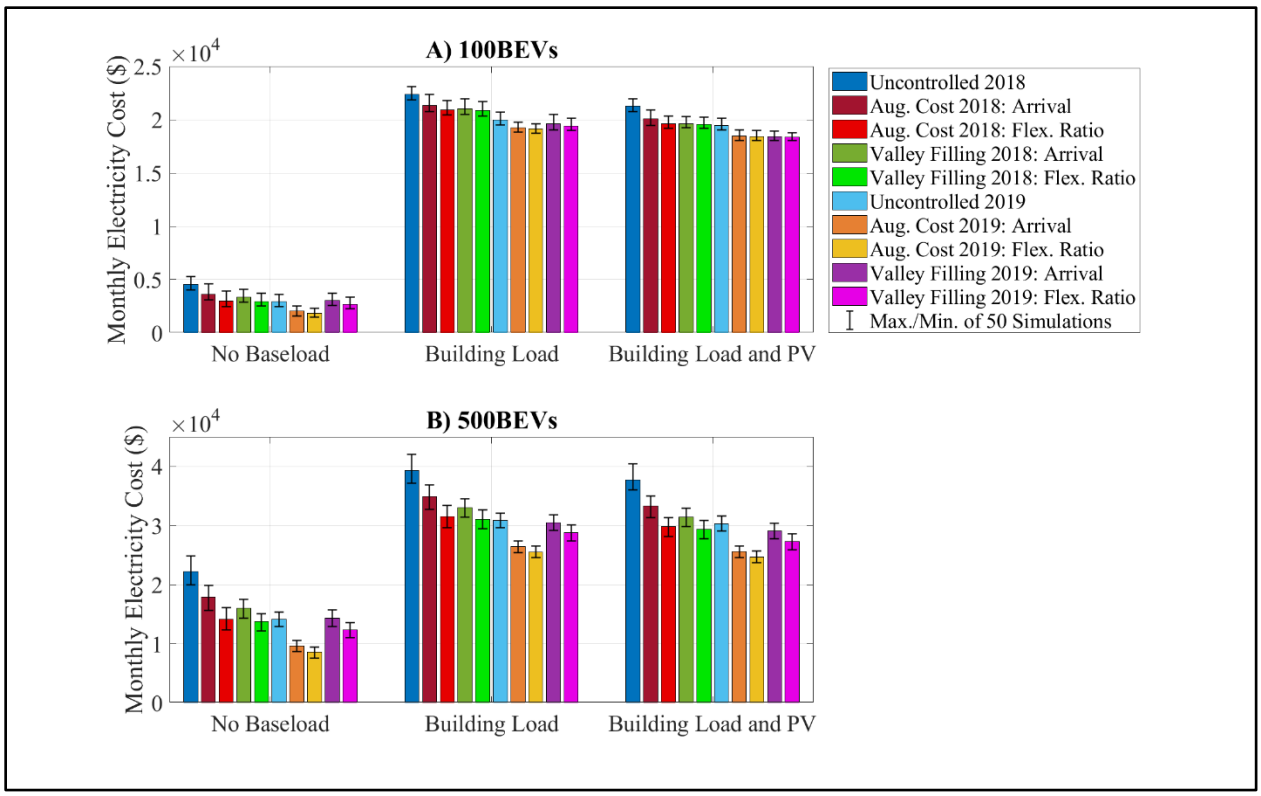

Figure 9 Estimated monthly cost of electricity for 50 simulated parking structures with A) 100 and B) 500 BEVs attempting to get a full charge

Average monthly savings between 20-31% are seen for all cases with no baseload and ordering via arrival time, except Valley Filling with 2019 rates (compared to Uncontrolled Charging). Ordering via arrival time requires the least amount of communication between the BEVs and the parking structure operator. Ordering via Flexibility Ratio, however, results in increased savings. All cases with no baseload and ordering via Flexibility Ratio resulted in monthly savings between 34-40%, except Valley Filling with 2019 rates.

Valley Filling with chronological ordering increases the monthly cost of electricity with 2019 rates and no baseload, compared to Uncontrolled Charging. This is because most charging occurs before 4 pm when it is uncontrolled. The Valley Filling strategy shifts charging to On-

Peak hours (see Figure 8-B), during high per kWh prices and On-Peak demand charges. Thus, non-augmented Valley Filling is not as effective at lowering electricity costs for 2019 prices as it was for 2018 prices. Electricity costs, however, are routinely changed or they may not always be the main concern of the parking structure operator, who might prefer to avoid overloading local power distribution components, for example. These argue for a flexible approach that can be modified to the specific needs of the operator.

5.9 Effects on Bin Assignment

Next, we focus on the use of octopus chargers. The algorithm from Section 5.5.1 was used to find the number of bins needed for each parking structure simulation. It is assumed that the number of BEVs assigned to each bin dictates the number of cables needed for each bin. The number of bins needed for each charging strategy and ordering strategy is presented in Figure 10.

On average, less than 40 and 182 bins are needed for 100 and 500 BEV parking structures, respectively. Valley Filling requires the lowest number of bins in all cases, as it has the lowest peaks. The average depth of all 50 simulations, described in Section 5.5.1, is included in Figure 10. The depth is given by the maximum number of BEVs charging at the same time, which is the smallest possible number of bins that can satisfy charging for the parking structure. On average, the difference between the number of bins needed and the depth is less than 8 and 38 bins for parking structures with 100 and 500 BEVs, respectively. The largest number of bins occurs when the 2018 Augmented Cost Signal strategy is used on a parking structure with a building load and PV. This occurs because PV generation reduces the baseload between 10am-12pm. This coincides with the time when the peaks for the Augmented Cost Signal strategy are highest (due to load shifting).

A key characteristic of Uncontrolled Charging is that charging is continuous during each dwell time. This means that the original Interval Partitioning algorithm can be used. Thus, the number of bins needed is equal to the depth for Uncontrolled Charging. The smart-charging strategies, however, require fewer bins and reduce monthly electricity costs in most cases and are thus preferred over Uncontrolled Charging.

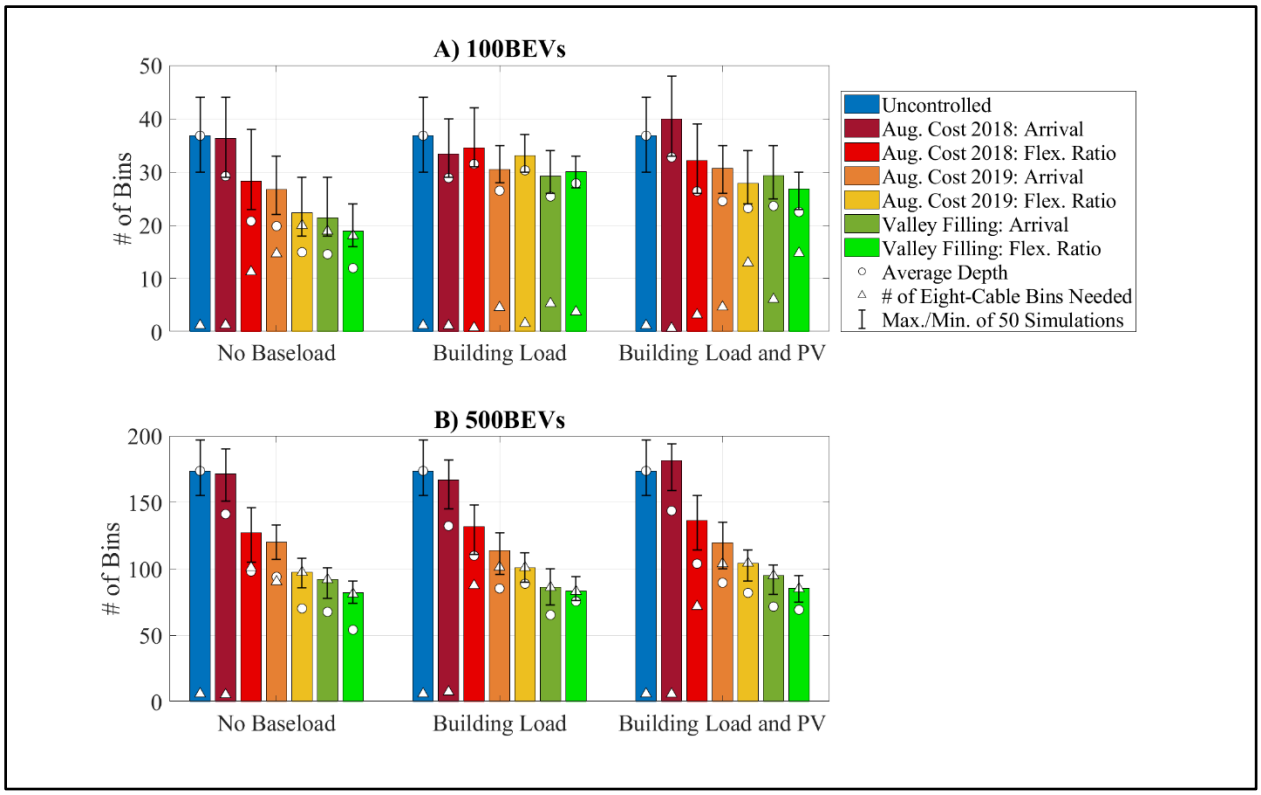

Figure 10 Number of bins required for 50 simulated parking structures with A) 100 and B) 500 BEVs attempting to get a full charge. Limit of eight cables per bin

The Sorted-Balance algorithm was used to assign bins to octopus chargers, to balance the number of cables needed by each octopus charger. The results for the Sorted-Balance assignment are shown in Table 6 and Table 7 for octopus chargers with two and three active cables, respectively. On average, less than 15 and 22 cables were needed for octopus chargers with two

and three active cables, respectively. The number of octopus chargers needed is obtained by dividing the number of bins needed (in Figure 10) by the number of active cables per octopus charger.

Table 6 Number of cables needed for each octopus charger with two assigned bins, for 50 simulated parking structures with 500 BEVs

Charging Strategy	Ordering Strategy	No Baseload		Building Load		Building Load & PV	
		Avg.	Max.	Avg.	Max.	Avg.	Max.
Uncontrolled	Arrival	7.29	11	7.29	11	7.29	11
Aug. Cost (2018)	Arrival	7.17	11	7.37	10	6.8	10
	Flex. Ratio	9.68	12	9.35	11	9.08	13
Aug. Cost (2019)	Arrival	10.09	14	10.71	13	10.17	12
	Flex. Ratio	12.57	15	12.2	14	11.8	14
Valley Filling	Arrival	12.64	16	13.59	16	12.41	15
	Flex. Ratio	14.59	18	14.32	17	14.01	17

Table 7 Number of cables needed for each octopus charger with three assigned bins, for 50 simulated parking structures with 500 BEVs

Charging Strategy	Ordering Strategy	No Baseload		Building Load		Building Load & PV	
		Avg.	Max.	Avg.	Max.	Avg.	Max.
Uncontrolled	Arrival	10.89	15	10.89	15	10.89	15
Aug. Cost (2018)	Arrival	10.71	13	11.03	14	10.18	13
	Flex. Ratio	14.46	18	13.99	17	13.59	17
Aug. Cost (2019)	Arrival	15.08	19	16	19	15.19	18
	Flex. Ratio	18.76	22	18.19	21	17.61	20
Valley Filling	Arrival	18.85	23	20.23	24	18.5	22
	Flex. Ratio	21.78	26	21.34	25	20.91	25

It may be preferable to assign each bin to a four-cable octopus charger with a single active cable (i.e., one bin per octopus charger), so that octopus chargers can be placed at the center of four neighboring parking spaces. Doing so would avoid the need for excessively long cables. The number of bins needed for four-cable octopus chargers is shown in Figure 11.

Parking structures with 100 and 500 BEVs require a maximum of 49 and 200 four-cable octopus chargers, respectively, for all cases (including fringe cases).

Utilization is the amount of charge received by BEVs divided by the total capacity of the chargers. The average utilization rate for traditional single-cable charging stations is 6.28%, for constant 3.6 kW charging rates. On average, Valley Filling required less than 100 bins/chargers to accommodate 500 BEVs in Figure 10-B. This reduces the number of the chargers to one fifth, resulting in utilization rates five times that of traditional single-cable charging stations (i.e., about 31.4%). Since less than 16% of BEVs are at work before 6:44 am or after 6:43 pm, utilization rates above 50% are unlikely (see Figure 1).

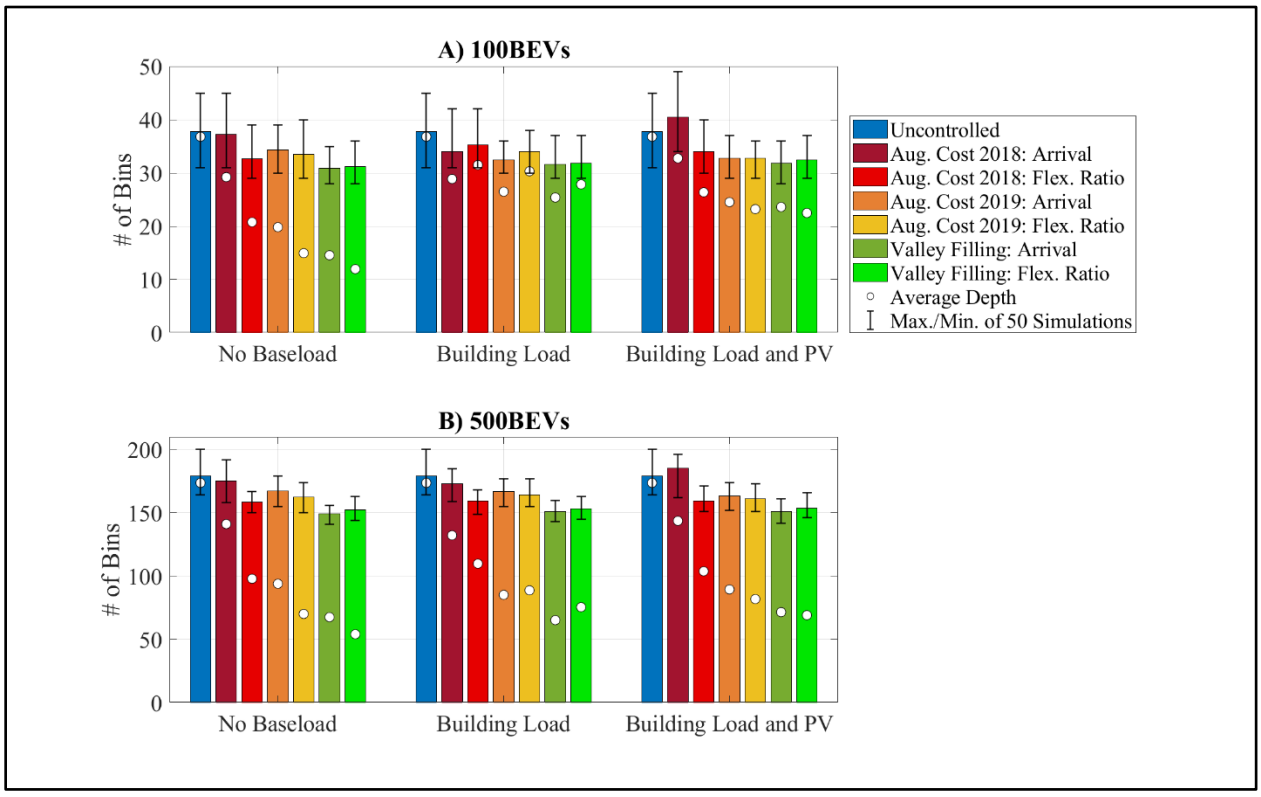

Figure 11 Number of bins required for 50 simulated parking structures with A) 100 and B) 500 BEVs attempting to get a full charge. Limit of four cables per bin

5.10 Sensitivity to Inaccurate Driving Patterns

In some cases, there may be discrepancies between predicted/scheduled driving patterns and actual driving patterns. Problems could arise if more driving is done than expected. In cases when driving after the workday is underestimated, drivers can request more energy than they need (see Section 4.4). If BEV drivers attempt to get a full charge at work (as is the case in all results presented, except for Figure 5), they can minimize the risk of not having enough charge at the end of the workday. This is particularly true for BEVs with large battery capacities that are generally maintained at a high state of charge.

If there are discrepancies in driving done between dwell times, then the BEV can keep track of large errors. If the BEV returns to the parking structure with a state of charge that is much smaller than expected, the BEV can cancel the rest of its reserved timeslots (i.e., charging profile) and re-run the charging strategy, generate a new charging profile, and request a new assignment from the parking structure operator (if necessary). For such cases, it may be necessary to keep some octopus chargers or single-cable chargers on reserve to accommodate reassignments. These reassigned BEVs then become chronological entries on top of the original Flexibility Ratio queue – the mixed case briefly mentioned in Section 5.4.2.

Furthermore, if a BEV needs the entire workday to charge and has little/no flexibility (due to long commutes), then it may not be compatible with any BEVs assigned to a bin/charger. Such BEVs might be best assigned to a single-cable charger. These details are omitted to focus on the main concepts of this work.

5.11 Conclusion

The second most opportune time to charge a BEV is at work [9]. Workplace charging, however, poses new challenges that arise from the multiple dwell times of BEVs. A decentralized smart-charging strategy that addresses the constraints and limitations of multiple dwell times is proposed in this work. The strategy allows BEVs to independently schedule charging for an entire workday. With simple modifications to the cost signal, this smart-charging strategy can be used to reduce parking structure load variation (Valley Filling) or shift charging away from On-Peak hours (Augmented Cost Signal). The Augmented Cost Signal strategy significantly reduced monthly electricity costs in all cases, when compared with Uncontrolled charging. Savings are significantly influenced by the charging strategy and electricity rate plans used.

A sorting strategy was developed to further improve the effectiveness of the proposed smart-charging strategies. Sorting via Flexibility Ratio resulted in improved peak reductions and increased savings for all cases when compared with sorting via arrival time but requires more communication. The increased communication requirements for the Flexibility Ratio strategy can be satisfied with internet communication, which is already included some BEVs.

An algorithm that assigns BEVs to bins/chargers is proposed. In all cases, a maximum of 49 and 200 chargers were needed to serve parking structures with 100 and 500 BEVs, respectively. When combined with smart charging, the assignment algorithm reduced the number of chargers needed in most cases, compared to Uncontrolled Charging. By reducing the number of bins (and thus octopus chargers) needed, the proposed assignment strategy can reduce investments needed for parking structures' charging infrastructures.

The comprehensive smart-charging protocol presented in this work can be used to reduce electricity and charging infrastructure costs associated with workplace charging, while increasing the utilization of renewable resources. Renewable energy is uncertain and electricity prices can vary significantly across regions, adding to the need for smart-charging protocols that are robust enough to deal with these variations (i.e., optimization based vs. ad-hoc). While this work focuses on daytime workplace charging, it has other applications. The smart-charging protocol can be used to coordinate charging for fleets of electric buses or delivery trucks.

The strategies proposed in this work can be developed further to estimate the energy storage capabilities of parking structures. On emergency days, the Augmented Cost Signal strategy can be used to provide as much charging as possible before On-Peak hours. Thus, giving the parking structure operator an estimate of the energy stored in the parked BEVs. Having this estimate gives the operator a valuable insight into each BEV's storage capabilities, so that an arbitrage (vehicle-to-grid and vehicle-to-vehicle charging) can be implemented. This is beyond the scope of this paper and is suggested as a future work.

6 Octopus Charger-Based Optimization Protocol

6.1 Introduction

While the overall market share of EVs is currently small, recent years have seen a significant increase in sales [7]. Significant increases in EV production/sales are imminent, with beneficial impacts on fossil fuel consumption and greenhouse gas emissions. Non-uniform concentrations of EV sales and increasing power levels, however, can cause difficulties for electricity delivery systems at the regional and/or residential levels [8]. As BEV battery sizes increase, faster charging rates become necessary. With enough BEVs and fast enough charging rates, BEV charging could create significant power demand. Large spikes in demand could negatively affect parking garage circuitry, increase electricity costs (e.g. demand charges), and exacerbate stress in critical times (e.g., high usage durations on hot days). These issues could be addressed by deploying smart-charging strategies in parking garages.

In Section 5, a charging protocol that allows BEVs to individually generate their charging profiles is presented. The parking structure aggregator gathers all of the charging profiles and assigns BEVs to charging stations such that multiple BEVs are charged by a single station (see Section 5.2 for a detailed overview of the charging protocol). The **BEV-based Optimization Protocol** can reduce peak loads, monthly electricity costs, and the number of needed charging stations. The decentralized nature of this protocol allows BEV owners to maintain a measure of privacy, while participating in smart charging.

If octopus chargers generate the charging profiles of their assigned BEVs, however, the benefits of smart charging can be further improved. Such an approach would require octopus chargers to use their assigned BEVs' driving data to generate their charging profiles. Thus,

privacy is not maintained for the participating BEVs. If privacy is not a high priority and drivers are willing to share their driving patterns, then this protocol can be used to reduce the number of octopus charger needed in a workplace parking structure.

Such a smart-charging protocol can also be applied to destination-charging locations where privacy is not a priority (e.g., delivery companies and bus terminals). Driving patterns for entire fleets of buses or delivery trucks, for example, are generally known. Furthermore, many delivery companies have announced plans to convert significant portions of their delivery trucks to battery-electric propulsion, in recent years [36],[37]. Such conversions require significant investments in charging stations. By using smart-charging protocols delivery companies (along with other businesses that require large fleets of EVs) can reduce electricity costs and charging infrastructure investments.

In this chapter, a comprehensive Octopus Charger-based mixed integer linear programming (MILP) protocol for workplace charging is proposed. The protocol is developed with the goal of reducing infrastructure and operational costs for a workplace parking structure, while meeting BEV drivers' charging needs. This work is focused on BEVs but applies to PEVs in general. The following are the main contributions of this work. **1)** A simple and well-known algorithm is used to assign BEVs to octopus chargers based on charging flexibility. **2)** A smart-charging strategy, that allows octopus chargers to schedule charging for their assigned BEVs via MILP methods is proposed (see Section 6.4.2). The **Octopus Charger-based MILP** strategy manages the parking structure demand load by allowing octopus chargers to act as individual agents. Thus, distributing the computational burden among the octopus chargers. By using the appropriate cost signal, the proposed smart-charging strategy can generate a parking structure demand load with desirable characteristics.

6.2 Overview of Octopus Charger-Based Optimization Protocol

For this charging protocol, it is assumed that a set number of Octopus Chargers with a set number of cables are installed in the parking structure. The Flexibility Ratios of all the participating BEVs are collected by the parking structure operator, in order to assign BEVs to octopus chargers. The parking structure operator then uses an assignment algorithm to assign each BEV to the octopus charger that it will be connected to, for the entire workday. Once assigned, BEVs share their expected driving patterns for the day (along with basic BEV specifications/information) to their assigned octopus chargers. A queue is then generated to dictate the order in which octopus chargers generate charging profiles for their assigned BEVs. Once an octopus charger is ready to generate the charging profiles of its assigned BEVs, it receives a cost signal. The octopus charger then uses mixed integer linear programming (MILP) techniques to generate the charging profiles. The octopus charger then sends the sum of all the charging profiles (i.e., the octopus charger's demand profile) to the parking structure operator, where it is aggregated for an updated cost signal. The process is repeated with the next octopus charger in the queue, until all BEV charging profiles have been generated.

In Section 5, it was necessary to execute the BEV-based protocol before the first BEV arrived at work when ordering BEVs via Flexibility Ratio. Similarly, this Octopus Charger-based MILP Protocol must be performed before the first BEV arrives (since each BEV needs to know which charger it is assigned to). Thus, each BEV driver inputs their expected driving patterns the night before or in the early morning via the BEV's user interface or a smartphone app. Once the information is gathered, the protocol above is executed.

In this protocol, the charging profiles of the BEVs assigned to an octopus charger are obtained by said octopus charger. Thus, this charging protocol is centralized at the octopus

charger level (with respect to the BEVs). The octopus chargers, however, generate the profiles as independent agents so this protocol is decentralized at the parking structure level (with respect to the octopus chargers).

This work assumes that BEV drivers participating in the proposed smart-charging protocol are willing to share their expected driving schedules (as well as basic BEV specifications/information). This assumption is based on the emergence and advancement of location and calendar information on smart phones (e.g., location reminders). Furthermore, this assumption is generally true when considering delivery and bus companies (where the schedules for the entire fleet are generally known).

6.3 Octopus Charger Assignment

In Section 5, octopus charger assignment was performed after each BEV individually obtained its charging profile. Since the BEVs must me assigned to each octopus charger before the charging profiles are obtained, a new assignment strategy must be developed. In order to effectively assign BEVs to octopus chargers, an appropriate assignment algorithm must have the following characteristics: 1) It must minimize the number of octopus chargers needed to accommodate all BEVs, 2) It must have a reasonably fast computational time, 3) It must maximize compatibility among BEVs assigned to the same octopus charger. In order to generate a suitable assignment, all BEVs assigned to an octopus charger must be able to meet their charging needs. Thus, grouping of BEVs with undesirable characteristics (large charging demands and/or low Flexibility Ratios) must be avoided.

6.3.1 Octopus Charger Assignment via Sorted-Balance

A well-established assignment problem is the Load Balancing Problem [35]. The Load Balancing Problem occurs when a set of n jobs must be assigned to m identical machines, M_i, such that the workload among the machines is as balanced as possible. The processing time of each job (i.e., load) is given by l_j. We can define the total load on each machine, L_i, as the sum of the processing times (l_j) of its assigned jobs. We define the makespan, L, as the maximum load on any machine (i.e., $L = \max(L_1, \dots, L_m)$). Thus, the objective is to minimize the makespan. Acquiring the optimal solution to the Load Balancing Problem is NP-hard, which could lead to long computational times. Two approximation algorithms that run in polynomial time exist, which can find solutions that are guaranteed to be close to the optimal solution [35].

The optimal solution to the Load Balancing Problem is unknown, however, a lower bound can be determined. The lower bound of the optimal solution is given by L^*, which has the following characteristics: $L^* \geq \frac{1}{m}\sum_j l_j$ and $L^* \geq \max_j l_j$ [35]. The first lower bound is the average work done by all the machines. The second lower bound is the case where the processing time of one job is longer than the combined processing time of all the other jobs.

Sorted-Balance is a well-known approximation algorithm that can find solutions to the Load Balancing Problem such that $L \leq \frac{3}{2}L^*$ (see [35] for details). The Sorted-Balance algorithm does this by first sorting jobs in decreasing order of processing time (l_j). The algorithm then goes through each job in the queue and assigns it to the machine with the smallest load (L_i) [35].

The Sorted-Balance algorithm above can be used to assign BEVs to octopus chargers such that BEVs with undesirable characteristics (e.g., low Flexibility Ratios) are distributed evenly among the chargers. In this case, The BEVs represent the jobs and the octopus chargers

represent the machines. The processing time of each job in the algorithm can represent each BEV's Inverse Flexibility Ratio, F_n^{-1}, given in (10). Balancing the Inverse Flexibility Ratios results in similar flexibility among the octopus chargers in the parking structure. By having some flexibility, the octopus chargers are less constrained when generating the charging profiles for their assigned BEVs. In this work, we focus on balancing BEVs' Inverse Flexibility Ratios, however any parameter can be used (see Section 6.5.1 for an example where requested charge is balanced).

$$F_n^{-1} = \frac{\left(\frac{-\left(BC_{n,0} - BC_{n,des}\right)}{\eta} + \sum_{k=1}^{D_n} \frac{y_{n,k}}{\eta}\right)/p_n}{\sum_i \Delta t_n(t_i)} \tag{10}$$

The assignment algorithm above can be implemented if the parking structure operator gathers the Inverse Flexibility Ratios of all participating BEVs ahead of time. This requires the operator to communicate the with the participating BEVs. If communication (before the BEV arrives at the parking structure) is not possible, then a different assignment algorithm must be used (see Section 7.3).

Note that the guarantee that the Sorted-Balance solution is close to the optimal solution ($L \leq \frac{3}{2} L^*$) is maintained only if the octopus chargers are assumed to have an unlimited number of cables. If a limit is placed on the number of cables per octopus charger, then the assignment could result solutions above the guaranteed limit. For example, an octopus charger could have the lowest load (L_i) but no more available cables. In this case, the current BEV will be assigned to the octopus charger with the smallest load and available cables. Due to the queue, however, these BEVs will have the smallest Inverse Flexibility Ratios (i.e., most flexibility). Thus, this

assignment algorithm is still effective. The focus of this work is on 4-Cable and 8-Cable octopus chargers.

The Sorted-Balance algorithm is used in this work without any modifications, except limiting the number of cables. Thus, no contributions are made to the assignment algorithm used in this work. The detailed description above is given only for ease of understanding to the reader. For more information see [35].

Note that the Inverse Flexibility Ratio and requested charge can also be used to limit participation in this protocol. For example, if a BEV has very little flexibility and will be charging for a long period, then said BEV might be better suited with a single-cable charging station. These details are omitted to focus on the main concepts of this work.

6.4 Smart Charging: Octopus Charger-Based Optimization

For this strategy, each octopus charger must generate the charging profiles of all its assigned BEVs. Thus, the octopus charger must have access to the expected driving patterns and basic specifications of all assigned BEVs. Two Octopus Charger-based Optimization strategies are described in the following sections.

A key observation of this strategy is that timeslots must be defined differently from the timeslots in BEV-based optimization. In BEV-based optimization, timeslots were dependent on each individual BEV. For example, a BEV that arrived at 1:18 pm and left at 7:33 pm had a dwell time of 6.25 hours. This BEV would have 6 one-hour timeslots and one 15-minute timeslot for BEV-based optimization. For octopus charger-based optimization, however, all BEVs must have identical timeslots. Timeslots in this chapter (and in Section 7) will have a resolution of one hour and start at the top of the hour (unless stated otherwise). Timeslots will, however, be split

up every time that a BEV connects or disconnects to/from an octopus charger. The following table contains sample BEV data, that will be used in examples in the following sections.

Table 8 Sample BEV data

	Arrival Time	Departure Time	Charge Needed	Charging Rate
BEV #1	6:20 am	9:35 am	12 kWh	6.6 kW
BEV #2	7:00 am	9:15 am	7 kWh	6.6 kW
BEV #3	7:30 am	9:15 am	8 kWh	6.6 kW

For the sample data there is initially a one-hour timeslot from 6-6:59 am. This timeslot is split into two timeslots of 20 and 40 minutes. Note that no charging occurs in the first (20-minute) timeslot, since there are no parked BEVs. The 7:00-7:59 am timeslot is split into two 30-minute timeslots, and so on. The following table contains the timeslots for the sample BEV data in Table 8.

Table 9 Timeslots for PEV data from Table 8

6:00-6:19	6:20-6:59	7:00-7:29	7:30-7:59	8:00-8:59	9:00-9:14	9:15-9:34	9:35-9:59

6.4.1 Octopus Charger-Based Optimization: Linear Programming

The problem formulation from the BEV-based Optimization strategy can be expanded to incorporate the constraints of the Octopus Charger-based strategy. The objective function from BEV-based Optimization (Equation (2)) is expanded to incorporate all the BEVs assigned to an octopus charger. Doing so results in the objective function given in Equation (11). The decision variables, $x_n(t_i)$, are defined as the energy requested by the n^{th} BEV during timeslot t_i. The cost signal for BEV n, during timeslot, t_i, is given by $C_n(t_i)$. Note that the cost signal can be the same or different for each BEV (see Section 6.4.2.1 for more details).

$$min \sum_{n=1}^{N} \sum_{i=1}^{I} C_n(t_i) x_n(t_i) \tag{11}$$

The total amount of energy requested by the n^{th} BEV is given by b_n in Equation (5) of BEV-based optimization strategy. Similarly expanding Equation (5) produces the following equality constraints for the assigned BEVs. Where the value of b_n for each BEV is still given by Equation (5) and I is the total number of universal timeslots.

$$\left.\begin{aligned} h_1(x) &= \sum_{i=1}^{I} x_1(t_i) - b_1 = 0 \\ &\vdots \\ h_3(x) &= \sum_{i=1}^{I} x_N(t_i) - b_N = 0 \end{aligned}\right\} \tag{12}$$

Expanding the lower and upper bounds in Equation (3) gives the constraints in Equations (13) and (14), respectively. Equation (13) sets charging during each timeslot to be positive (i.e. no vehicle-to-grid or vehicle-to-vehicle charging).

$$\left.\begin{aligned} g_{lb,1}(x) &= \begin{bmatrix} -x_1(t_1) \\ \vdots \\ -x_1(t_I) \end{bmatrix} \leq \begin{bmatrix} 0 \\ \vdots \\ 0 \end{bmatrix} \\ &\vdots \\ g_{lb,\mathrm{N}}(x) &= \begin{bmatrix} -x_N(t_1) \\ \vdots \\ -x_N(t_I) \end{bmatrix} \leq \begin{bmatrix} 0 \\ \vdots \\ 0 \end{bmatrix} \end{aligned}\right\} \tag{13}$$

Equation (14) limits the amount of charging that each BEV can do during each timeslot. The limit, $r_n(t_i)$, is given by Equation (4) and based on each BEVs' maximum charging rate and

timeslot length. For example, a BEV with a 3.6 kW charging rate can only charge 1.8 kWh during a 30-minute timeslot.

$$\left.\begin{aligned} g_{ub,1}(x) &= \begin{bmatrix} x_1(t_1) - r_1(t_1) \\ \vdots \\ x_1(t_5) - r_1(t_5) \end{bmatrix} \leq \begin{bmatrix} 0 \\ \vdots \\ 0 \end{bmatrix} \\ &\vdots \\ g_{ub,\mathrm{N}}(x) &= \begin{bmatrix} x_N(t_1) - r_N(t_1) \\ \vdots \\ x_N(t_I) - r_N(t_I) \end{bmatrix} \leq \begin{bmatrix} 0 \\ \vdots \\ 0 \end{bmatrix} \end{aligned}\right\} \tag{14}$$

In order to respect the maximum charging rate of the octopus charger, a limit must be placed on the amount of charging that can be done by the assigned BEVs during each timeslot. Equation (15) limits the amount of charging can be provided by the octopus charger, $R(t_{\mathrm{i}})$, during each timeslot, t_{i}. For example, a 7.2 kW charging station can only provide 7.2 kWh of charging during a one-hour timeslot. Thus, the combined charging done by all assigned BEVs must be less than 7.2 kWh.

$$g_{station}(x) = \begin{bmatrix} x_1(t_1) + \cdots + x_N(t_1) - R(t_1) \\ \vdots \\ x_1(t_I) + \cdots + x_3(t_I) - R(t_I) \end{bmatrix} \leq \begin{bmatrix} 0 \\ \vdots \\ 0 \end{bmatrix} \tag{15}$$

Note that the equations above are given for the case where each BEV has a single, continuous dwell time. In order to take the constraints of multiple dwell times into consideration (as in Section 5) the additional inequality constraints from Equations (5)-(8) must be applied to each BEV.

6.4.1.1 Proof of Characteristics

This strategy allows all BEVs to charge at their maximum charging rate, except for one timeslot (similar to [19]) during each dwell time and when the maximum capacity of the

charging station is reached. A proof of this can be found below. For simplicity, the case where BEVs has one dwell time is presented. The following notation will be used in the proof.

$$x_n = \begin{bmatrix} x_n(t_1) \\ \vdots \\ x_n(t_{\mathrm{I}}) \end{bmatrix} \tag{16}$$

$$x = \begin{bmatrix} x_1 \\ \vdots \\ x_{\mathrm{N}} \end{bmatrix} \tag{17}$$

$$r = \begin{bmatrix} r_1 \\ \vdots \\ r_{\mathrm{N}} \end{bmatrix} \tag{18}$$

$$\frac{\partial f}{\partial x} = \begin{bmatrix} \frac{\partial f}{\partial x_1} & \cdots & \frac{\partial f}{\partial x_m} \end{bmatrix} \tag{19}$$

The Lagrangian for the problem stated by Equations (11)-(15) is given below.

$$\begin{aligned} \mathcal{L} = [C^T \quad C^T \quad C^T]x - \nu_1 \left[\sum_{i=1}^{\mathrm{I}} x_1(t_i) - b_1\right] - \cdots - \nu_{\mathrm{N}} \left[\sum_{i=1}^{\mathrm{I}} x_{\mathrm{N}}(t_i) - b_{\mathrm{N}}\right] + \lambda^T x \\ + \mu^T[x - r] + p^T[x_1 + \cdots + x_{\mathrm{N}} - R] \end{aligned} \tag{20}$$

The gradient of the Lagrangian is found to be

$$\begin{aligned} \frac{\partial \mathcal{L}}{\partial x} = [C^T \quad C^T \quad C^T] - [\nu_1 \quad \cdots \quad \nu_1 \quad \cdots \quad \cdots \quad \cdots \quad \nu_{\mathrm{N}} \quad \cdots \quad \nu_{\mathrm{N}}] + \lambda^T + \mu^T \\ + [p^T \quad p^T \quad p^T] = 0 \end{aligned} \tag{21}$$

The gradient gives the following KKT Conditions.

$$\frac{\partial \mathcal{L}}{\partial x} = C_n(t_i) - \nu_n + \lambda_n(t_i) + \mu_n(t_i) + p(t_i) = 0 \tag{22}$$

$$\nu_n \left[\sum_{i=1}^{\mathrm{I}} x_n(t_i) - b_n \right] = 0 \tag{23}$$

$$\lambda_n(t_i) x_n(t_i) = 0 \tag{24}$$

$$\mu_n(t_i)[x_n(t_i) - r_n(t_i)] = 0 \tag{25}$$

$$p(t_i) \left[\sum_{n=1}^{\mathrm{N}} x_n(t_i) - R(t_i) \right] = 0 \tag{26}$$

We now look at all the possible cases for the KKT Conditions above.

Case 1: $\boldsymbol{x_n(t_i) \neq 0}$

We are interested in charging time, so that means that $\lambda_n(t_i) = 0$. Which changes Equations (22)-(26) to the following.

$$\frac{\partial \mathcal{L}}{\partial x} = C_n(t_i) - \nu_n + \mu_n(t_i) + p(t_i) = 0 \tag{27}$$

$$\nu_n \left[\sum_{i=1}^{\mathrm{I}} x_n(t_i) - b_n \right] = 0 \tag{23}$$

$$\lambda_n(t_i) = 0 \tag{28}$$

$$\mu_n(t_i)[x_n(t_i) - r_n(t_i)] = 0 \tag{25}$$

$$p(t_i) \left[\sum_{n=1}^{\mathrm{N}} x_n(t_i) - R(t_i) \right] = 0 \tag{26}$$

Case 1.1: $\boldsymbol{x_n(t_i) \neq 0}$ and $\boldsymbol{\mu_n(t_i) \neq 0}$

If $\boldsymbol{\mu_n(t_i) \neq 0}$, then the timeslot charges at maximum power.

$$\frac{\partial \mathcal{L}}{\partial x} = C_n(t_i) - \nu_n + \mu_n(t_i) + p(t_i) = 0 \tag{27}$$

$$\nu_n \left[\sum_{i=1}^{\mathrm{I}} x_n(t_i) - b_n \right] = 0 \tag{23}$$

$$\lambda_n(t_i) = 0 \tag{28}$$

$$x_n(t_i) = r_n(t_i) \tag{29}$$

$$p(t_i) \left[\sum_{n=1}^{\mathrm{N}} x_n(t_i) - R(t_i) \right] = 0 \tag{26}$$

Case 1.2: $\boldsymbol{x_n(t_i) \neq 0}$ and $\boldsymbol{\mu_n(t_i) = 0}$

If $\mu_n = 0$, we get the following equations. We now look at $p(t_i)$.

$$\frac{\partial \mathcal{L}}{\partial x} = C_n(t_i) - \nu_n + p(t_i) = 0 \tag{30}$$

$$\nu_n \left[\sum_{i=1}^{\mathrm{I}} x_n(t_i) - b_n \right] = 0 \tag{23}$$

$$\lambda_n(t_i) = 0 \tag{28}$$

$$\mu_n(t_i) = 0 \tag{31}$$

$$p(t_i) \left[\sum_{n=1}^{\mathrm{N}} x_n(t_i) - R(t_i) \right] = 0 \tag{26}$$

Case 1.2.1: $\boldsymbol{x_n(t_i) \neq 0}$, $\boldsymbol{\mu_n(t_i) = 0}$, and $\boldsymbol{p(t_i) = 0}$

If $p(t_i) = 0$, it means that the charging capacity of the octopus charger has not been reached. Thus, we have $C_n(t_i) = \nu_n$. There is only one ν_n for each BEV. If all $C_n(t_i)$ values are distinct, then there is only one timeslot that that will not charge at maximum power under these conditions.

$$C_n(t_i) = \nu_n \tag{32}$$

$$\nu_n \left[\sum_{i=1}^{\mathrm{I}} x_n(t_i) - b_n \right] = 0 \tag{23}$$

$$\lambda_n(t_i) = 0 \tag{28}$$
$$\mu_n(t_i) = 0 \tag{31}$$
$$p(t_i) = 0 \tag{33}$$

Case 1.2.2: $\boldsymbol{x_n(t_i) \neq 0}$, $\boldsymbol{\mu_n(t_i) = 0}$, and $\boldsymbol{p(t_i) \neq 0}$

If $p(t_i) \neq 0$, then that means that the charging capacity for the station is reached. In this case, BEVs may not charge at the maximum power.

$$C(t_i) = \nu_n - p(t_i) \tag{34}$$
$$\nu_n \left[\sum_{i=1}^{\mathrm{I}} x_n(t_i) - b_n \right] = 0 \tag{23}$$
$$\lambda_n(t_i) = 0 \tag{28}$$
$$\mu_n(t_i) = 0 \tag{31}$$
$$\sum_{n=1}^{\mathrm{N}} x_n(t_i) - R(t_i) = 0 \tag{35}$$

Thus, all BEVs will charge at their maximum charging rate, except for one timeslot (if there is one dwell time only) and when the maximum capacity of the charging station is reached. This is based on the requirement that all values of the cost signal are distinct (as in [19]). A basic example of these characteristics is presented in the following section.

6.4.1.2 Example of Characteristics

A simple example of the characteristics described above are presented in Figure 12. The three sample BEVs from Table 8 are assigned to an octopus charger with a maximum output rate of 15 kW. The cost signal used was set up such that earlier timeslots had a lower cost.

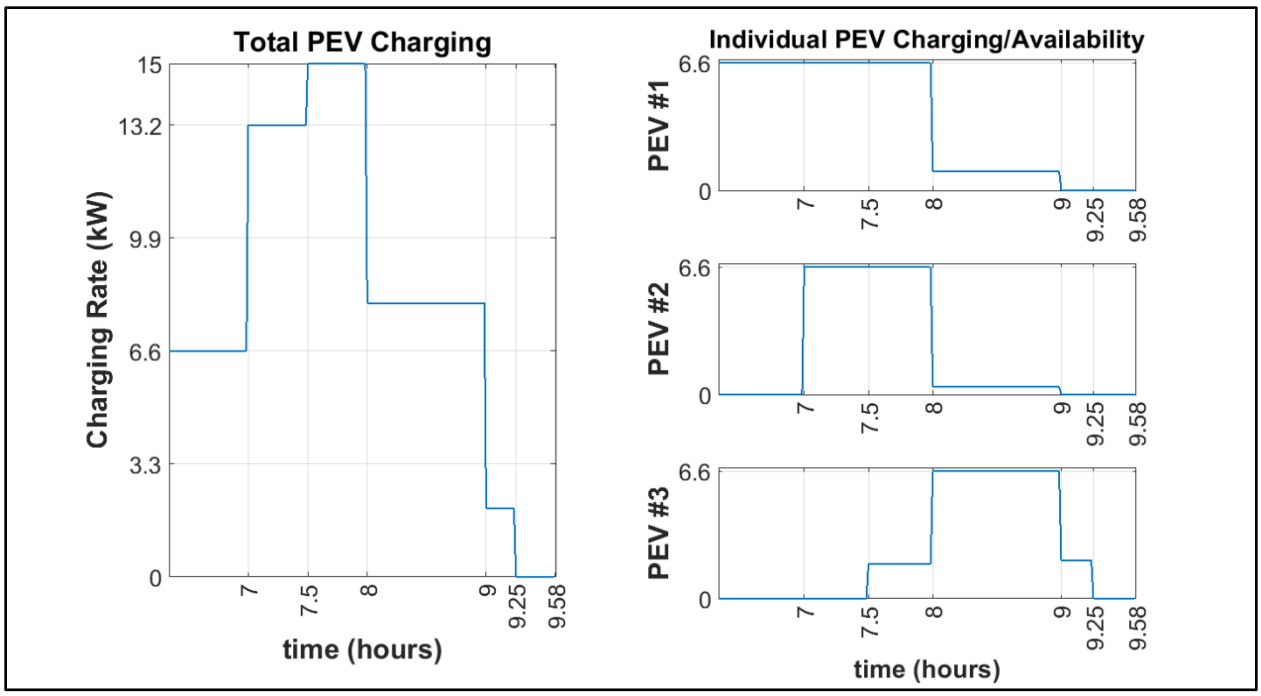

Figure 12 Linear programming solution for Octopus Charger-based Optimization for a 15 kW octopus charger with the BEVs from Table 8

BEVs #1 and #2 charge at the maximum rate during all timeslots except for their last one. BEV #3 contains two timeslots that do not charge at the maximum rate. The first occurs at 7:30 am, when the maximum capacity of the charging station is reached, and the second occurs at 9:00 am. If the BEVs can charge at variable rates, then there can be a subset of BEVs charging at a rate lower than the maximum power (when the station capacity is reached).

To avoid the first non-maximum timeslot for BEV #3 at 7:30 am, the constraint on the charging possible by each octopus charger during each dwell time ($R(t_i)$) can be modified to be dependent on maximum charge possible by the BEVs (i.e., $[Modified\ Capacity] = r_n(t_i) \times floor\left(\frac{R(t_i)}{r_n(t_i)}\right)$). This workaround, however, requires that all assigned BEVs have the same charging rate and would prevent the grouping of BEVs with different charging rates. An

example of this modification is given in Figure 13. All BEVs charge at the maximum rate for all timeslots except for one. The maximum output rate of the octopus charger is 13.2 kW, due to the modified capacity.

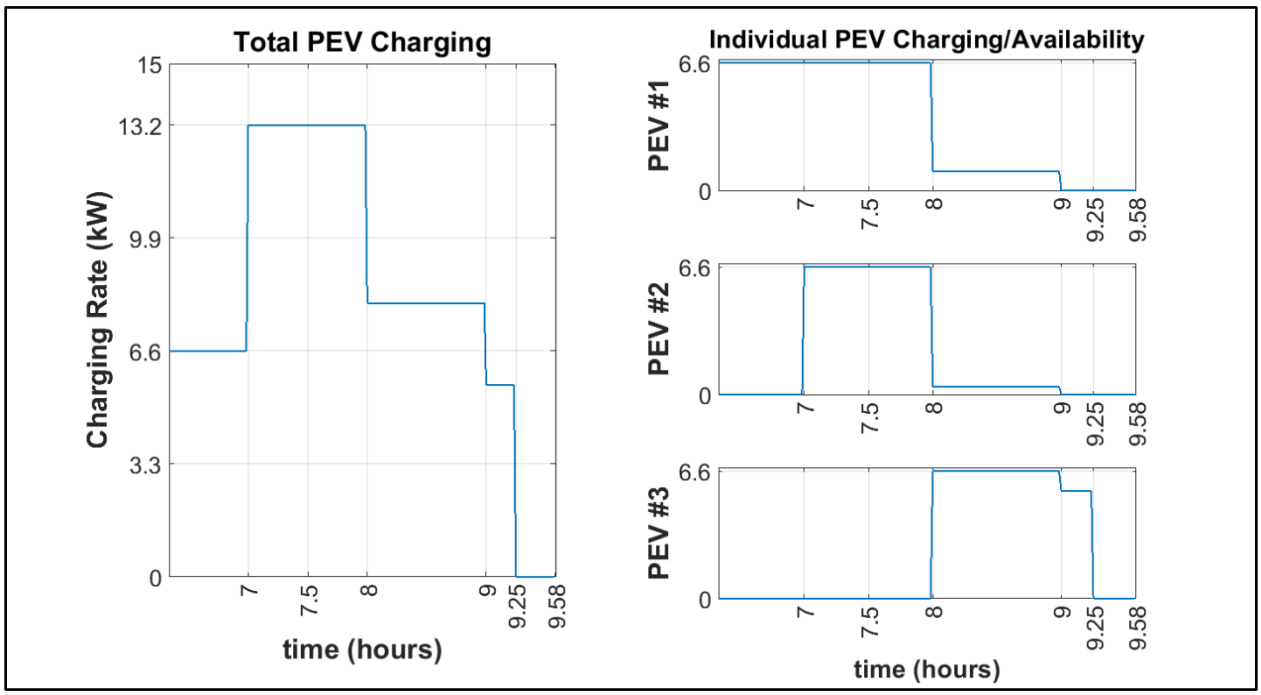

Figure 13 Linear programming solution for octopus charger-based optimization for a 13.2 kW charging station with BEVs from Table 8

As seen in Figure 12 and Figure 13, choosing the cost signal such that earlier timeslots are cheaper forces charging to occur as early as possible. This can be very beneficial as it would allow the charging station to accommodate charging for unexpected BEV arrivals that occur later in the day (since most charging is done as early as possible).

This charging strategy is suitable for BEVs that can charge at variable rates. It is, however, is not fully developed for BEVs that can only (or prefer to only) charge at their maximum charging rate. As seen in the 7:30 am timeslot of Figure 12, all three BEVs cannot

charge at the maximum rate, as this would result in a 19.8 kW power rate. Therefore BEV #3 must charge below its maximum charge rate. This can be overcome if all BEVs have the same maximum charging rate (Figure 13) but prevents BEVs with different maximum charging rates from being grouped together. This charging strategy will not be pursued in this work. It does, however, provide some valuable insight into the characteristics of the mixed integer linear programming approach discussed in the following section.

6.4.2 Octopus Charger-Based Optimization: Mixed Integer Linear Programming

In order to ensure that all BEVs can charge at their maximum rate during all timeslots except for one, modifications and constraints from mixed integer linear programming (MILP) can be applied. The objective function from Equation (11) is modified to include binary variables. As in Equation (11) the decision variables, $x_n(t_i)$, are defined as the energy requested by the n^{th} BEV during timeslot t_i. The cost signal for BEV n, during timeslot, t_i, is given by $C_n(t_i)$. Note that the cost signal can be the same or different for each BEV (see Section 6.4.2.1 for more details). The binary variables, $l_n(t_i)$, can be constrained such that they equal one when $x_n(t_i)$ is nonzero (see Equation (37) for details). The variable B is the cost associated with charging a BEV during any timeslot and must be positive. The total number of assigned BEVs and the total number of timeslots are given by N and I, respectively.

$$min \sum_{n=1}^{N} \sum_{i=1}^{I} C_n(t_i) x_n(t_i) + \sum_{n=1}^{N} \sum_{i=1}^{I} B l_n(t_i) \tag{36}$$

The equality constraints that dictate total charging for each BEV are the same as in the linear programming case. The total amount of energy requested by the n^{th} BEV is given by b_n in Equation (5) of BEV-based Optimization strategy (in Section 5.3.2).

$$\left.\begin{aligned} h_1(x) &= \sum_{i=1}^{I} x_1(t_i) - b_1 = 0 \\ &\vdots \\ h_3(x) &= \sum_{i=1}^{I} x_N(t_i) - b_N = 0 \end{aligned}\right\} \tag{12}$$

The lower bounds used for MILP are the same as in the linear programming case and are repeated for clarity. Equation (13) sets charging during each timeslot to be positive (i.e. no vehicle-to-grid or vehicle-to-vehicle charging).

$$\left.\begin{aligned} g_{lb,1}(x) &= \begin{bmatrix} -x_1(t_1) \\ \vdots \\ -x_1(t_I) \end{bmatrix} \leq \begin{bmatrix} 0 \\ \vdots \\ 0 \end{bmatrix} \\ &\vdots \\ g_{lb,\mathrm{N}}(x) &= \begin{bmatrix} -x_N(t_1) \\ \vdots \\ -x_N(t_I) \end{bmatrix} \leq \begin{bmatrix} 0 \\ \vdots \\ 0 \end{bmatrix} \end{aligned}\right\} \tag{13}$$

The upper bound on BEV charging during each timeslot can be set with the following constraints. Where $r_n(t_i)$ is the maximum amount of charging that the n^{th} BEV can do during timeslot t_i. If the n^{th} BEV performs any amount of charging during timeslot t_i, the constraint below can only be satisfied if $l_n(t_i)$ is equal to one. If there is no charging, then the value of $l_n(t_i)$ can be either zero or one. The cost associated with each binary variable, B, in the objective function, however, prevents nonzero values for $l_n(t_i)$ when there is no charging. Thus, $l_n(t_i)$ equals zero when $x_n(t_i) = 0$ and one when $x_n(t_i)$ is nonzero.

$$\left.\begin{aligned} g_{ub,1}(x) &= \begin{bmatrix} x_1(t_1) - r_1(t_1)l_1(t_1) \\ \vdots \\ x_1(t_I) - r_1(t_I)l_1(t_I) \end{bmatrix} \leq \begin{bmatrix} 0 \\ \vdots \\ 0 \end{bmatrix} \\ &\vdots \\ g_{ub,N}(x) &= \begin{bmatrix} x_N(t_1) - r_N(t_1)l_N(t_1) \\ \vdots \\ x_N(t_I) - r_N(t_I)l_N(t_I) \end{bmatrix} \leq \begin{bmatrix} 0 \\ \vdots \\ 0 \end{bmatrix} \end{aligned}\right\} \quad (37)$$

With the binary variables, the constraint on the octopus charger can be changed to consider charging power (kW), as opposed to charge (kWh) as in Equation (15). The constraints set on charging power, during each timeslot are given below. Where p_n is the maximum charging rate of the n^{th} BEV and P_{oct} is the maximum output rate of the octopus charger.

$$g_{oct}(x) = \begin{bmatrix} l_1(t_1)p_1 + \cdots + l_N(t_1)p_N - P_{oct} \\ \vdots \\ l_1(t_I)p_1 + \cdots + l_N(t_I)p_N - P_{oct} \end{bmatrix} \leq \begin{bmatrix} 0 \\ \vdots \\ 0 \end{bmatrix} \quad (38)$$

The sum of the charging rates of all connected BEVs, p_n, must be less than or equal to the maximum output rate of the octopus charger, P_{oct}. Thus, the charging capacity of the octopus charger cannot be exceeded.

Note that the equations above are given for the case where each BEV has a single, continuous dwell time. In order to take the constraints of multiple dwell times into consideration (as in Section 5) the additional inequality constraints from Equations (5)-(8) must be applied to each BEV.

Each octopus charger generates the charging profiles for its assigned BEVs as an individual agent. Thus, this strategy is centralized at the octopus charger level with respect to the

BEVs. It is, however, decentralized at the parking structure level with respect to the octopus chargers. While this strategy can used by the parking structure to generate the charging profiles of all the BEVs in a centralized manner, it may not scale well in a computational sense. Thus, leading to a heavy computational burden on the parking structure operator [38]. The decentralized nature of this strategy allows for the computational burden to be distributed among the octopus chargers and results in fast running times.

The chances of satisfying all assigned BEVs are maximized if the octopus charger has access to all of the BEVs' driving patterns by the time that the first BEV connects to the octopus charger. If the driving patterns for all BEVs are known, then all BEVs will be satisfied when feasible. Thus, it is may preferable to run the protocol in the morning (like the ordered BEV-based protocol). If the driving patterns of all assigned BEVs are not known when the charging profiles are first generated, then the optimization problem above must be re-run when the other driving patterns become available. The worst case occurs when driving patterns are not known until the BEV connects to the octopus charger. This scenario is studied in Section 7.

As with BEV-based Optimization, an appropriate cost signal must be chosen in order to develop a final parking structure demand load with desirable characteristics. Details on various potential cost signals are described below.

6.4.2.1 Cost Signal

Cost Signal: Early Charging

The cost signal for the nonbinary variables, $C_n(t_i)$, depends each BEV (n) and each timeslot (t_i). While the cost signal is chosen to be distinct, these distinct values can be chosen such that priority is given to some BEVs over others. In this work, priority is always given to

BEVs that arrive first. The value n dictates the order of arrival of each BEV that is assigned to the octopus charger (i.e., BEVs with smaller values of n are prioritized).

If it is preferred to charge BEVs as early as possible, then earlier timeslots can be given a lower cost by satisfying Equation (39). Doing so, allows octopus chargers to accommodate charging for unexpected BEV arrivals that occur later in the workday. If priority for early charging is given to BEVs that arrive earlier, then the cost signal must be chosen such that Equation (40) is satisfied. Suppose that there are two timeslots, t_j and t_k such that $j < k$, and both BEV n and BEV $n + 1$ can charge during either of these timeslots. If any charging by the prioritized BEV (n) is done during the later timeslot (t_k) when it can be done during the earlier timeslot (t_j), then a higher cost will be incurred. Suppose, however, that BEV $n + 1$ can only charge during the earlier timeslot (t_j), if its charging needs are to be satisfied. If BEV n can charge during either timeslot, then BEV $n + 1$ is charged earlier so that all BEVs can satisfy their charging needs.

$$C_n(t_i) < C_n(t_{i+1}) \quad \forall\, i, n \tag{39}$$

$$|C_n(t_{i+1}) - C_n(t_i)| > |C_{n+1}(t_I) - C_{n+1}(t_1)| \quad \forall\, i, n \tag{40}$$

A sample cost signal, that satisfies Equations (39) and (40), for three BEVs ($N = 3$) and with four universal timeslots ($I = 4$) is given in Equation (41). Note that the true values of the cost signal are not relevant. Only their values relative to each other are important. For example, multiplying C_n by a constant will still satisfy Equations (39) and (40) above.

$$C = [C_1(t_i)|C_2(t_i)| \dots |C_N(t_i)] = [18\ 34\ 50\ 66 \mid 5\ 9\ 13\ 17 \mid 1\ 2\ 3\ 4] \tag{41}$$

Cost Signal: Valley Filling

As previously mentioned, the true values of the cost signal are not relevant. Only their values relative to each other are important. Reordering the cost signal of each individual BEV Equation (41) in any order will always satisfy Equation (40). Thus, the cost signal of each individual BEV can be rearranged to develop a final demand profile with desirable characteristics (i.e., Valley Filling). The smart-charging strategy for the BEV-based Optimization Strategy can be used to perform Valley Filling when the cost signal is an aggregation of the initial parking structure baseload and all previously scheduled BEV charging profiles (represented by $C_{load}(t_i)$). If each BEV charging profile is rearranged such that Equations (40) and (42) are satisfied, then the cost signal can be used to perform valley filling. By changing the values of C_n, such that the lowest values of each BEV's cost signal coincide with the lowest values of the current parking structure demand load, the valleys in the demand load can be filled.

$$C_n(t_j) < C_n(t_k) \quad iff \quad C_{load}(t_j) < C_{load}(t_k) \quad \forall\, j,k,n \tag{42}$$

A sample parking structure demand load (averaged at each timeslot) is given in Equation (43). A sample cost signal that satisfies Equations (40) and (42) is given in Equation (44). Note that all BEVs will attempt to charge during timeslot t_3 if they are available. Priority is given to the earliest arrivals, but it can be changed as needed.

$$C_{load}(t_i) = [C_{load}(t_1) \;\; C_{load}(t_2)\; C_{load}(t_3)\; C_{load}(t_4)] = [100\ 90\ 60\ 70] \tag{43}$$

$$C = [C_1|C_2|\ldots|C_N] = [66\ 50\ 18\ 34 \mid 17\ 13\ 5\ 9 \mid 4\ 3\ 1\ 2] \tag{44}$$

Cost Signal: Augmented Cost

The cost signal for Valley Filling above reduces peaks throughout the day. In some cases, however, it may be beneficial to avoid charging during certain periods of the day. This could be due to high electricity prices, limitations in the local charging infrastructure, or the need to reduce the load during scheduled maintenance. With minor modifications to the initial parking structure demand load, $C_{load}(t_i)$, the Octopus Charger-based MILP Strategy can steer demand away from (or towards) specific hours. The initial load used for Valley Filling is artificially increased during certain times to generate an augmented load (and, thus, augmented cost signal). The artificially high cost signal, thus, discourages BEVs from charging during those times.

For example, if we wish to avoid charging during the third timeslot, then the value of $C_{load}(t_3)$ can be increased from 60 to 1,000. A simple application of this strategy is avoiding charging during the more expensive On-Peak hours of Time-Of-Use (TOU) electricity rate plans. Thus, the demand load, $C_{load}(t_i)$, used by octopus chargers is artificially increased during On-Peak hours in order to reduce electricity costs for the parking structure.

6.4.2.2 Visual Example of Characteristics

A simple example of the MILP octopus charger-based optimization is presented in Figure 14. The three sample BEVs from Table 8 are assigned to an octopus charger with a maximum output rate of 15 kW. The cost signal used is set up for early charging (i.e., Equations (39) and (40) are satisfied). All BEVs charge at their maximum charging rate except for one timeslot. A simple post-processing can be performed on the non-maximum charging timeslot such that charging during said timeslot is done at the maximum rate. For example, the charging done by BEV #1 between 8:00 and 9:00 am is about 1 kWh. This can be accomplished by charging the at

6.6 kW for about 9 minutes instead. Doing so, however, leaves a large gap between 8:10 and 9:00 am that goes unused. Such gaps, however, can be reduced choosing a smaller timeslot resolution (e.g., 15 minutes instead of one hour). In cases where valley filling is performed, the post-processing can be performed such that the 9 minutes of 6.6 kW charging above are set to fill the valleys of non-maximum timeslots.

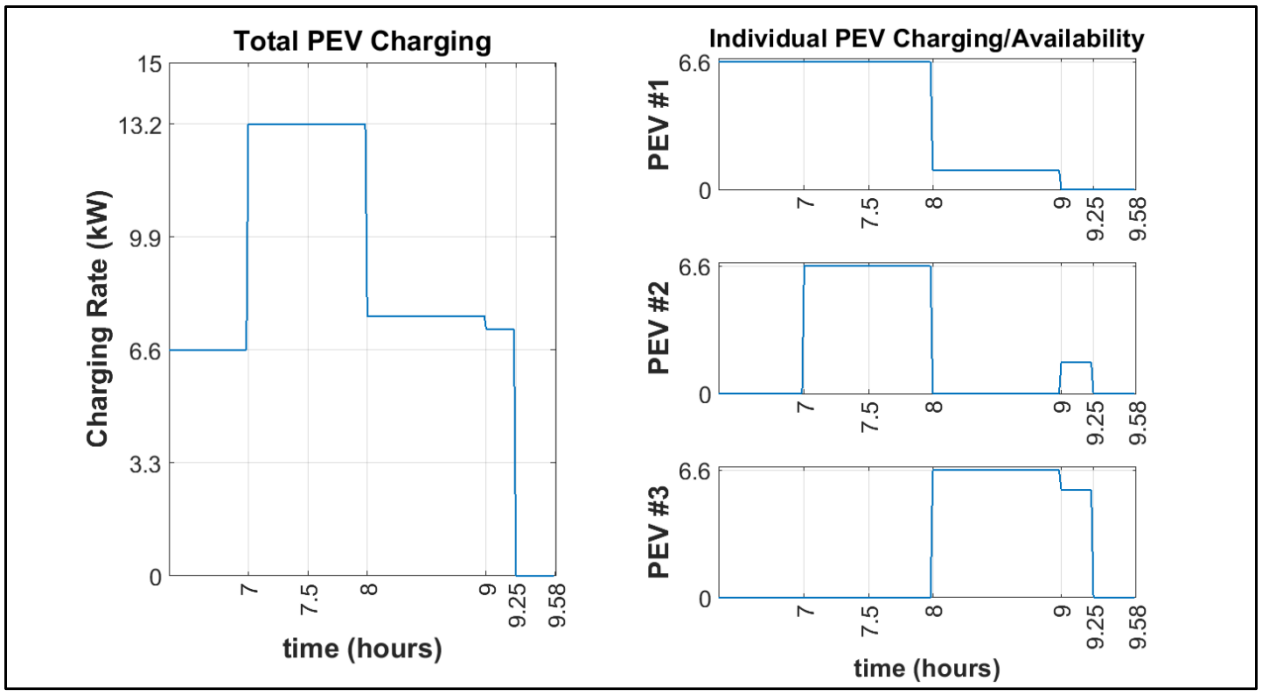

Figure 14 Mixed integer linear programming solution for octopus charger-based optimization for a 15 kW octopus charger with the BEVs from Table 8

6.5 Results

Results for the Octopus Charger-based MILP Strategy are presented in the following sections. The same parking structures and BEVs from Section 5 were tested under the same conditions (i.e., same driving patterns, same baseloads, etc.). For more details see Section 4. Unless stated otherwise, all charging scenarios presented here assume that all BEVs attempt to

get the highest possible SOC by the end of the day (i.e., they attempt to get a 100% SOC when possible). All BEVs charge at a rate of 3.6 kW. All 4-Cable and 8-Cable octopus chargers have maximum output rates of 3.6 kW and 7.2 kW, respectively. Thus, 4-Cable octopus chargers can charge one BEV at a time and 8-Cable octopus chargers can charge two BEVs at a time.

6.5.1 Octopus Charger Assignment

The Sorted-Balance algorithm was used in conjunction with the Octopus Charger-based MILP Strategy to find the number of 4-Cable and 8-Cable octopus chargers needed to satisfy the charging requirements of 100 and 500 BEV parking structures. The minimum number of octopus chargers were initially used (i.e., 25 4-Cable or 13 8-Cable chargers for a 100 BEV parking structure). If all the BEVs received their requested charge (b_n in Equation (12)), then that number of octopus chargers was used for that parking structure. If at least one BEV did not receive its requested charge, then the number of octopus chargers was increased iteratively until a feasible assignment was found.

The Sorted-Balance algorithm was evaluated for 50 simulated parking structures with two cases. For the first case, the BEVs' requested charge (b_n) was balanced among the octopus chargers. For the second case, the BEVs' Inverse Flexibility Ratio was balanced among the octopus chargers. The number of octopus chargers needed to satisfy 50 simulated 100 BEV parking structures are presented in Table 10. The largest number of octopus chargers needed is 27, which is only two more octopus chargers than the minimum. On average, balancing the Inverse Flexibility Ratio results in the lowest number of required octopus chargers.

Table 10 Number of octopus chargers needed for 50 simulated 100-BEV parking structures

		Min.	Avg.	Max.
Four-Cable	Sorted-Balance: Requested Charge	25	25.14	26
	Sorted-Balance: Inverse Flex. Ratio	25	25.1	27
Eight-Cable	Sorted-Balance: Requested Charge	13	13	13
	Sorted-Balance: Inverse Flex. Ratio	13	13	13

The number of octopus chargers needed to satisfy 50 simulated 500 BEV parking structures are presented in Table 11. The largest number of octopus chargers required is 130, which is only five more than the minimum. Note that the minimum number of bins satisfied all cases when the Inverse Flexibility Ratio was balanced among 8-Cable octopus chargers. This is likely because it is easier for a "problematic" BEV (with large charging demands or low flexibility) to cause a disruption for a 4-Cable octopus charger than an 8-Cable octopus charger. Thus, if there is a mixture of 4-Cable and 8-Cable octopus chargers, then it is better to place more problematic BEVs in 8-Cable chargers. In this work, however, we focus on the two extremes where all chargers have 4 cables or 8 cables.

Table 11 Number of octopus chargers needed for 50 simulated 500-BEV parking structures

		Min.	Avg.	Max.
Four-Cable	Sorted-Balance: Requested Charge	125	125.86	130
	Sorted-Balance: Inverse Flex. Ratio	125	125.48	129
Eight-Cable	Sorted-Balance: Requested Charge	63	63.02	64
	Sorted-Balance: Inverse Flex. Ratio	63	63	63

In general, balancing the Inverse Flexibility Ratio among the octopus chargers requires less chargers. Since these results only check for the feasibility of satisfying all BEV charging requests, any cost signal can be combined with the Octopus Charger-based MILP Strategy. Thus, the same number of octopus chargers will be used if we wish to perform valley filling or if we wish to shift BEV charging to the morning (i.e., the Augmented Cost Signal).

A key observation of the Sorted-Balance assignment is that while a set number of octopus chargers may satisfy a parking structure, adding another octopus charger will affect the assignment. This can potentially lead to an assignment that does not satisfy all BEVs. This can be overcome by developing more specialized assignment algorithms. These details are omitted to focus on the main concepts of this work and are suggested as future works

6.5.2 Octopus Charger-Based MILP: Early Charging

Representative results from parking structure #2 (out of 50 simulated parking structures) are presented in the following sections. The Octopus Charger-based MILP Strategy from Section 6.4.2 was used to set charging for BEVs to occur as early as possible. Thus, allowing BEVs to accommodate unexpected arrivals to the parking structure later in the day. Results for the Early Charging strategy are presented in Figure 15. Cases where both 4-Cable and 8-Cable octopus chargers were installed at the parking structure were studied. The maximum load experienced in both cases is slightly above 400 kW. The profile of the demand load has a saw-tooth pattern with peaks at the top of the hour. This is caused by the simple post-processing done to charge BEVs at their maximum rate during non-maximum timeslots (see Section 6.4.2.2). This saw-tooth pattern

can be reduced by using a finer resolution when generating the timeslots for the octopus charger (i.e., using 15 minutes instead of an hour).

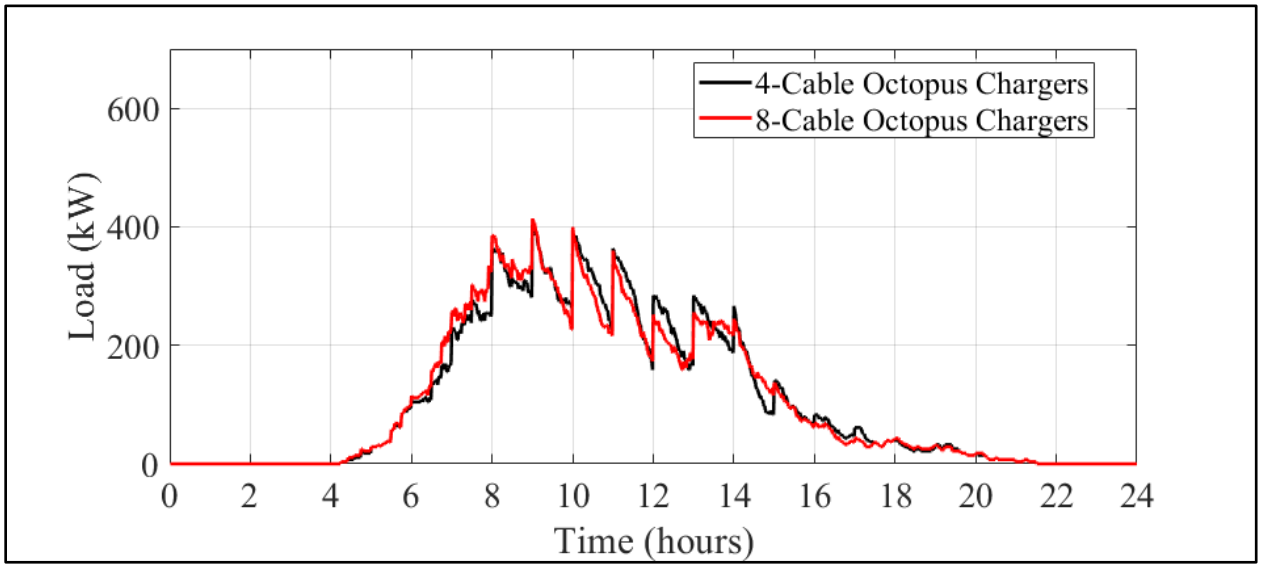

Figure 15 Early Charging demand profiles for a simulated parking structure with 500 BEVs attempting to get a full charge and no baseload

6.5.3 Octopus Charger-Based MILP: Valley Filling

The Octopus Charger-based MILP strategy from Section 6.4.2 can be used to perform Valley Filling when the cost signal is an aggregation of the initial parking structure baseload and all previously assigned BEV charging profiles. Results for the Valley Filling strategy are given in Figure 16. The maximum peaks experienced when using 4-Cable and 8-Cable octopus chargers were both about 190 kW for 500 BEV parking structures. This is comparable to the 184 kW peaks generated when the BEV-based strategy was paired with ordering via Flexibility Ratio in Section 5.6.2.

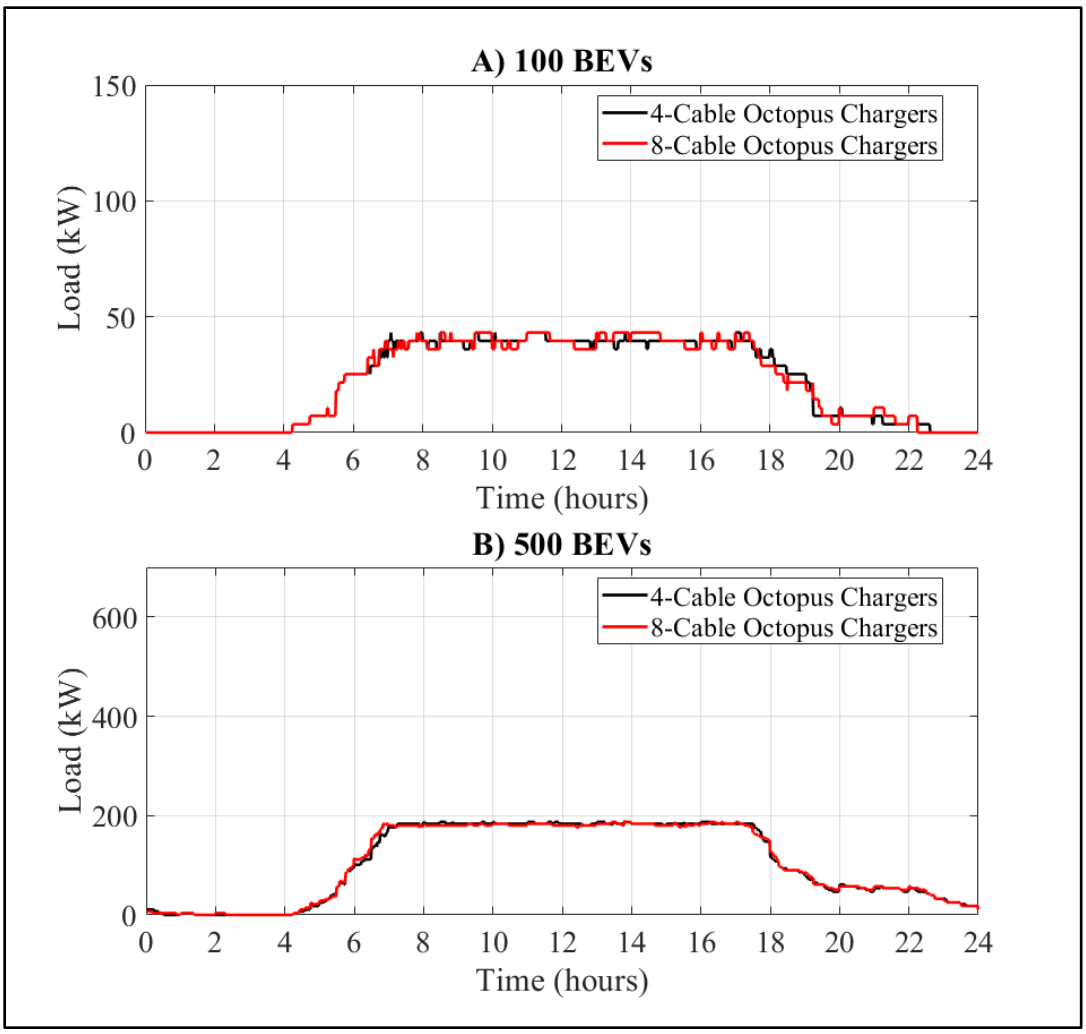

Figure 16 Valley Filling demand profiles for a simulated parking structure with A) 100 and B) 500 BEVs attempting to get a full charge and no baseload

6.5.4 Octopus Charger-Based MILP: Augmented Cost Signal

Simulation results for the Augmented Cost Signal Strategy with 2018 On-Peak-Hours (12 pm – 6 pm) and 2019 On-Peak Hours (4 pm – 9 pm) are presented in Figure 17 and Figure 18, respectively. The load during On-Peak Hours is lowered in both cases. As in Section 5.6.3, the Augmented Cost Signal strategy avoids charging during the 2019 On-Peak hours more effectively than with the 2018 On-Peak hours. This is because 2019 On-Peak hours (4 pm – 9

pm) occur during the decline of BEV availability at work. A small dip is seen in Figure 17 as 6 pm approaches. This is because a subset of BEVs that can avoid charging during On-Peak hours shift their charging after 6 pm.

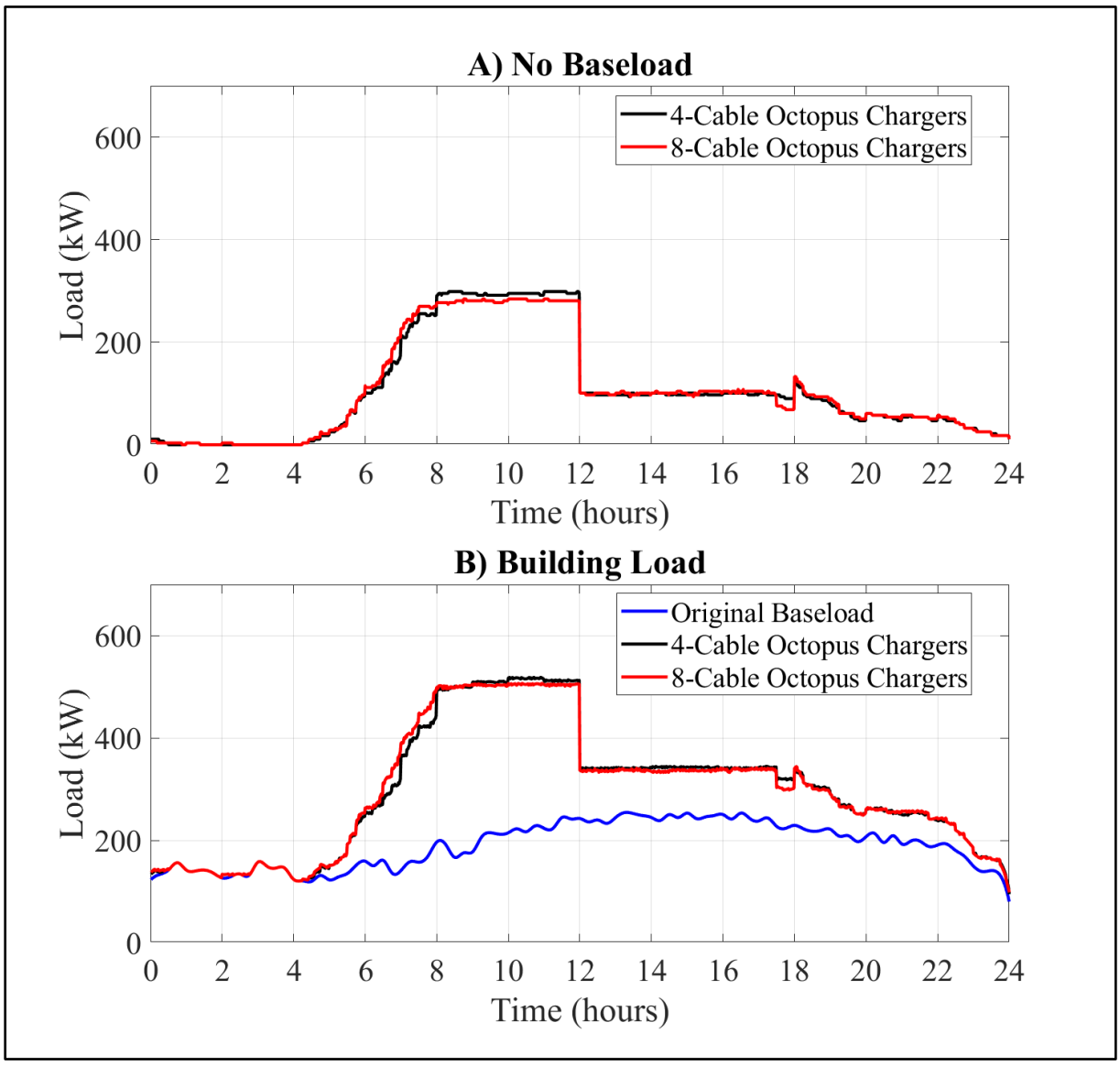

Figure 17 Augmented Cost Signal demand profiles with 2018 On-Peak Hours for a simulated parking structure with 500 BEVs attempting to get a full charge and no initial load

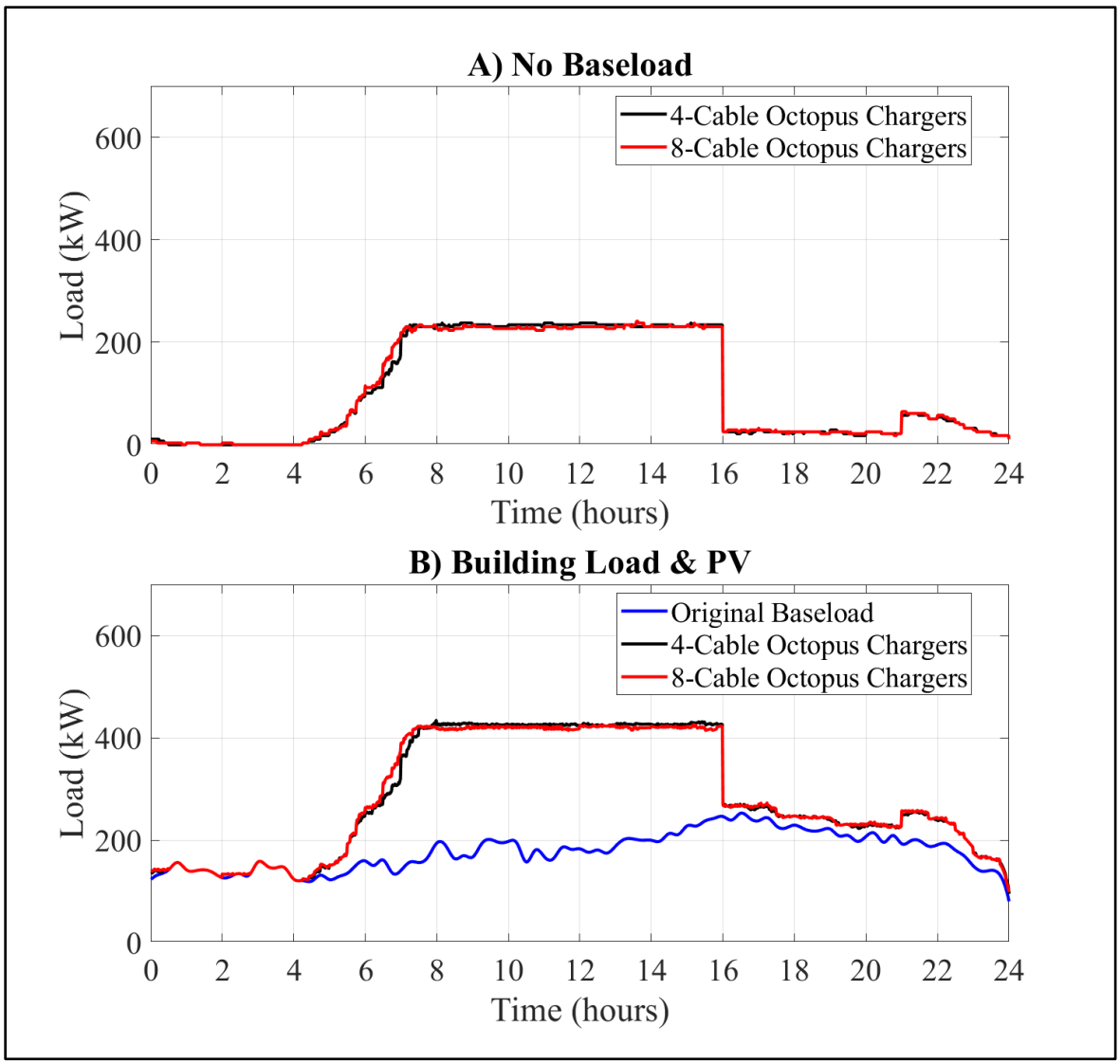

Figure 18 Augmented Cost Signal demand profiles with 2019 On-Peak Hours for a simulated parking structure with 500 BEVs attempting to get a full charge and no initial load

6.5.5 Effects on Parking Structure Demand Load

The maximum 24-hour loads experienced by 500 BEV parking structures are presented in Figure 19-A. The respective values from Uncontrolled Charging in Section 5 are included for comparison. Early Charging reduces the maximum load compared to Uncontrolled Charging but

has the highest load among the smart-charging strategies. Valley Filling results in the lowest loads in all cases, demonstrating its peak reduction capabilities. In all cases, the Octopus Charger-based MILP Protocol resulted in reduced loads when compared with Uncontrolled Charging.

The maximum On-Peak loads experienced by 500 BEV parking structures are given in Figure 19-B. The Augmented Cost Signal strategy reduces the maximum On-Peak load when compared with all other strategies. The flattening nature of the Valley Filling strategy shifts charging and results in the highest On-Peak load for all cases with 2019 On-Peak hours. Early charging results in the highest On-Peak loads for all cases with 2018 On-Peak hours.

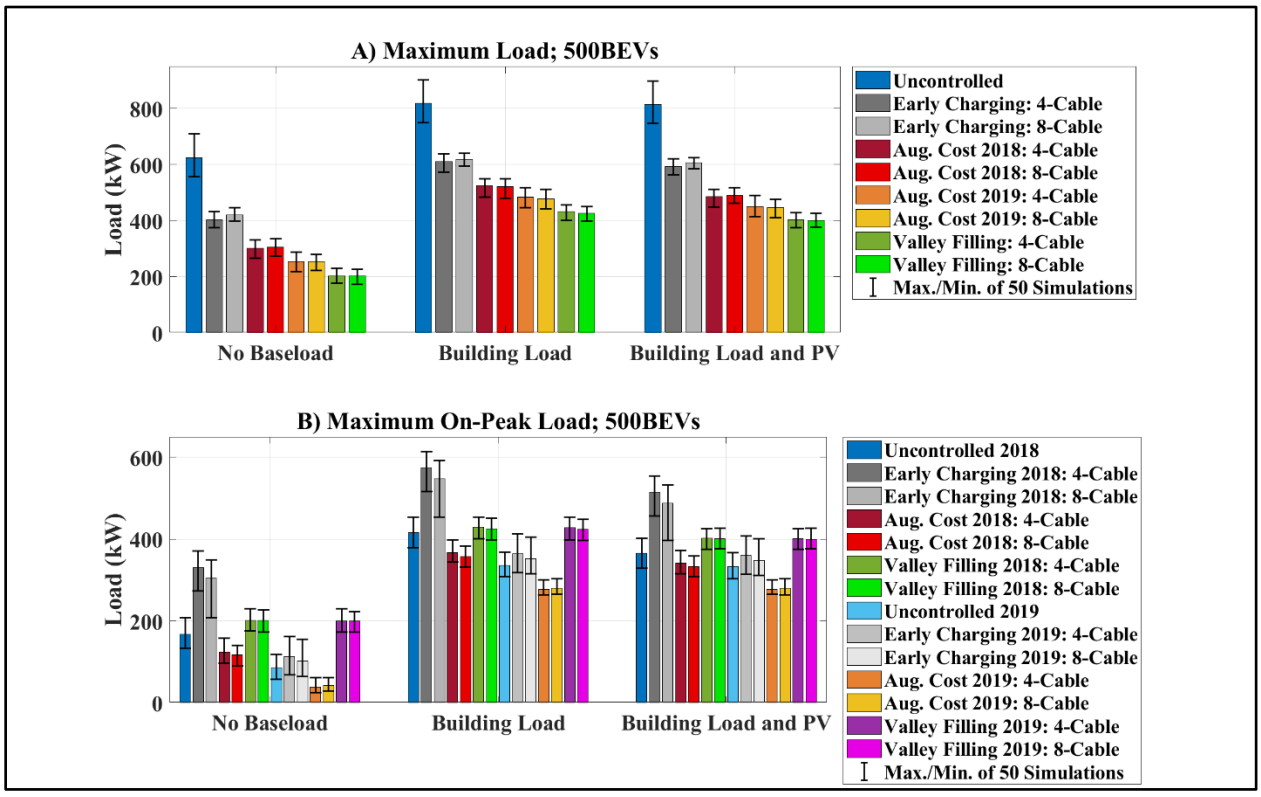

Figure 19 A) Maximum 24-hour load and B) Maximum On-Peak load for 50 simulated parking structures with 500 BEVs attempting to get a full charge with the Octopus Charger-based MILP Protocol

6.5.6 Effects on Electricity Costs

The monthly cost of electricity was calculated for each parking structure demand load. For simplicity, the demand load for each simulation was assumed to be the same for each weekday of the month. It was also assumed that the month contained 20 weekdays and that there was no charging or electricity usage during the weekends. The fixed monthly charge associated with each rate schedule was also included in the calculated costs.

For simplicity and consistency, electricity costs for all parking structures were calculated with the corresponding TOU-GS-3 summer rate schedule, except for 100 BEV parking structures without a baseload. For more details on the rate plans used, see Section 4.5 and 5.8.

The monthly electricity costs for the simulated parking structures are given in Figure 20. The Valley Filling and Augmented Cost Signal strategies reduce monthly electricity costs in all cases where 2018 On-Peak hours are used. With 2019 On-Peak Hours, however, Valley Filling results in monthly costs that are comparable to those of Early Charging. As in Section 5.8, this occurs because Valley Filling shifts charging to the more expensive On-Peak Hours.

Average monthly savings between 32-40% are seen for all cases with no baseload, except for Early Charging and Valley Filling with 2019 rates (compared to Uncontrolled Charging). Note that these savings are comparable to those seen when the BEV-based strategy was paired with ordering via Flexibility Ratio (34-40%) in Section 5.6.2.

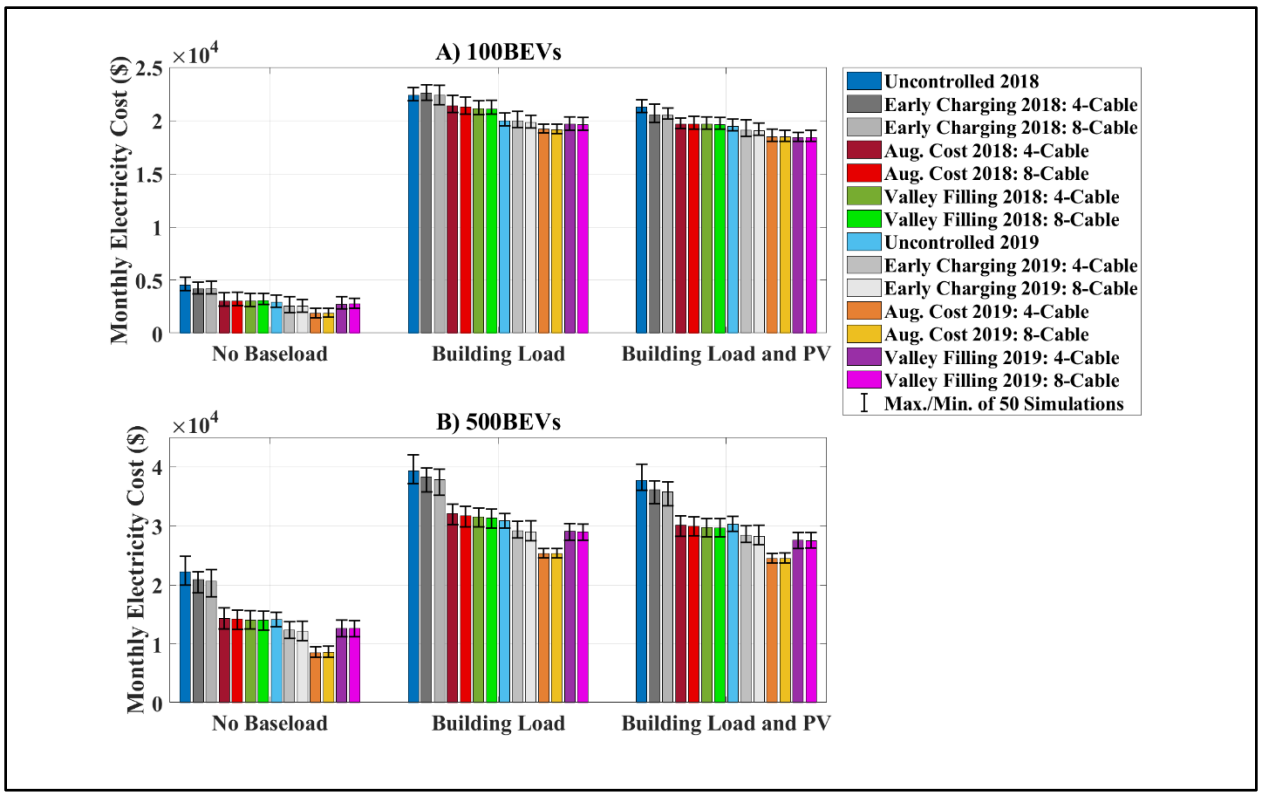

Figure 20 Estimated monthly cost of electricity for 50 simulated parking structures with A) 100 and B) 500 BEVs attempting to get a full charge with the Octopus Charger-based MILP Protocol

6.6 Conclusion

A mixed integer linear programming strategy that allows octopus chargers to independently generate charging profiles for their assigned BEVs is proposed in this work. By allowing the octopus charger to act as independent agents, the computational burden is distributed among all chargers. With simple modifications to the cost signal, this smart-charging strategy can be used to charge BEVs as early as possible, reduce parking structure load variation (Valley Filling), or shift charging away from On-Peak hours (Augmented Cost Signal). The Augmented Cost Signal strategy significantly reduced monthly electricity costs in all cases, when compared with Uncontrolled Charging from Section 5.3.1 and the Early Charging strategy proposed here. Furthermore, savings from the Augmented Cost Signal strategy in this work were

comparable to those seen when the BEV-based strategy was paired with ordering via Flexibility Ratio in Section 5.6.2.

A simple and well-known algorithm is used to assign BEVs to octopus chargers. In all cases, the assignment algorithm required less than five extra 4-Cable octopus chargers to satisfy the charging demands of 50 simulated parking structures. No extra octopus chargers were needed when using 8-Cable octopus chargers. By reducing the number of octopus chargers needed, the proposed assignment strategy can reduce investments needed for parking structures' charging infrastructure. Such an assignment, however, requires the driving patterns of all BEVs before the protocol is performed. In some cases, privacy may not be a high priority. For example, schedules for delivery trucks and public buses are generally known. Thus, this charging strategy can be used to generate the charging schedules for the entire fleet of a bus or delivery company. If driving schedules are not known until each BEV arrives, then the assignments used here may not be feasible. In this case, driving patterns are obtained in real time and more octopus chargers may be needed. Such a real-time charging strategy is studied in the following section.

The comprehensive smart-charging protocol presented in this work can be used to reduce electricity and charging infrastructure costs associated with workplace charging, while increasing the utilization of renewable resources. Renewable energy is uncertain and electricity prices can vary significantly across regions, adding to the need for smart-charging protocols that are robust enough to deal with these variations (i.e., optimization based vs. ad-hoc).

7 Real-Time Octopus Charger-Based Optimization

7.1 Introduction

Access to electric vehicle chargers can mitigate the negative effects of range anxiety and charger anxiety. In [5] it is found that increases in charging station deployment result in increases of EV sales. In [29] a survey found that 71.7% of participants placed a high degree of importance on having recharging facilities at work or near businesses they frequent, when considering a future PHEV purchase. Some BEV manufacturers have capitalized on this by donating charging stations to qualifying businesses and property owners [34]. Significant investments in charging infrastructure would, however, be required if single-cable charging stations remain the standard. In Section 4.2, it is shown that single-cable charging stations go unused for large portions of time (when BEVs are connected, but not charging). By charging multiple BEVs with a single charging station, utilization rates can be improved. Thus, resulting in more cost-effective infrastructure investments for workplace parking structures.

In [30], “octopus chargers” are proposed as a cost-effective solution for charger anxiety. Octopus chargers are designed to contain several cables, such that a single octopus charger can charge multiple PEVs. Thus, octopus chargers allow workplace parking structure operator to reduce charging infrastructure investments by reducing the number of needed charging stations. Some utility companies offer Demand Response programs that provide incentives for reducing electricity usage when the demand is high [39]. Thus, smart-charging strategies for octopus chargers can be used in conjunction with demand response programs such that savings businesses (with large fleets of PEVs) are maximized.

In Section 6, it is necessary to execute the Octopus Charger-based MILP Protocol in the morning (before the first BEV arrives). To do this, the parking structure operator must gather the charging flexibility of all participating BEVs ahead of time. This approach requires somewhat more complex interaction between the BEVs and the octopus chargers but provides significant benefits. In some cases, however, drivers may be unable or unwilling to share their expected driving patterns ahead of time. In this case, the driving patterns of each BEV are obtained in real time as each car connects to its assigned octopus charger. In order to do this, an assignment strategy that does not depend on the BEV's driving patterns must be used. Furthermore, eliminating the communication requirements from Section 6 allows octopus chargers to be installed in more destination-charging locations that can service multiple BEVs (e.g., apartment buildings, shopping malls, universities).

In this chapter, a comprehensive Real-Time Octopus Charger-based mixed integer linear programming (MILP) protocol for workplace charging is proposed. The protocol is developed with the goal of reducing infrastructure and operational costs for a workplace parking structure, while meeting BEV drivers' charging needs. The following are the main contributions of this work. **1)** A simple and well-known algorithm is used to assign BEVs to octopus chargers, without prior information about the BEVs. **2)** A smart-charging strategy, that allows octopus chargers to schedule charging for their assigned BEVs in real time is proposed (see Section 7.2). The **Real-Time Octopus Charger-based MILP Protocol** requires that drivers share their expected driving patterns with their assigned octopus chargers. Thus, user privacy is not maintained. This protocol, however, eliminates communication requirements from the BEV-based Optimization Protocol and the Octopus Charger-based MILP Protocol. Once the driver parks, they can simply input their expected driving patterns via the octopus charger's user

interface. The Real-Time Octopus Charger-based MILP strategy manages the parking structure demand load by allowing octopus chargers to act as individual agents. Thus, distributing the computational burden among the octopus chargers.

7.2 Overview of Real-Time Octopus Charger-Based Optimization Protocol

For this charging protocol, it is assumed that a set number of Octopus Chargers with a set number of cables are installed in the parking structure. As each BEV arrives to the parking structure, it is assigned to the octopus charger with the most flexibility (without any prior information about the BEV). As the driver connects their BEV to the octopus charger, the BEV's expected driving patterns for the day become available to the octopus charger. If it is the first BEV to connect, then Octopus Charger-based MILP Strategy (from Section 6.4.2) is executed on the lone BEV. If other BEVs were previously connected, then the connected BEVs cancel their charging profile for the rest of the day and the Octopus Charger-based MILP Strategy is executed on all BEVs whose driving patterns have already been provided. Thus, updating the charging profiles of all previously connected BEVs. The octopus charger then sends the sum of all the charging profiles (along with the cancelled profiles) to the parking structure operator, where they are aggregated for an updated cost signal. The process is repeated with the next BEV to arrive, until all BEV charging profiles have been generated.

As each BEV arrives, it is assigned to the octopus charger with the smallest workload, that has available cables. The driver's assignment can be provided by a parking structure attendant, by electronic signs, or via short-range communication with the BEV. Once the BEV is parked, the driver can input their expected driving patterns via the octopus charger's user interface. Of course, if the BEV can communicate with the octopus charger (via the cable or

short-range communication), then the driver can input their expected driving patterns into their BEV computer or a smart-phone application.

7.3 Octopus Charger Assignment via Greedy-Balance

In Section 6.3.1, BEVs are assigned to octopus chargers ahead of time by collecting the Inverse Flexibility Ratios of all of the participating BEVs. The Sorted-Balance algorithm does this by queueing all Inverse Flexibility Ratios in decreasing order and then assigning them to the octopus chargers with the smallest sum of Inverse Flexibility Ratios. Since BEVs must me assigned as they arrive, with no prior information, a variation of the Sorted-Balance algorithm must be used.

Greedy-Balance is another well-known approximation algorithm that can be used to find solutions to the Load Balancing Problem [35]. The structure of Greedy-Balance is generally the same as Sorted-Balance, except that the loads (i.e., Inverse Flexibility Ratios) are not initially queued. Thus, Greedy-Balance can be set to assign BEVs in no particular order. The Greedy-Balance algorithm can find solutions to the Load Balancing Problem such that $L \leq 2L^*$ [35]. See Section 6.3.1 for more details.

The Greedy-Balance algorithm above can be used to assign BEVs to octopus chargers such that charging flexibility is distributed among the chargers. By distributing flexibility, the octopus chargers are less constrained when generating the charging profiles for their assigned BEVs. The guarantee that the Greedy-Balance solution is close to the optimal solution ($L \leq 2L^*$) is maintained only if the octopus chargers are assumed to have an unlimited number of cables. Since a limit is placed on the number of cables per octopus charger here, the assignment could result solutions above the guaranteed limit.

7.4 Results

Results for the Real-Time Octopus Charger-based MILP Strategy are presented in the following sections. The same parking structures and BEVs from Sections 5 and 6 were tested under the same conditions (i.e., same driving patterns, same baseloads, etc.). For more details see Section 4. All charging scenarios presented here assume that all BEVs attempt to get the highest possible state of charge by the end of the day (i.e., they attempt to get a full charge when possible). All parking structures in the following results were simulated without a baseload. All BEVs charge at a rate of 3.6 kW and 8-Cable octopus chargers have a maximum output rate of 7.2 kW (i.e., 8-Cable octopus chargers can charge two BEVs at a time).

7.4.1 Octopus Charger Assignment via Greedy-Balance

The Greedy-Balance algorithm was used to assign BEVs to octopus chargers in real time. The Octopus Charger-based MILP Strategy was used to find the number of chargers needed to satisfy the charging demands of all BEVs in 100 and 500 BEV parking structures. The minimum number of octopus chargers were initially used (i.e., 25 4-Cable or 13 8-Cable chargers for a 100 BEV parking structure). If all charging requests were satisfied, the number of octopus chargers was determined for the parking structure. If at least one BEV did not receive its full requested charge, then the number of octopus chargers was increased iteratively until a feasible assignment was found.

The Greedy-Balance algorithm was used to assign BEVs to octopus chargers in 50 simulated parking structures, such that the flexibility among octopus chargers was distributed evenly. It was found that several cases with 4-Cable octopus chargers resulted large numbers of octopus chargers. Specifically, several 500 BEV parking structures required more than 200 4-

Cable octopus chargers; an amount larger than those required for the BEV-based optimization strategies in Section 5. Results for the real-time assignment of 4-Cable octopus chargers are, thus, omitted from this work.

While the Greedy-Balance algorithm resulted in large numbers of 4-Cable octopus chargers, it should be noted that Greedy-Balance is a general algorithm that is not tailored for octopus charger assignment. Several modifications can be made to the Greedy-Balance algorithm to improve its performance when dealing with 4-Cable octopus chargers. For example, the Inverse Flexibility Ratio and requested charging can be used to limit the BEVs that can use octopus chargers. If a BEV has very little flexibility and will be charging for a long period, then said BEV might be better suited with a single-cable charging station. These details are omitted to focus on the main concepts of this work and suggested as future works.

The number of 8-Cable octopus chargers needed to satisfy 50 simulated 100 BEV parking structures are presented in Table 12. The largest number of octopus chargers needed is 17 and occurs when Valley Filling is performed. On average, only one extra octopus charger is required to satisfy the charging demands of all BEVs.

Table 12 Number of 8-Cable octopus chargers needed for 50 simulated 100-BEV parking structures

Charging Strategy	No Baseload		
	Min.	Avg.	Max.
Real-Time: Early Charging	13	13.12	15
Real-Time: Aug. Cost Signal (2018)	13	13.22	15
Real-Time: Aug. Cost Signal 2019	13	13.28	16
Real-Time: Valley Filling	13	13.78	17

The number of 8-Cable octopus chargers needed to satisfy 50 simulated 500 BEV parking structures are presented in Table 13. The largest number of octopus chargers required is 101; which occurs when Valley Filling is performed. This occurs because some BEVs, that arrive early, delay charging to fill valleys in the afternoon. By doing so, they do not charge earlier in the day and decrease the charging flexibility of the octopus charger when new arrivals connect. All other strategies, on the other hand, shift charging to the morning and require less octopus chargers. On average, less than 3 extra octopus chargers are required for all charging strategies, except for Valley Filling.

Table 13 Number of 8-Cable octopus chargers needed for 50 simulated 500-BEV parking structures

Charging Strategy	No Baseload		
	Min.	Avg.	Max.
Real-Time: Early Charging	63	63.96	74
Real-Time: Aug. Cost Signal (2018)	63	65.7	72
Real-Time: Aug. Cost Signal (2019)	63	65.44	70
Real-Time: Valley Filling	64	78.56	101

7.4.2 Real-Time Octopus Charger-Based MILP: Early Charging

Representative results from parking structure #2 (out of 50 simulated parking structures) are presented in the following sections. The Real-Time Octopus Charger-based MILP Protocol was used to set BEV charging as early as possible, to allow octopus chargers to accommodate unexpected arrivals. Results for the Real-Time Early Charging strategy are presented in Figure 21. As previously mentioned, only cases with 8-Cable octopus chargers and no initial baseload were studied. The maximum load experienced is about 425 kW, which is slightly higher than the

loads seen in Figure 15 (about 400 kW). The saw-tooth pattern in the demand profile caused by the post-processing is seen here again (see Section 6.4.2.2 and Section 6.5.2). This saw-tooth pattern can be avoided by using a finer resolution when generating the timeslots for the octopus charger (i.e., using 15 minutes instead of an hour).

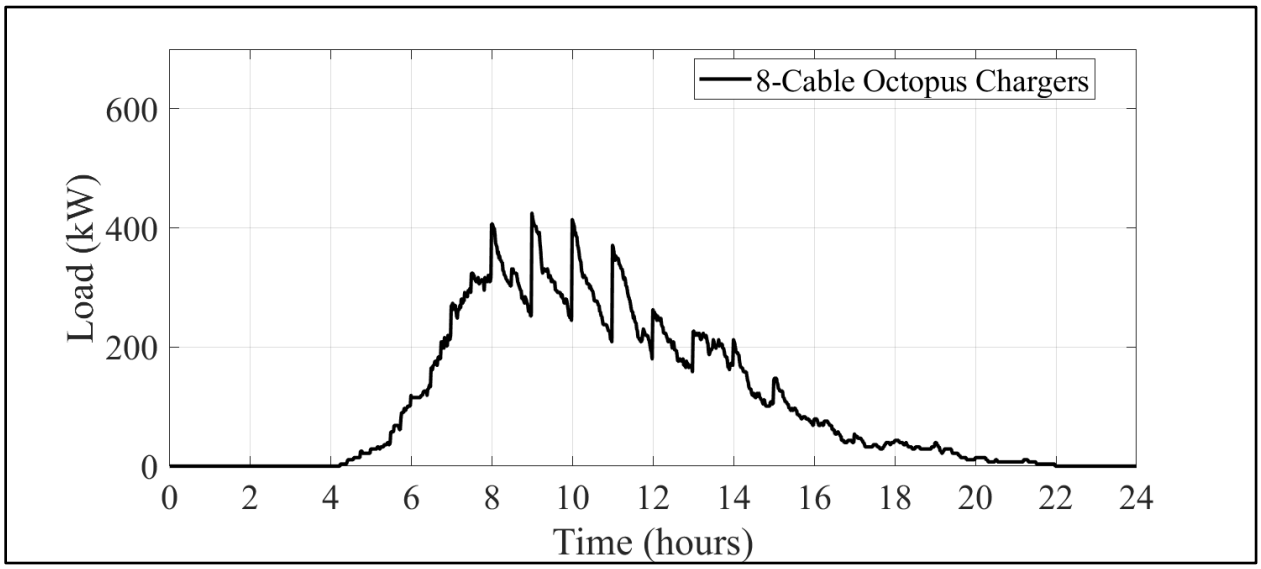

Figure 21 Real-Time Early Charging demand profile for a simulated parking structure with 500 BEVs attempting to get a full charge, no initial baseload, and 8-Cable octopus chargers

7.4.3 Real-Time Octopus Charger-Based MILP: Valley Filling

Results for the Real-Time Valley Filling strategy are given in Figure 22. The maximum peak experienced in this simulation is about 230 kW. This is significantly higher than the loads experienced when the Octopus Charger-based MILP Protocol is executed ahead of time (about 190 kW in Figure 16). This is, however, comparable to the 230 kW peaks experienced when the BEV-based strategy was ordered by arrival time in Section 5.6.2.

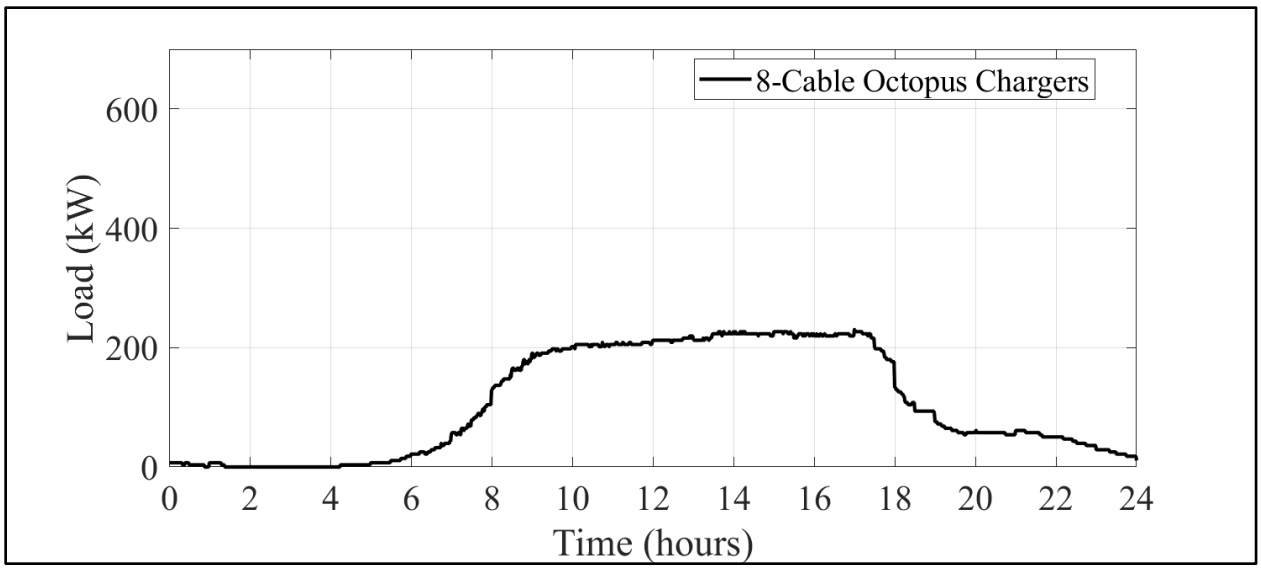

Figure 22 Real-Time Valley Filling demand profile for a simulated parking structure with 500 BEVs attempting to get a full charge, no initial baseload, and 8-Cable octopus chargers

7.4.4 Real-Time Octopus Charger-Based MILP: Augmented Cost Signal

Simulation results for the Real-Time Augmented Cost Signal Strategy 2018 On-Peak-Hours (12 pm – 6 pm) and 2019 On-Peak Hours (4 pm – 9 pm) are presented in Figure 23 and Figure 24, respectively. The load during On-Peak Hours is lowered in both cases. As in Section 5.6.3, the Augmented Cost Signal strategy avoids charging during the 2019 On-Peak hours more effectively than with the 2018 On-Peak hours. When compared to Figure 17 (when the protocol is executed ahead of time), the peaks are increased by 32 kW and 43 kW during On-Peak and non-On-Peak hours.

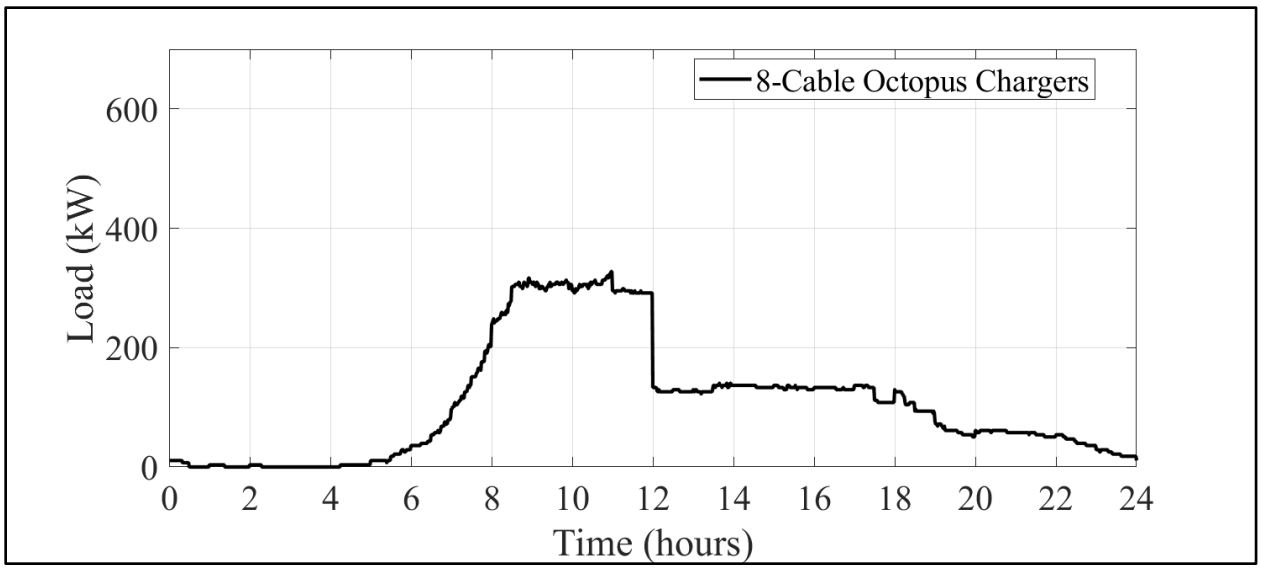

Figure 23 Augmented Cost Signal demand profile with 2018 On-Peak Hours for a simulated parking structure with 500 BEVs attempting to get a full charge, no initial baseload, and 8-Cable octopus chargers

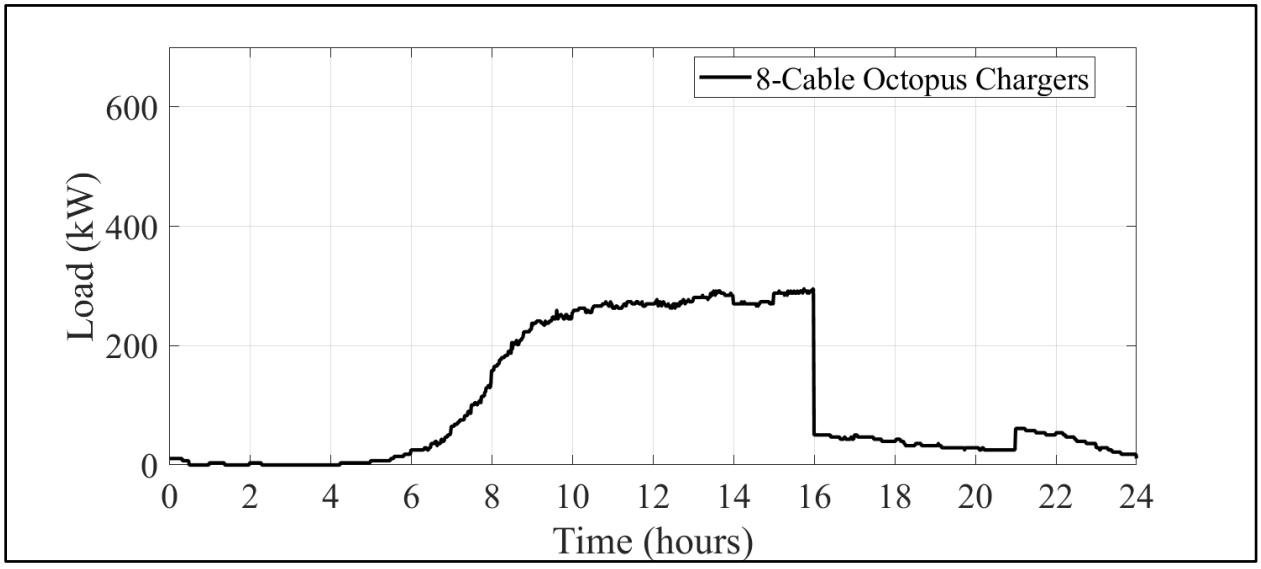

Figure 24 Augmented Cost Signal demand profile with 2019 On-Peak Hours for a simulated parking structure with 500 BEVs attempting to get a full charge, no initial baseload, and 8-Cable octopus chargers

7.4.5 Effects on Parking Structure Demand Load

The maximum 24-hour loads and the maximum On-Peak loads experienced by 500 BEV parking structures are presented in Figure 25-A and Figure 25-B, respectively. Similar trends to those found in Figure 19 (in Section 6.5.5) are found here. Valley Filling gives the lowest 24-hour loads and the Augmented Cost Signal strategy give the lowest On-Peak loads. The Real-Time strategies, however, result in higher loads in all cases when compared to the strategies in Section 6.5.5. Since the driving patterns of BEVs are not known until each BEV connects, the octopus charger cannot schedule charging as effectively. Thus, resulting in higher peaks during On-Peak and non-On-Peak hours.

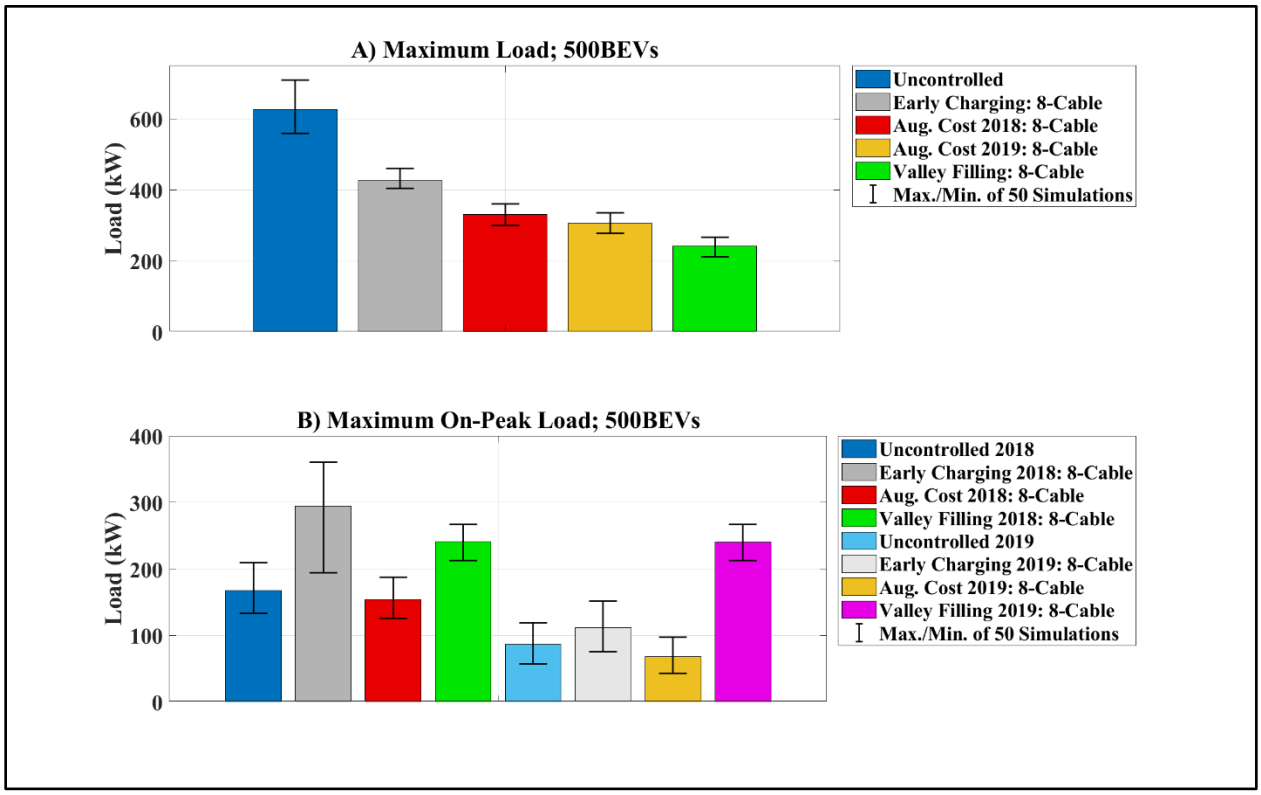

Figure 25 A) Maximum 24-hour load and B) Maximum On-Peak load for 50 simulated parking structures with 500 BEVs attempting to get a full charge with the Real-Time Octopus Charger-based MILP Protocol

7.4.6 Effects on Electricity Costs

The monthly cost of electricity was calculated for each parking structure demand load. For simplicity, the demand load for each simulation was assumed to be the same for each weekday of the month. It was also assumed that the month contained 20 weekdays and that there was no charging or electricity usage during the weekends. The fixed monthly charge associated with each rate schedule was also included in the calculated costs.

For simplicity and consistency, the TOU-GS-2 and TOU-GS-3 summer rate schedules were used to calculate the electricity costs for parking structures with 100 and 500 BEVs, respectively. The B and D versions of the above rate plans were used for 2018 and 2019 TOU schedules, respectively. For more details on the rate plans used, see Section 4.5 and 5.8.

The monthly electricity costs for the simulated parking structures are given in Figure 26. Valley Filling significantly increased monthly electricity costs for 2019 On-Peak Hours when compared to Early Charging. The Augmented Cost Signal strategy resulted in the lowest costs for all cases.

Average monthly savings between 25-30% are seen for all cases here, except for Early Charging and Valley Filling with 2019 rates (compared to Uncontrolled Charging). Note that these savings are comparable to those seen when the BEV-based strategy was paired with ordering via arrival time (20-31%) in Section 5.6.2. When compared to the strategies in Section 6.5.6, however, the Real-Time strategies resulted in higher costs for most cases.

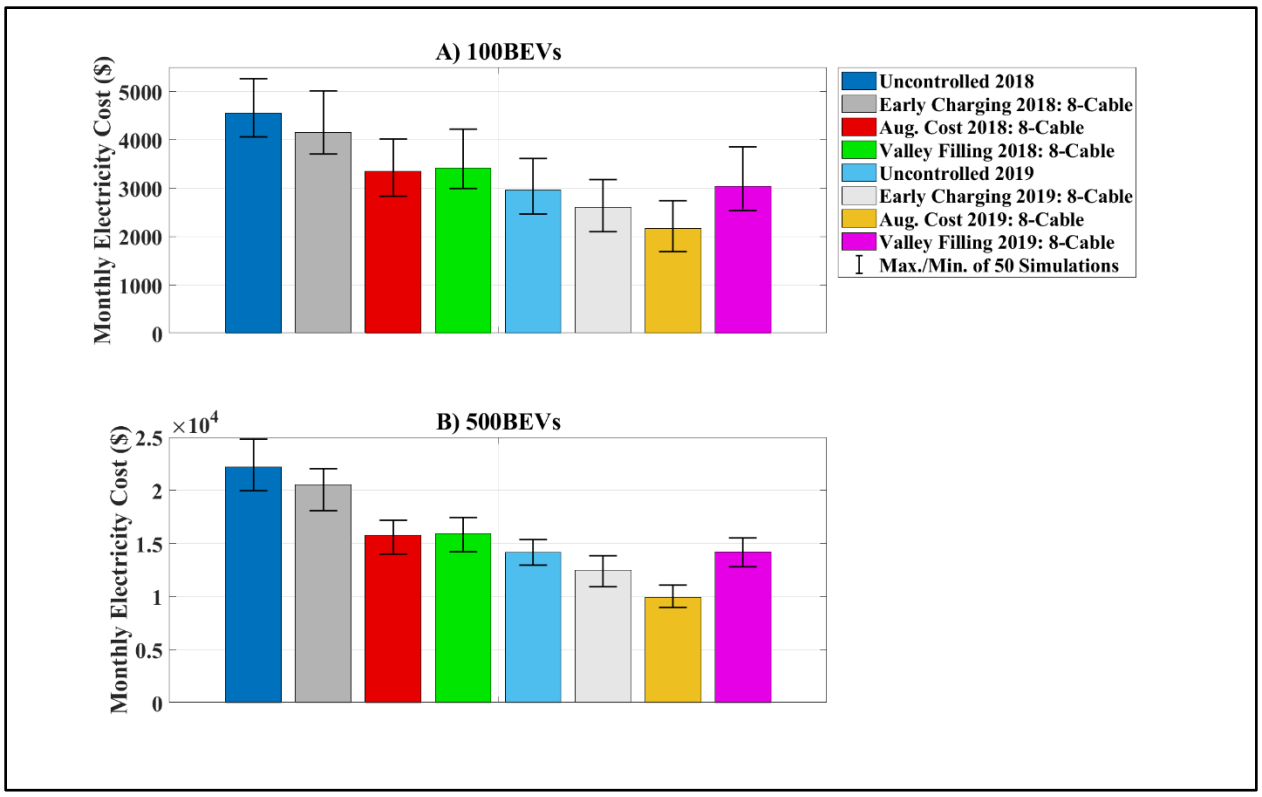

Figure 26 Estimated monthly cost of electricity for 50 simulated parking structures with A) 100 and B) 500 BEVs attempting to get a full charge with the Real-Time Octopus Charger-based MILP Protocol

7.5 Conclusion

A mixed integer linear programming strategy that allows octopus chargers to generate charging profiles for BEVs as they arrive in real time is proposed in this work. By scheduling charging in real time, the burden of communication with the parking structure operator (from Sections 5 and 6) is eliminated. Before drivers connect their BEV to their assigned octopus charger, they can simply enter their expected driving patterns into the octopus charger's user interface. Furthermore, by allowing the octopus charger to act as independent agents, the computational burden is distributed among all chargers. By contrast, centralized charging strategies would place the entire computational burden on the parking structure operator. Such

computations would be even more challenging for real-time charging if the protocol is expected to be executed/updated after each BEV arrival.

With simple modifications to the cost signal, this smart-charging strategy can be used to charge BEVs as early as possible, reduce parking structure load variation (Valley Filling), or shift charging away from On-Peak hours (Augmented Cost Signal). The Augmented Cost Signal strategy significantly reduced monthly electricity costs in all cases, when compared with Uncontrolled Charging from Section 5.3.1 and the Early Charging strategy proposed here.

A simple and well-known algorithm is used to assign BEVs to octopus chargers in real time, without any prior information about the BEVs. On average, the Early Charging and Augmented Cost Signal strategies required less than 66 8-Cable octopus chargers for 500 BEV parking structures (i.e., less than three additional chargers). The Valley Filling strategy required 79 and 101 8-cable octopus chargers on average and in the worst case, respectively. By reducing the number of octopus chargers needed, the proposed assignment strategy can reduce investments needed for parking structures' charging infrastructure.

The comprehensive smart-charging protocol presented in this work can be used to reduce electricity and charging infrastructure costs associated with workplace charging, while providing charging opportunities to long-range commuters and workers without access to home charging (i.e., apartment dwellers).

While the results for the assignment algorithm were quite underwhelming for 4-Cable octopus chargers, modifications can be made to the Greedy-Balance algorithm to improve its performance. For example, limits can be placed so that "problematic" BEVs are assigned to single-cable octopus charger. Machine learning algorithms can also be used to anticipate and

plan for predicted BEV arrivals. These topics are beyond the scope of this work and are suggested as a future works.

8 Conclusions

Three comprehensive smart-charging protocols with varying applications are proposed in this work. Each protocol is developed with varying degrees of focus on communication requirements and privacy concerns. The **BEV-based Optimization Protocol** is a decentralized, non-iterative strategy that allows BEVs to individually generate their own charging profiles via linear programming methods. The **Octopus Charger-based MILP Protocol** is a smart-charging strategy that allows octopus chargers to independently schedule charging for their assigned BEVs via MILP methods. The **Real-Time Octopus Charger-based MILP Protocol** is a smart-charging strategy that allows octopus chargers to independently schedule charging for their assigned BEVs in real time, without any prior BEV information.

Simulations were performed to verify and quantify the effectiveness of each of the proposed protocols. By using octopus chargers, all protocols were able to reduce the number of charging stations needed at parking structures, while meeting the charging requests of all BEVs. With simple modifications to the cost signal, the proposed protocols can manage the demand load of a parking structure to reduce parking structure load variation (Valley Filling) or shift charging away from On-Peak hours (Augmented Cost Signal). The Augmented Cost Signal strategy significantly reduced monthly electricity costs in all cases, when compared with Uncontrolled charging.

All three smart-charging protocols can reduce operational and charging infrastructure costs associated with workplace charging, while providing charging opportunities to long-range commuters and workers without access to home charging. Savings, however, were significantly influenced by the charging strategy and electricity rate plans used. Electricity prices can vary

significantly across regions, thus, adding to the need for smart-charging protocols that are robust enough to deal with these variations (i.e., optimization based vs. ad-hoc).

The implementation of the proposed protocols require investment to parking structures' charging infrastructure (i.e., octopus chargers). Such investments have already been proposed as possible methods of mitigating charger anxiety [30]. Future iterations of octopus chargers should be designed with smart-charging capabilities in order to reduce infrastructure and electricity costs for parking structure operators further. In order to implement the strategies proposed here, limited communication is required between the BEVs and the charging stations (traditional or octopus). This technology is currently feasible and can be implemented in new octopus charger models.

8.1 BEV-based Optimization Protocol

A decentralized smart-charging strategy that addresses the constraints and limitations of multiple dwell times is proposed. The protocol first uses an ordering strategy, based on each vehicle's load shifting flexibility, to develop a queue. Next, a decentralized smart-charging strategy that allows BEVs to individually generate their own charging profile is used. Finally, an assignment algorithm is used to assign BEVs to octopus chargers.

By allowing BEVs to individually generate their charging profiles, drivers can avoid sharing their driving patterns with the parking structure operator. Thus, maintaining a measure of user privacy. For this protocol, the parking structure operator must gather the charging flexibility of all participating BEVs in the morning (before the first BEV arrives). The operator then generates a queue and executes the appropriate smart-charging strategy. Thus, this approach

requires somewhat more complex communication between the BEVs and the parking structure operator but provides significant benefits.

8.2 Octopus Charger-based MILP Protocol

The Octopus Charger-based MILP Protocol can manage a parking structure demand load by having octopus chargers schedule charging for their assigned BEVs. By allowing octopus chargers to act as individual agents, the protocol distributes the computational burden among the octopus chargers. This protocol requires that the octopus chargers have access to their assigned BEVs' driving data, so privacy is not maintained for the participating drivers. In some cases, however, privacy may not be a concern. For example, driving patterns for entire fleets of buses or delivery trucks are generally known. Thus, this protocol can be used to reduce electricity costs and charging infrastructure investments for public transportation and delivery companies.

This protocol must be executed ahead of time, which requires more communication between the BEVs and the octopus chargers. These increased communication requirements, however, provide significant benefits. A simple and well-known algorithm is used to assign BEVs to octopus chargers. The Octopus Charger-based MILP Protocol significantly reduced the number of charging stations required when compared to the BEV-based Optimization Protocol. In all cases, the assignment algorithm required less than five extra 4-Cable octopus chargers to satisfy the charging demands of 50 simulated parking structures. No extra octopus chargers were needed when using 8-Cable octopus chargers.

8.3 Real-Time Octopus Charger-based MILP Protocol

A comprehensive protocol that allows octopus chargers to independently schedule charging for their assigned BEVs in real time is proposed. The Real-Time Octopus Charger-

based MILP Protocol requires that drivers share their expected driving patterns with their assigned octopus chargers, so user privacy is not maintained. This protocol, however, eliminates the communication requirements from the BEV-based Optimization Protocol and the Octopus Charger-based MILP Protocol. Once the driver parks, they can simply input their expected driving patterns via the octopus charger's user interface. By eliminating these communication requirements octopus chargers can be installed in more destination-charging locations that typically service multiple BEVs (e.g., apartment buildings, shopping malls, universities).

Furthermore, by allowing the octopus chargers to act as independent agents, the computational burden is distributed among all chargers. By contrast, centralized charging strategies would place the entire computational burden on the parking structure operator. Such computations would be even more challenging for real-time charging, if the protocol is expected to be executed/updated after each BEV arrival.

A simple and well-known algorithm is used to assign BEVs to octopus chargers in real time, without any prior information about the BEVs. On average, the Early Charging and Augmented Cost Signal strategies required less than three additional 8-cable octopus chargers to satisfy charging for all BEVs. A significant reduction compared to the BEV-based Optimization Protocol. The Valley Filling strategy required 101 octopus chargers in the worst-case scenario. The Real-Time Octopus Charger-based MILP Protocol, however, required more than 200 4-cable octopus chargers for several cases; an amount larger than those required for the BEV-based Optimization Protocol.

8.4 Future Work

While the results for the assignment algorithm were quite underwhelming for 4-Cable octopus chargers, modifications can be made to the Sorted-Balance algorithm to improve its performance. For example, if a BEV needs the entire workday to charge and has little/no flexibility (due to long commutes), then it may not be compatible with any BEVs assigned to an octopus charger. Such BEVs might be best assigned to a single-cable charger. Furthermore, machine learning algorithms can also be used to anticipate and plan for predicted BEV arrivals. These topics are beyond the scope of this work and are suggested as a future works.

In some cases, there may be discrepancies between predicted/scheduled driving patterns and actual driving patterns. BEV drivers can attempt to get a full charge at work, to minimize the risk of not having enough charge at the end of the workday. This is particularly true for BEVs with large battery capacities that are generally maintained at a high state of charge. If driving between dwell times is underestimated, however, more complications could arise. Thus, robust methods to handle the effects or random deviations from typical driving patterns must be developed.

The strategies proposed in this work can be developed further to estimate the energy storage capabilities of parking structures. On emergency days, the Augmented Cost Signal strategy can be used to provide as much charging as possible before On-Peak hours. Thus, giving the parking structure operator an estimate of the energy stored in the parked BEVs. Having this estimate gives the operator a valuable insight into each BEV's storage capabilities, so that an arbitrage (vehicle-to-grid and vehicle-to-vehicle charging) can be implemented. This is beyond the scope of this paper and is also suggested as a future work.

9 Appendix

A draft of the manuscript that appeared in Volume 113 of *Energy* by Edgar Ramos Muñoz, Ghazal Razeghi, Li Zhang, and Faryar Jabbari is provided below.

9.1 Electric Vehicle Charging Algorithms for Coordination of the Grid and Distribution Transformer Levels

9.1.1 Abstract

The need to reduce greenhouse gas emissions and fossil fuel consumption has increased the popularity of plug-in electric vehicles. However, a large penetration of plug-in electric vehicles can pose challenges at the grid and local distribution levels. Various charging strategies have been proposed to address such challenges, often separately. In this paper, it is shown that, with uncoordinated charging, distribution transformers and the grid can operate under highly undesirable conditions. Next, several strategies that require modest communication efforts are proposed to mitigate the burden created by high concentrations of plug-in electric vehicles, at the grid and local levels. Existing transformer and battery electric vehicle characteristics are used along with the National Household Travel Survey to simulate various charging strategies. It is shown through the analysis of hot spot temperature and equivalent aging factor that the coordinated strategies proposed here reduce the chances of transformer failure with the addition of plug-in electric vehicle loads, even for an under-designed transformer while uncontrolled and uncoordinated plug-in electric vehicle charging results in increased risk of transformer failure.

Keywords:

Plug-in electric vehicle, Valley filling, Distribution transformer, PEV charging, BEV, Loss of life

Notation

The symbols used in this paper are as follows.

b_n	Energy used by each BEV, between charging cycles
$C_{grid}(t_i)$	Broadcast cost from the grid for each timeslot
$C_{trans}(t_i)$	Broadcast cost from the transformer for each timeslot
I_{CD}	Cooling down period
J	Total charging cost
n	PEV number
P_{lim_i}	Desired maximum power limit for the transformer
$\overline{P_{lim_i}}$	Desired maximum power limit for the transformer with cooling down period
$p_n(t_i)$	Charging power for each BEV
$r_n(t_i)$	Maximum charging energy for each BEV *n*, at each timeslot
t_i	Timeslot *i*
$\overline{\Delta t_n(t_i)}$	Time each BEV *n* is plugged in during timeslot *i*
$x_n(t_i)$	Charging energy for each BEV *n*, at each timeslot
η	BEV charging efficiency

The abbreviations used in this paper are as follows.

AAF Aging Acceleration Factor

BEV Battery Electric Vehicle

BSOC Battery State of Charge

EAF Equivalent Aging Factor

HST Hot Spot Temperature

PEV Plug-in Electric Vehicle

PHEV Plug-in Hybrid Electric Vehicle

TOU Time-of-Use

9.1.2 Introduction

Plug-in electric vehicles (PEVs) have been gaining popularity in recent years due to the need to reduce fossil fuel consumption and greenhouse gas emissions [1]. PEVs include plug-in hybrid electric vehicles (PHEVs) and battery electric vehicles (BEVs). In [3], it is shown that meeting ambitious reduction in greenhouse gasses, such as those planned for California, requires large numbers of PEVs. According to [40] market share of PHEVs is expected to increase to 25% by 2020. This would lead to an overall PHEV penetration of about 9% of all vehicles in use. While this penetration level might seem low, concentrations of PEVs could become quite high in more affluent and tech savvy neighborhoods (e.g. Silicon Valley) [19]. This uneven distribution can occur across national boundaries. For example, the Tremove model predicts a PHEV penetration as high as 30% for Belgium by 2030 [41]. Here, it is assumed that the vehicles rely on electric power primarily, therefore the focus is on BEVs.

Interactions between large number of electric vehicles and power networks have been studied by several groups. In [42], integration of PEVs is studied with regard to reconfigurable microgrids, while [43] analyzes the impact of 100% PEV penetration on the power transmission network. Reference [44] shows that PEVs can be used as storage, in vehicle-to-grid (V2G) charging, to reduce reliance on coal/natural gas. In [18], similarly, PEVs are studied as alternative energy storage, for high renewable penetration levels, given the intermittency of renewable sources (see, e.g., [45] and [46] on challenges in integrating wind and solar energy into a conventional grid). In [47], PEV batteries (although only at their automotive end of life) are repurposed as stationary storage systems to integrate intermittent wind power. In [23], it is found that large number electric vehicles that recharge at night, can level the electricity demand, and increase the amount of wind power that can be used. High concentrations of PEVs, however, can also cause grid level challenges during high demand periods if vehicle charging is uncoordinated.

Large, and non-uniform penetration levels have the potential to pose additional challenges, namely at the local level through distribution transformers. These transformers are often designed and sized for the non-BEV power demand of a group of residences (e.g., a street). Large loads, extended over long periods can shorten the life, as well as increase the risk of serious damage [1] to distribution system equipment (including transformers). While transformers are designed to tolerate certain levels of overload, excessive overloads can be problematic. Overloading can increase the hot spot temperature (HST), which can increase the equivalent aging factor (EAF). This would cause more frequent replacement of transformers [1] and upgrades to the distribution system.

Scheduling EV charging properly, may reduce the daily cycling of power plants and the operational cost of the electric utility [11]. The issue of accommodating the charging needs of a large number of PEVs without placing extreme stress on the electricity distribution network have been studied by a number of research groups. EV charging control strategies fall into three main categories: time-of-use (TOU), centralized control, and decentralized control [48]. In [41] quadratic and dynamic programming techniques are used to generate charging profiles for PEVs by minimizing power losses in the distribution grid. In [14] a decentralized charging strategy is proposed for the case where all EVs have identical characteristics (same charging horizon, power consumption, and maximum charging rate). In [48] another decentralized charging strategy is proposed which alleviates the necessity for the identical characteristics assumed in [14].

In this paper, the focus is on leveling the grid scale power demand by developing a smart charging strategy for high electric vehicle penetrations, while avoiding excess damage to the infrastructure (e.g., distribution transformers). Due to the communication and computational requirements for a real-world application, the focus is on a decentralized approach. This paper starts with the simple algorithm proposed in [19], in which a non-iterative approach is developed that results in maximum charging rates for all charging periods, is capable of achieving valley filling (when desired), and can be modified easily to follow specific grid level demand profiles (e.g., to accommodate the integration of renewable power generation in the grid, thought that is not the main focus). It is then shown that under reasonably mild conditions, a large number of distribution transformers can operate under undesirable conditions (i.e. significantly higher than designed power levels), be it under a grid level coordination or uncoordinated charging.

Charging strategies have also been developed to improve performance at the distribution level as well. The effects of uncontrolled and off-peak charging are studied in [1] and [40]. Both

papers find that smart-charging strategies can mitigate the negative effects of PEV charging. Two smart-charging strategies are proposed in [40]. The first prevents transformers from overloading by delaying charging of PEVs. The second sheds or defers non-critical household loads (e.g. water heaters and dryers) during PEV charging. Load shedding is not considered in this work due to communication, technical, and privacy concerns. Neither algorithm addresses grid level concerns and deal with the safety of local transformers only. Another local control strategy is proposed in [49] that depends only on local network conditions and the battery state of charge (BSOC) of the PEV. A centralized control charging strategy where a single controller manages the charging rates of all PEVs is then also proposed.

In [50], Distribution Feeder Reconfiguration (DFR) is used to coordinate PEV operation in a stochastic framework. The DFR strategy is employed to minimize operational costs and increase the penetration of PEVs with the use of V2G. An application of the proposed approach demonstrates its robustness and effectiveness. In this paper, V2G is not investigated and focus is given to more readily available technologies. In [51] the integration of a high number of electrical vehicles in a renewable-dominated power system is studied. The problem is formulated using a two-stage stochastic programming model.

A critical issue that remains unresolved is that improved grid performance can negatively affect local distribution components. In [52] decentralized charging protocols are developed that use cost signals to achieve a valley filling profile at the grid. The charging strategy from [48] is expanded to develop three different iterative algorithms that incorporate capacity constraints, relying on stochastic optimization techniques using nested iterative algorithms. The capacity constraints in [52] can be used to prevent failure and/or improve the efficiency of local components (e.g. transformers).

The focus of this work is on the development of a decentralized algorithm, with minimal communication and delay considerations (e.g., non-iterative) that addresses both grid level concerns (i.e., utility level economics) and local levels (e.g., safety and maintenance concerns), with priority given to local concerns. Here, the two concerns are combined by expanding the algorithm in [19], with only slight increases in communication and computation requirements. The algorithm from [19] requires modest communication between the grid operator and the BEV. As in [52], the modifications made to the algorithm from [19] requires communication between the BEV and the local distribution transformer. However, since iterative techniques are not used, the increase in computational effort (performed by the BEV) is negligible. This communication is used to prevent charging during times that could cause overloading. Naturally, the algorithm proposed here is not limited to only distribution transformers. With minor modifications, this algorithm can be used in conjunction with any (or indeed multiple) other local infrastructure components affected by BEV charging. Finally, this paper compares key performance variables of the transformers (load factor, HST, and life span) for different algorithms to gain a better, and quantitative, understanding of the benefits.

9.1.3 Parameters, Data, and Related Assumptions

The parameters, data, and related assumptions used in the following simulations are described below.

9.1.3.1 Transformer Data

Measured data from a 75-kVA transformer, from a residential area in Irvine, California is used to obtain a Baseload for the simulations performed. The Baseload is the load demand on the transformer. See the black curve in Figure 27-A. Transformer data from Irvine (for which

measured data has already been obtained) is used, because of its suitable socio-economic population regarding PEV sales. The measured 75 kVA transformer serves 20 homes. Eight of these homes have air conditioning. These homes range in size from 177 to 269 square meters (1900 to 2900 square feet). These attributes are relatively common for the socio-economic groups most enthusiastic about BEVs. The Baseload transformer data used throughout this paper did not include any electric vehicle charging.

The Baseload was obtained from the transformer data on Thursday September 25, 2014. The temperature on this day had highs of 31.7° C and lows of 21.7° C [53]. The transformer data have a sampling time of five minutes. This sampling time could exaggerate changes in the load (see Figure 27-A). The transformer profile chosen here is used as a representative load for all transformers in the following simulations. For a clear presentation of the results, a smoother profile would be desirable, since many short-term peaks clutter the figures (without altering the main findings). In practice, a predicted (or average – based on history) profile is used and it is unlikely that such a predicted history would have a large number of significant jumps over 5 or 15-minute time slots. Without smoothing, the results are quite similar, though with higher peaks and lower valleys (which might be more problematic for transformers in hot days). Furthermore, we use this representative profile, in Figure 33, for grid level impact. As a result, some form of averaging or smoothing is needed to represent a large number of transformers. Therefore, the data are first "smoothed out" with a central moving average with nine data points. The data are then interpolated on MATLAB, to obtain a one minute resolution. A power factor of 1 was assumed for the transformer at all times.

During August and September of 2014 (months for which transformer data were recorded), there were 17 days (28%) with highs of at least 31.7° C. Figure 27-B shows a

comparison of the Baseload used here with Baseloads from two other days: August 25, 2014 and September 16, 2014. The temperature on September 16 had highs of 37.8° C and lows of 24.4° C. August 25 had highs of 26.7° C and lows of 21.1° C. Similar traits can be seen in the three Baseloads. To use an intermediate – and relatively common – condition, the Baseload from September 25 (which is represented by the middle curve in Figure 27-B) will be used in all of the following simulations unless otherwise stated.

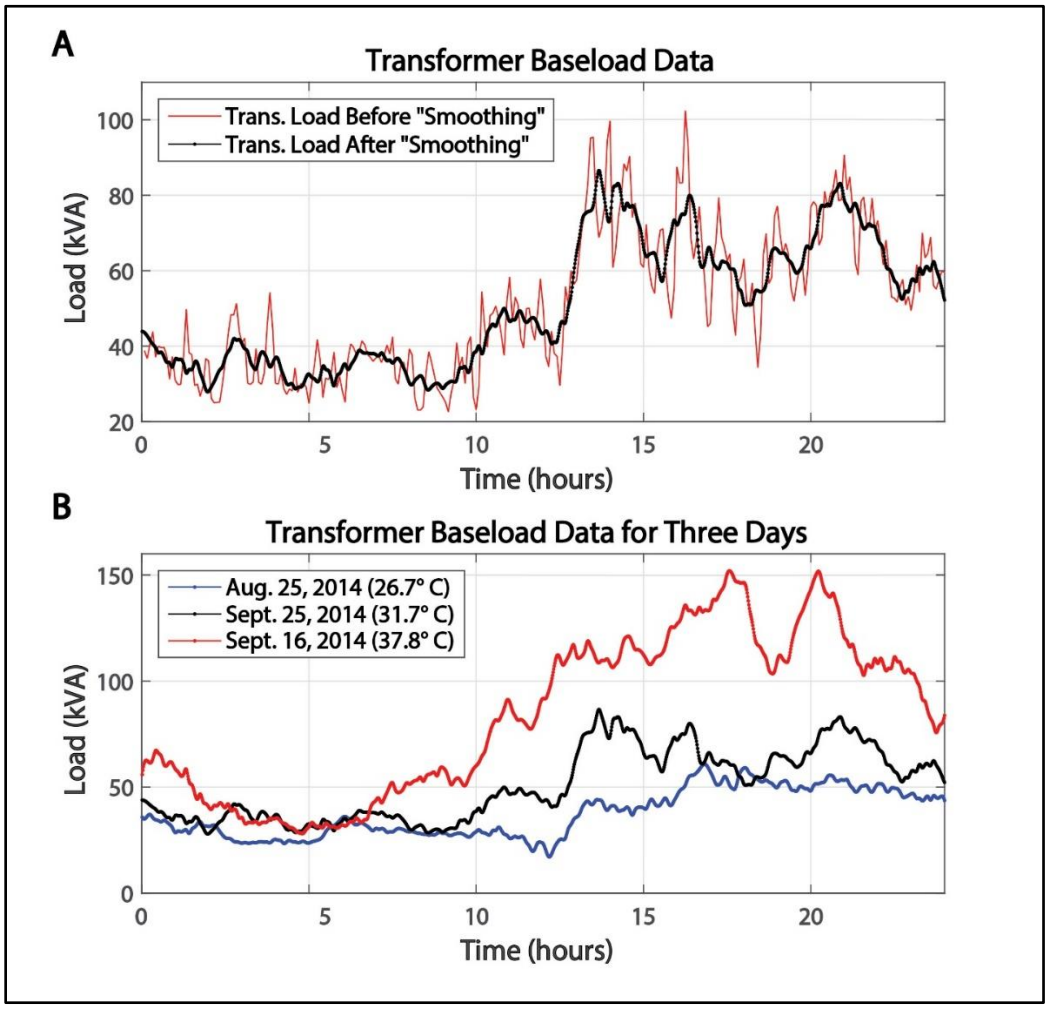

Figure 27 Transformer Baseload data a) before and after "smoothing" and b) for three days

9.1.3.2 PEV Data

The 2009 National Household Travel Survey (NHTS), [54], is used to obtain the vehicle travel behavior data for the following simulations. The same processing steps from [19] were used to prepare the data. Trips without a personally owned vehicle were deleted, person-chain data was converted to vehicle chain data, daily trip data with unlinked destinations or significant over-speed were deleted, and tours were organized to start and end at home. This processing resulted in travel data for 20,295 vehicles.

Main Electric Vehicle Assumptions: (i) An all-electric range of 40 miles (64.4 km) (which is a conservative number), (ii) A rate of 0.34 kWh/mi (0.21 kWh/km), (iii) BEVs in the simulation are either given a 3.3 kW or 7.2 kW charging rate with a charging efficiency of 0.85, (iv) If PHEV, vehicles will try to use battery power before gasoline (the focus of this work is on BEVs).

Penetration Assumptions: Electric vehicle sales will vary depending on regions. Current prices suggest that sales will be higher in areas with people of higher socio-economic standing. This, added with the fact that views on PEVs vary depending on regional affiliation, results in the clustering of sales in certain areas (e.g. California leads the United States in PEV sales). Consistent with the notion of non-uniform distribution of PEV sales, it is assumed that PEVs have higher penetration in individual neighborhoods and streets. Here it is assumed that (i) An overall penetration of 10%, (ii) Average penetration on streets with PEVs of 25%, (iii) A ratio of 1.86 cars per household [55], and (iv) 20 houses per distribution transformer. These assumptions lead to 9 BEVs per transformer.

Given that there are 20,295 vehicles in the data-set (and it is assumed they are all BEVs), the vehicles are served by 2,255 transformers that need to be studied for possible damage. The 20,295 BEVs are randomly assigned to the 2,255 transformers, to maintain a ratio of 9 BEVs per transformer. The original random assignment is maintained throughout all simulations. In practice, there could be many variations in the number of BEVs a transformer supports, as well as the expected demand of these vehicles. The assignment can be interpreted as an estimation of the chance of overloading due to variations in BEV usage. For example, if 225 transformers overload, then this could also be interpreted as a 10% chance of a transformer overloading.

9.1.3.3 Charging Power

Most electric vehicles have charging rates of 3.3 kW [56]. Others have 6.6, 7.2, or 10 kW charging rates. The Tesla Model S even has an optional 20 kW twin charger. In the current study, only charging rates of 3.3 and 7.2 kW are used in all simulations. For each of the algorithms, the three following charging scenarios are simulated:

i. 3.3 kW Charging: All BEVs have a charging rate of 3.3 kW

ii. Mixed Charging: Half of the BEVs have a charging rate of 3.3 kW and the other half have a rate 7.2 kW.

iii. 7.2 kW Charging: All BEVs have a charging rate of 7.2 kW

High levels of BEVs with 7.2 kW charging could exacerbate the issues discussed here. For the mixed charging method, the 7.2 kW BEVs were randomly assigned to the 2,255 transformers. Since the assignment was random, some transformers have more BEVs with 7.2 charging than others.

9.1.4 Algorithms

In the following, we describe different charging scenarios.

9.1.4.1 Uncontrolled Charging

BEV charging is first simulated in an uncontrolled charging scenario. In this scenario, charging begins as soon as the driver arrives home and plugs in their BEV. The BEV continues to charge until it has a full battery state of charge (BSOC).

9.1.4.2 TOU Charging

Time-Of-Use (TOU) is a pricing structure that charges different rates for electricity [57]. The varying rates depend on the season and time of the day. The TOU pricing structure from Southern California Edison (SCE) is used in these simulations. The SCE TOU pricing scheme includes two seasons: summer and winter. The summer season is June-September, while winter season is October-May. SCE refers to its three pricing periods as On-Peak, Off-Peak, and Super Off-Peak. With On-Peak having the highest energy price and Super Off-Peak having the lowest. During the summer season, the On-Peak hours are 2 pm to 8 pm. The Super Off-Peak hours are 10 pm to 8 am. The rest are Off-Peak hours. Winter hours are the same as summer hours for residential customers, but prices are generally lower. Table 1 contains the typical periods for the TOU pricing structure during the summer (the actual prices can vary significantly across regions).

Table 14 Summer residential time-of-use hours

Super Off-Peak	Off-Peak	On-Peak
10 pm – 8 am	8 am – 2 pm & 8 pm – 10 pm	2 pm – 8 pm

For this strategy, the BEVs attempt to charge during times when the electricity price is the lowest. If the BEV cannot get a full charge during Super Off-Peak hours, then it tries to only avoid On-Peak hours. If this is not possible either, then there are no limitations set on when the BEV can charge.

9.1.4.3 Grid Valley Filling

In this section, the protocol in Zhang et al. [19] is briefly reviewed. The non-iterative protocol in [19] ensures maximum charging power during the scheduled charging times for BEVs, to achieve close to "valley filling" profile or other desired profile (e.g., to accommodate renewable resources). This is done to the extent that the arrival and departure times of BEVs allow. The algorithm works by having the grid operator send a "cost" signal to the BEV. The BEV then optimizes its own cost with the cost signal in order to form a charging profile. The charging profile is then sent to the grid operator. The cost signal is updated after a certain amount of time has passed or certain number of BEVs have established their profile (see [19] and the Appendix for more details).

The power needed by each BEV n, for each timeslot t_i is given by $x_n(t_i)$. The total charging cost is

$$J = \sum_i C_{grid}(t_i) \times x_n(t_i) \tag{45}$$

where $C_{grid}(t_i)$ is the most recent broadcast cost for each timeslot. The cost used in Equation 45 is the net grid level load. It is broadcasted by the grid operator and updated throughout the day. The grid load, without BEV charging, is estimated through forecast, based on historical data.

The following constraints are needed for the optimization problem. The energy consumed by the BEV must be equal to the energy used in between charging cycles, b_n.

$$\sum_i x_n(t_i) = b_n \tag{46}$$

The lower bound for the power is set to zero. The upper bound is set as the product of the charging power $p_n(t_i)$, the charging efficiency η (0.85), and the fraction of dwell time during each timeslot $\overline{\Delta t_n(t_\iota)}$. The value of $\overline{\Delta t_n(t_\iota)}$ depends on the dwelling time of the vehicle. For example, for a dwelling time of 6.25 hours, $\overline{\Delta t_n(t_\iota)}$ would equal one for the first six timeslots and 0.25 for the final timeslot.

$$0 \leq x_n \leq r_n(t_i) \tag{47}$$

$$r_n(t_i) = p_n(t_i) \times \overline{\Delta t_n(t_\iota)} \times \eta \tag{48}$$

The algorithm is thus the following: Once a BEV is connected, it receives the current predicted load for the next 24 hours (including all the previously assigned BEV charges). It then uses that as the cost, $C_{grid}(t_i)$ in Equation 45. The charging power at each timeslot (i.e., $x_n(t_i)$) are the variables that minimize the cost in Equation 45 subject to Equations 46-48. This is a linear program and a variety of fast and robust algorithms exist to obtain the unique solution.

Figure 28 (which is similar to Figure 8 of [19]) is a typical result. The BEV power demand in mustard yellow clearly achieves near complete valley filling. The red lines are the power forecast at each successive update (i.e., the signal that is broadcasted), started from the lowest level upward.

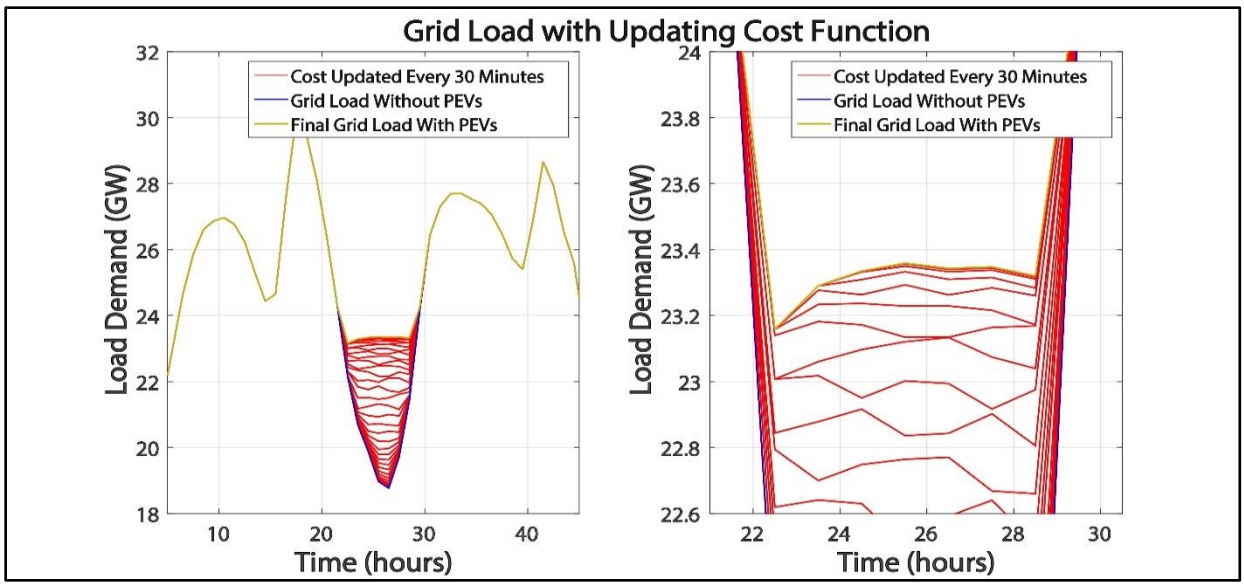

Figure 28 Grid load and updating cost function for Grid Valley Filling charging strategy with 3.3 kW charging rates and b) zoomed in view (similar to Figure 8 in [19])

9.1.5 Grid Valley Filling with Timeslot Rejection (By Transformer)

While the above protocol results in near ideal valley filling solution, it can lead to significant overload and overheating in a large portion of distribution transformers. To address this problem, the following adjustments are made:

A. At the time the BEV engages the network, the local transformer sends it the predicted demand profile (household use plus power usage planned by earlier BEVs) with a desired max power limit. For now, let this P_{lim_i} = 75 kVA $\forall i$.

B. If at any timeslot t_i, the current forecasted demand on the transformer ($C_{trans}(t_i)$) plus the charging power of the BEV violates P_{lim_i}, the upper bound for allowable power in that t_i is set to zero, which leads to $r_n(t_i) = 0$ in *(4)*.

C. The BEV attempts to solve the valley filling problem — i.e. minimizing the cost function in *(1)* subject to *(2), (3)* and *(5)* - - i.e., now *(4)* is replaced with *(5)*

$$r_n(t_i) = \begin{cases} p_n(t_i) \times \overline{\Delta t_n(t_i)} \times \eta & if\ C_{trans}(t_i) + p_n(t_i) < P_{lim_i} \\ 0 & else \end{cases} \quad (49)$$

Note that the algorithm can be modified easily for BEVs with advanced power management technology that allows multiple charging power — it simply reduced the value of $p_n(t_i)$ to the amount that does not violate P_{lim_i}.

If some BEVs, with high energy requirements, engage the network late in the evening, the modification above can result in an insufficient number of timeslots for those BEVs. If the vehicle is a PHEV, this might not be problematic. If it is a pure BEV, the following further enhancement can be used. It is based on the fact that transformers can operate at higher levels than the nameplate capacity, for a limited time — as long as this period is relatively brief, or there is a "cooling off" period in which the transformer is operating below capacity (more on this below).

It should be noted that this and the following two charging strategies require modest communication between transformers and BEVs. There are no iterations and vehicle receives the current grid level demand estimates from the grid operator (say 96 data points corresponding to the overall demand at 15 minute intervals) and the capacity availability from the transformer for the same time slots, which can be used to avoid charging during high transformer load times. The simple optimization is performed at the vehicle level and the resulting charging times are sent to the grid operator and the local transformer to be aggregated.

9.1.5.1 Grid Valley Filling with Modified Timeslot Rejection

Failure of the Timeslot Rejection algorithm implies that the BEV has limited number of timeslots to charge. To accommodate this BEV, the value of P_{lim_i} is increased by the power level of the BEV (see Equation 50 below). For example, if a 3.3 kW BEV cannot get a full charge and P_{lim_i} is 50 kVA, then P_{lim_i} is increased to 53.3 kVA.

$$P_{lim_i} = P_{lim_i} + p_n(t_i) \tag{50}$$

This would open up all timeslots. However, for safety and transformer lifetime considerations, it would be desirable to first use the timeslots that would violate the limits only slightly. For this, it minimizes the cost in Equation 50 and thus solves the local (transformer level) valley filling problem; i.e., minimizing the cost in Equation 51 subject to Equations 46 and 47 with $r_n(t_i)$ and P_{lim_i} from Equations 49 and 50. The local (i.e., transformer level) valley filling is used to ensure the lowest transformer load periods are used first – i.e., for these rare (and late) cases, the safety of the transformer is made higher priority than the grid level economic considerations. Thus, instead of Equation 45, the cost to minimize is now

$$J = \sum_i C_{trans}(t_i) \times x_n(t_i) \tag{51}$$

where $C_{trans}(t_i)$ is the current forecasted total load on the transformer and Equation 49 is updated to reflect the new value of P_{lim_i} from Equation 50.

This algorithm ensures that the BEV will receive significant charge, as long as it is physically feasible (i.e., the BEV has enough time to charge without any other grid/transformer restrictions). The use of local demand for cost ensures that the BEV uses the timeslots in which the violation of the old P_{lim_i} is the smallest [19].

9.1.5.2 Forced Cool-Down Period Method

The previous modification would face challenges if the limit is raised for multiple vehicles. In that case, increasing the power limit repeatedly would be counter to the main safety concern. To address this situation, a slight modification can be made: There would be an upper limit for the maximum power for certain timeslots for cooling down. This is implemented through placing a maximum value for P_{lim_i} , say $\overline{P_{lim_i}}$. For cooling down periods, say $i \in \{I_{CD}\}$ (e.g., 8-10 pm, just after typically high usage period) this value can be, for example, 65kVA. The rest of the timeslots ($i \notin \{I_{CD}\}$) would be set at a higher value (e.g. 75 kVA). Again, if the cooling down periods do not allow a BEV to get a full charge, then the maximum value for the cooling down period is raised (meeting the energy requirement while staying close to the cooling down plan). The BEV attempts to solve Equations 45-47 with Equation 53. If the BEV cannot get a full charge, then it implements Equation 52 and solves Equations 51, 46, 47, and 53 until it can obtain a full charge.

$$P_{lim_i} = P_{lim_i} + p_n(t_i) \quad for\ i \notin \{I_{CD}\} \tag{52}$$

$$r_n(t_i) = \begin{cases} p_n(t_i) \times \overline{\Delta t_n(t_i)} \times \eta & if\ C_{trans}(t_i) + p_n(t_i) < \overline{P_{lim_i}} \\ 0 & else \end{cases} \tag{53}$$

9.1.6 Results at the Transformer Level

The results of the different charging scenarios described in Section 9.1.4 are presented below.

9.1.6.1 Uncontrolled Charging

Figure 29-A shows the result of Uncontrolled Charging for the scenario in which of all the simulated BEVs have a 3.3 kW charging rate. It is also assumed that the 20 homes are served by either a 50 kVA or 75kVA transformer. In this plot, the cyan curves represent the load on all 2,255 randomly assigned transformers. The black curve represents the Baseload (i.e., the load on the transformer without any BEV charging). As each vehicle selects its charging times, the power use is added to the Baseload to obtain the new demand for the transformer. The final profile for each individual transformer is plotted in Figure 29-A, below.

It can be seen that charging occurs throughout the day. The highest load reaches about 109 kVA and the BEV charging significantly increases overloading in the transformers. This type of loading would cause overloading even in a 75 kVA transformer. With 3.3 charging, 955 (42.4 %) of the 75 kVA transformers experience loads greater than 100% of rated capacity for more than an additional two hours. It should be noted that when discussing additional overload, overloading caused by the Baseload is not considered. Only the extra overloading caused by BEVs is considered. This number is raised to 1,377 (61.1%) with 7.2 kW charging. With 3.3 kW and mixed charging, all BEVs except for one were fully recharged. This vehicle turns out to be a BEV which was not at home long enough to get a full recharge (without any transformer related restrictions). In these results, a BEV with a BSOC above 98% will be considered fully recharged.

For the sake of brevity, representative simulations will be included. Figure 29-B shows the results for the charging strategy with only 7.2 kW charging rates. A total of 722 (32%) transformers are subjected to loads above 100 kVA. Of these transformers, 30 (1.3%) maintained the 100kVA load for over an hour. This means that these transformers would be overloaded to over 200% capacity for more than an hour if they had a 50kVA rating. The highest load now

appears to reach over 120 kVA. This change is attributed to the fact that 7.2 kW charging has been introduced. Similar results were found for the mixed charging method. The effects on the transformer are discussed in Section 9.1.7 in detail.

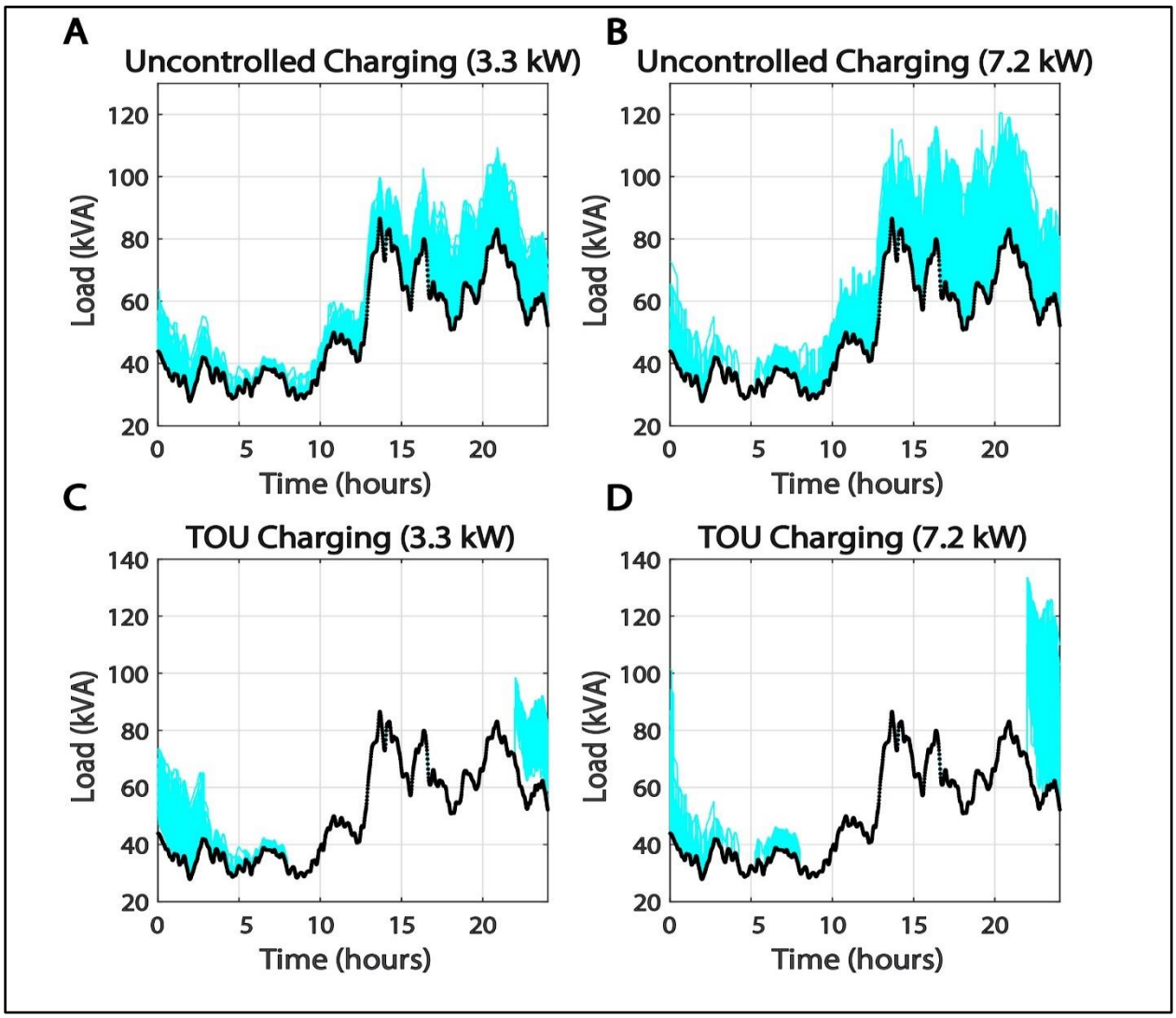

Figure 29 Transformer loads for uncontrolled charging strategy with a) 3.3 kW, b) 7.2 kW charging rates and TOU charging strategy with c) 3.3 kW, d) 7.2 kW charging rates

9.1.6.2 TOU Charging

The results for the TOU charging strategy with only 3.3 kW charging rates can be seen in Figure 29-C. All BEVs are able to get a full charge during Super Off-Peak hours. As mentioned in [19], 80% of vehicles are home between 8 pm and 7 am. This is the reason why all BEVs are able to charge during Super Off-Peak hours. It can be seen that the TOU charging strategy causes a big "jump" at 10 pm. This is because a large number of BEVs are waiting for the lower price and start charging at 10 pm. The maximum load appears to occur at 10 pm at about 98 kVA.

Figure 29-D shows the results for the TOU charging strategy with only 7.2 kW charging rates. The magnitude of the 10 pm peak increases significantly. The peak is at about 134 kVA. It is found that all of the 2,255 transformers are subject to loads above 100kVA. This would place all 50 kVA transformers at 200% capacity at some point during the day. Of these transformers, 603 (26.7%) were subjected to loads above 100kVA for at least one hour. While individual owners have attempted to be responsible, uncoordinated actions can lead to transformer damage and grid issues using this scheduling strategy. Any changes made to the time-of-use pricing structure would cause the same problems in this charging strategy. For example, suppose that the electric company decided to shift the load by shifting TOU times by two hours. A similar peak would occur, just two hours later. Thus, an intelligent approach is needed.

9.1.6.3 Grid Valley Filling

Figure 30-A gives the results for the Grid Valley Filling strategy with 3.3 kW charging rates. Most charging occurs between 10 pm and 6 am, since that is the overall grid level objective; similar to the TOU charging strategy. However, the problem with the 10 pm jump is not present. The highest load appears to stay below 92 kVA (less than the 98 kVA peak seen in

the TOU strategy in Figure 30-C). The highest load for 7.2 kW charging, in Figure 30-B, is approximately 104 kVA with this charging strategy. Here 1,667 (73.9%) transformers were subjected to additional overloading above 75 kVA. Of those, 86 (3.8%) transformers experienced additional overloading above 75 kVA for longer than an hour.

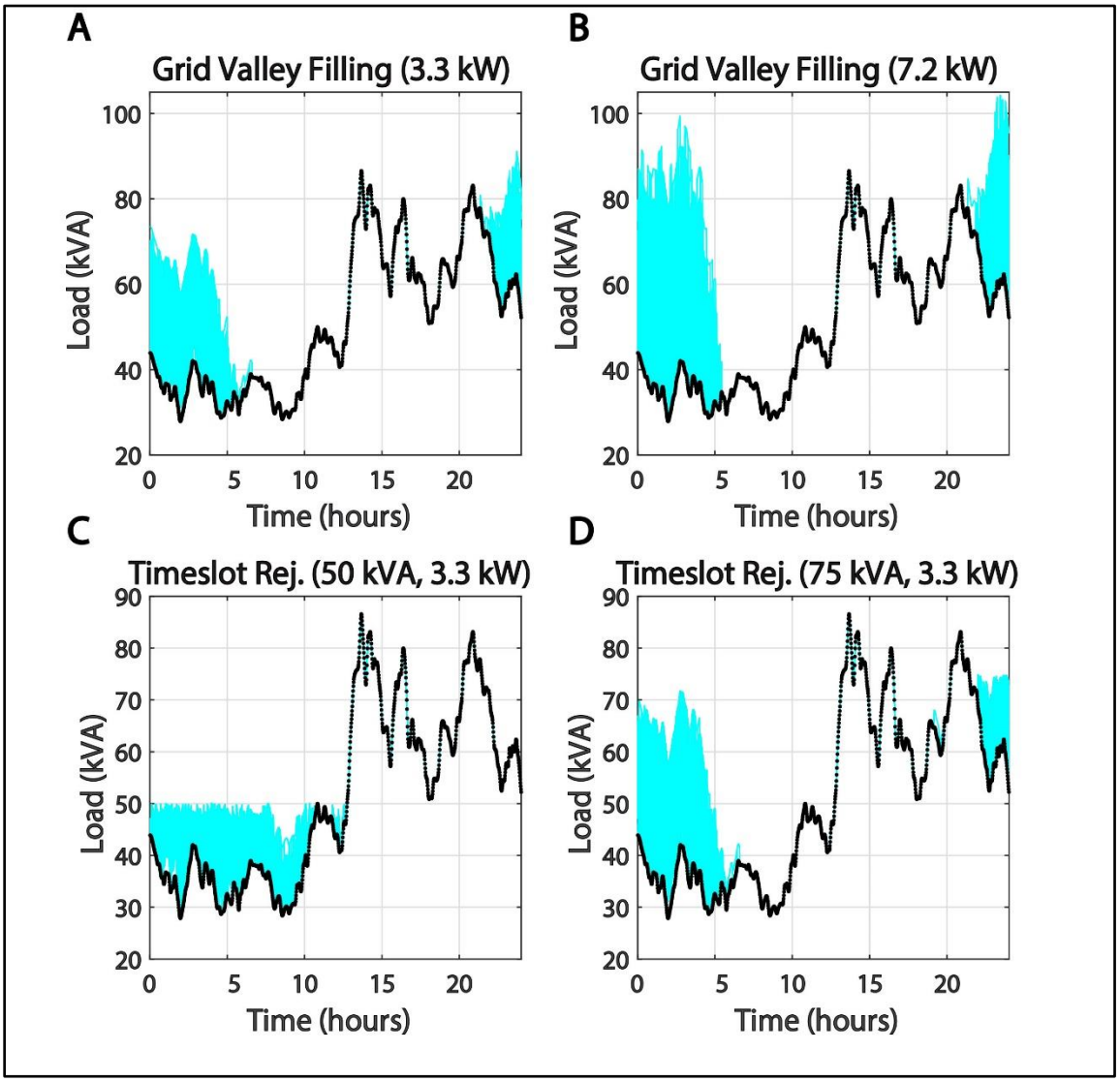

Figure 30 Transformer loads for Grid Valley Filling charging strategy with a) 3.3 kW, b) 7.2 kW charging rates and Grid Valley Filling with Timeslot Rejection charging strategy with only 3.3 kW charging rates for c) 50 kVA transformers and d) 75 kVA transformers

9.1.6.4 Grid Valley Filling with Timeslot Rejection (By Transformer)

In these simulations P_{lim_i} is set to 50 and 75 kVA to examine the effects on both 50 and 75 kVA transformers. For this Baseload, the 50kVA transformer is undersized but since all transformers are capable of withstanding some level of overload, it is possible that a lower capacity transformer is used even when the peak power exceeds the limits occasionally. Figure 30-C shows the result of the Grid Valley Filling with Timeslot Rejection algorithm with 50kVA transformers, while Figure 30-D corresponds to 75 kVA transformers. Note that the BEV charging does not force the transformers to go above 50 or 75 kVA limits in each case (further than the durations that were due to Baseload –non-BEV – energy demand). In order to prevent overloading, some BEVs were denied the opportunity to charge.

With 50kVA transformers, in 3.3 kW charging only, a total of 23.7 MWh of electric energy was denied to BEVs. The amount denied is 12.7% of the total charge requirements of all vehicles. A total of 37.5 MWh and 51.2 MWh of charge were denied to the scenarios with mixed charging and 7.2 kW charging, respectively. Their respective percentages of the total charge were 20.1% and 27.5%. These percentages might seem modest, but a significant number of BEVs did not get fully charged as a result of their charge requests being denied in this strategy. Table 15 shows the number of BEVs that received the given percentage of charge that they originally requested. For example, with mixed charging, 437 BEVs received only 70-80% of the charge that they originally requested upon arrival, while nearly 1,500 cars received less than 10% of the requested charge. It can be seen that BEVs with 7.2 kW charging had more timeslots rejected than those with 3.3 kW charging. This is due to the fact that 7.2 kW charging is more likely to cause violation of the transformer rated capacity. This suggests that when the transformer is undersized (or nearly so) a further modification is needed.

With 75kVA transformers, vast majority of cars received at least 90% of requested charge, as shown in the lower half of Table 15. Even in this case, guaranteeing full charge would need the modification discussed in the following subsection. Of course, even with 75kVA the problem would be more severe in hotter days (e.g., consider the higher Baseload in Figure 27-B).

Table 15 Percentage of required charge consumed (50 and 75 kVA Trans.)

	0-10%	10-20%	20-30%	30-40%	40-50%	50-60%	60-70%	70-80%	80-90%	90-98%	Full Charge
50 kVA Transformers											
3.3	259	150	252	297	372	391	600	531	667	1,007	15,769
Mixed	1,465	229	264	268	465	343	448	437	667	1,218	14,491
7.2	2,670	295	286	220	567	341	273	286	658	1,528	13,171
75 kVA Transformers											
3.3	0	0	0	0	0	0	1	0	17	570	19,707
Mixed	0	0	0	0	0	0	1	16	34	931	19,313
7.2	0	0	0	0	0	1	0	34	47	1,359	18,854

9.1.6.5 Grid Valley Filling with Modified Timeslot Rejection

Figure 31-A/B shows the results for the Modified Timeslot Rejection strategy. The transformers in these simulations have a 50 kVA rating, since there is little need for this modification for the 75kVA transformers, in this relatively warn – but not hot – day. With this charging strategy, all BEVs obtain a full charge (except for the single one that was not at home long enough to receive full charge even without any constraints, as previously mentioned). In these simulations, the highest load is about 87 kVA. This load is caused by the Baseload. The loads caused by BEV charging stay below about 66 kVA for 3.3 kW charging and below 64 kVA for 7.2 kW charging. Vehicle charging is shifted and occurs throughout the day as the result of attempting to reduce transformer overloading. This is due to the management of the charging schedules of the small portion of BEVs at home between 6am and 4 pm.

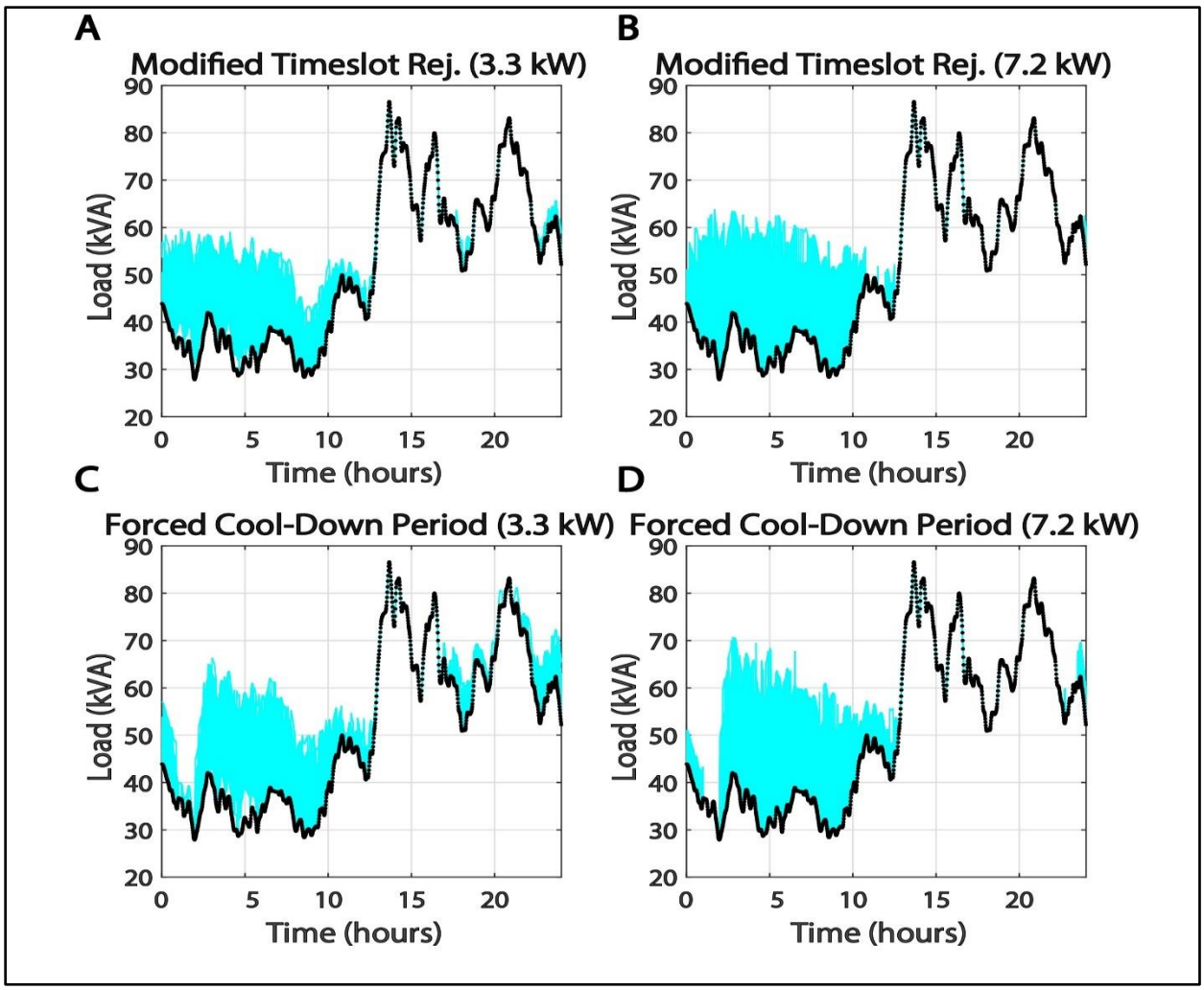

Figure 31 50 kVA transformer loads for Grid Valley Filling with Modified Timeslot Rejection charging strategy with a) 3.3 kW, b) 7.2 kW charging rates and Forced Cool-Down Period charging strategy with c) 3.3 kW, d) 7.2 kW charging rates

9.1.6.6 Forced Cool-Down Period Method

Figure 31-C/D shows the results for the Forced Cool-Down Period Method. The transformers in these simulations have a 50 kVA rating. $\overline{P_{lim_t}}$ is set at 40 kVA for the cooling down period. The cooling period is set for 1-2 am. It can be seen that all transformers maintain a load below 87 kVA throughout the day. Note that this peak load is caused by the Baseload and BEV load is considerably smaller, due to fact that in this approach, the local demand is used as

the broadcast cost, guiding the vehicles to low demand timeslot, whenever possible. All transformers also stay below 40 kVA during the cooling down period.

9.1.6.7 Grid Valley Filling with Modified Timeslot Rejection using a Different Baseload

For comparison, the Grid Valley Filling with Modified Timeslot Rejection strategy was simulated with a different Baseload. The Baseload from August 25, 2014 shown in Figure 27-B was used. This Baseload was taken from a day with a lower temperature than the Baseload that has been used in all the other simulations. The lower temperature results in lower loads on the transformer. This is most likely partly caused by the lower demand of electricity by the eight homes with air conditioning. The results for the simulation can be seen in Figure 32. The smaller Baseload allows the transformer to maintain lower loads throughout the day when compared to the original Baseload. Note that although the results may vary depending on the specific day simulated, the trends are similar, and thus the outcomes and conclusions of the study are not limited to a specific day and instead correspond to an “average” summer day in southern California.

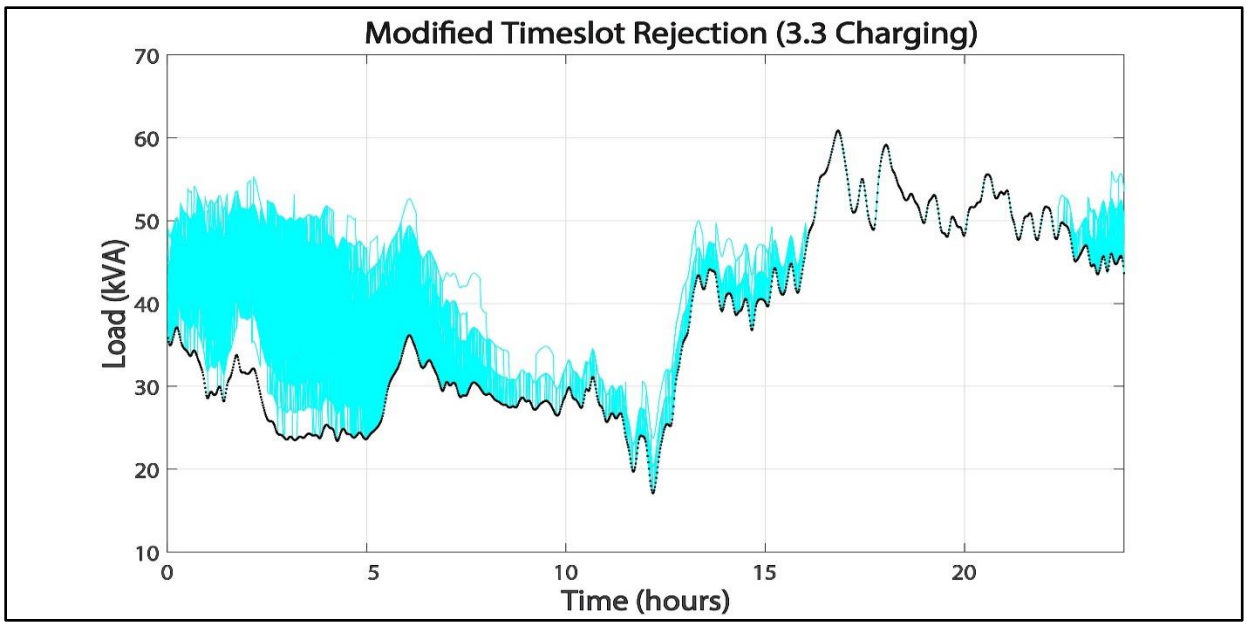

Figure 32 Transformer loads for Grid Valley Filling with Modified Timeslot Rejection charging strategy using a new Baseload with only 3.3 kW charging rates

9.1.7 Effects on the Grid and Distribution Life Cycle

The effects of the different charging scenarios on the grid and distribution cycle are discussed below.

9.1.7.1 Grid Level Demand

The effect of the charging strategies on the grid load can be seen in Figure 33, which is based on a typical demand profile for California. To estimate the effect at the grid level, the number of BEVs used is scaled to represent 10% of vehicles, with the same 9 vehicles per transformer (the same distribution used above). As expected, the left panel shows that Uncontrolled and TOU charging strategies do not result in a desirable grid load. Uncontrolled charging increases the existing peak, while TOU charging creates another one. The valley filling uses the low demand region for vehicle charging, resulting in a flat demand profile from 10 p.m. to 6 a.m. Left panel shows that the Modified Timeslot Rejection strategy does not maintain a

valley filling profile with only 50 kVA transformers. Of course, this is an exaggerated effect since it is based on the assumption that all BEVs are connected to 50kVA transformers, which is highly unlikely and it is used as a "worst case" scenario. When 75 kVA transformers are used, due to their higher capacity, the strategy maintains a valley filling profile while preventing transformers from overloading. The overall load in this case essentially overlaps with the "Grid Valley Filling", since the 75 kVA transformers have less timeslot rejection in the algorithm.

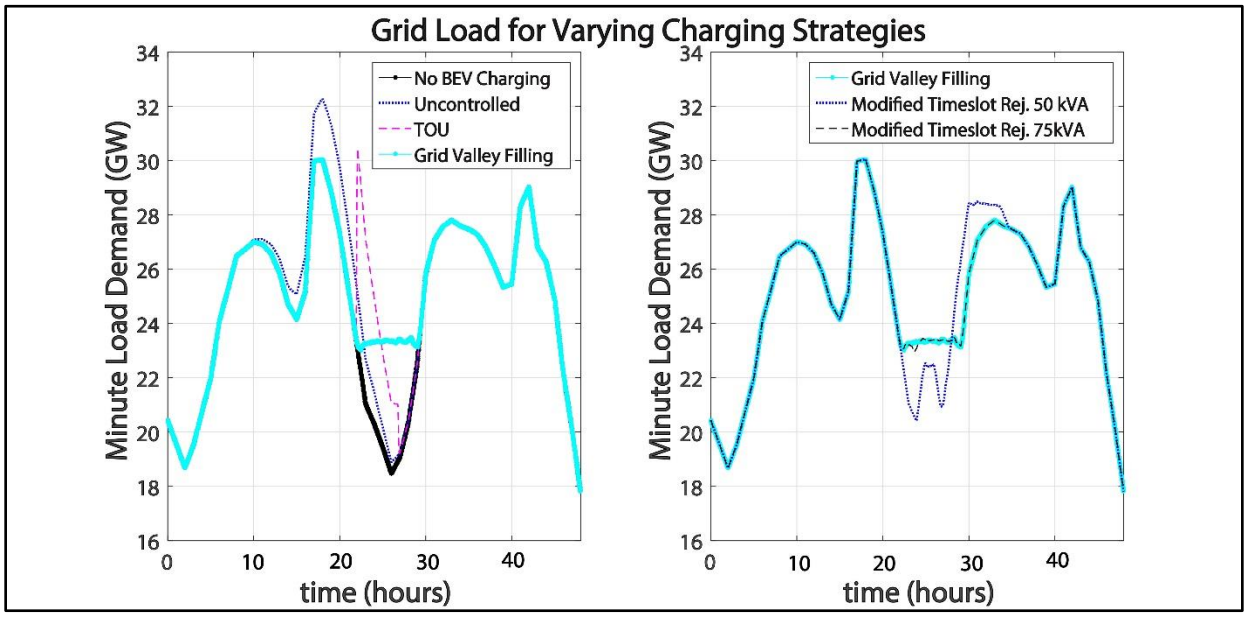

Figure 33 Grid load for various charging strategies (3.3 kW charging)

9.1.7.2 Effects on Distribution Transformers

As previously mentioned, the electricity demand imposed on the distribution transformer by the BEVs might result in transformer accelerated loss of life and even failure. The major factor in transformer loss of life is degradation of the winding insulation due to thermal, electrical and to induced mechanical stresses [58]. The thermal stress is considered as the most important factor affecting the life of an oil-immersed transformer [59], which can be predicted

by estimating the hot spot temperature (HST), the highest temperature observed in the winding [60]. Furthermore, residential transformers are more likely to be affected by peak temperatures during very high short-term loads [61]. A heat transfer model for oil-immersed transformers, previously developed by Razeghi et al. [1], is used to determine the HST of the transformers in each of the scenarios. Ambient temperatures consistent with the daily temperature profile for a summer day in southern California are used in the model.

First the load factor and the HST are compared to the limits recommended by IEEE C.57.91 [60] (Table 16). If any one of these three limits is reached, the transformer is highly likely to fail. The IEEE standard is then used to determine the Equivalent Aging Factor (EAF) and loss of life based on the dynamic HST calculations.

Table 16 Recommended limits of temperature and loading for a distribution transformer

Oil temperature	120°C
Winding hot spot temperature	200°C
Short time loading (30 minutes or less)	300 %

9.1.7.2.1 Load Factor

In cases and scenarios discussed above (including both transformer sizes), none of the transformers experience a load factor of 3 or higher for more than 30 minutes. In some scenarios with 50 kVA transformers, some transformers experience a load factor of 2 or greater for 30 minutes or longer (Table 17). Although these transformers might not fail, the manufacturer should be consulted before overloading the transformers for an extended period of time.

Table 17 Number of 50 kVA transformers (out of 2255) experiencing a load factor of 2 or greater for more than 30 minutes

Charging Profile	Charging Level (kW)	Number of Transformers Exceeding 200% Loading
Uncontrolled	3.3	8
	7.2	67
	Mixed	37
TOU	7.2	1876
	Mixed	940
Grid Valley Filling	Mixed	1

9.1.7.2.2 Hot Spot Temperature

The model developed in [1] is used to determine the HST for the transformers in each scenario. The results for the Baseload – i.e., before any BEV charging is added (for 50 kVA and 75 kVA transformers), shown in Figure 34-A, reveal that the Baseload 50 kVA transformer does not exceed the 200°C limit; however, this transformer is operating at temperatures higher than 140°C. At these temperatures, gassing in the solid insulation and the oil might result in significant transformer loss of life and even failure.

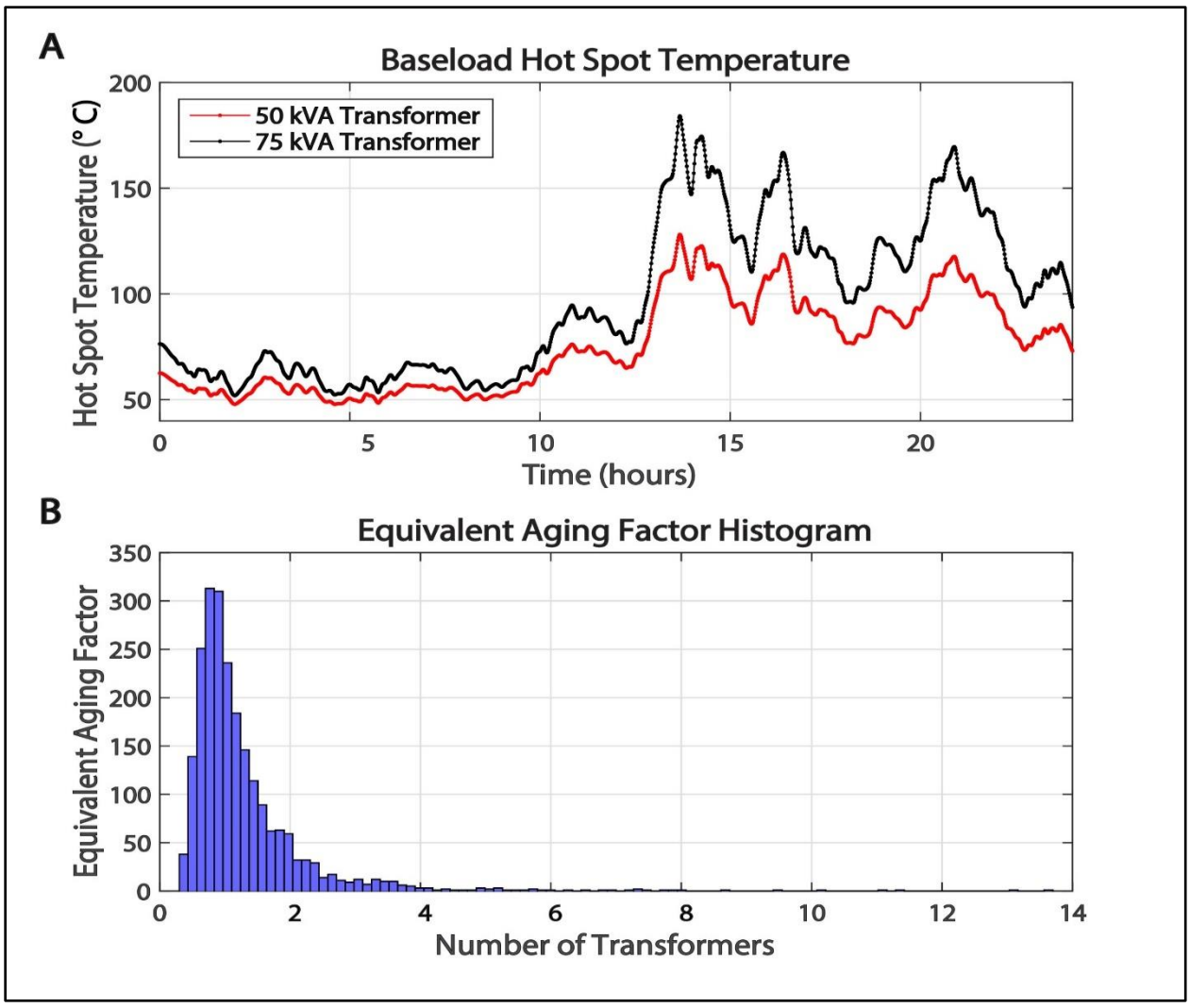

Figure 34 a) Hot spot temperature for the Baseload and b) Equivalent aging factor histogram for uncontrolled charging at 7.2 kW for 75 kVA transformer

The scenarios that might result in transformer failure and the corresponding percent of transformers that exceed the HST limit of 200°C and are thus susceptible to failure are shown in Table 18. The scenarios not shown in the table do not result in transformer failure. In all of the scenarios with 50 kVA transformer, and in the Uncontrolled charging at 7.2 kW and mixed charging with 75 kVA transformer, temperatures higher than 140° C are observed, justifying caution.

All the Uncontrolled and TOU charging profiles result in transformer failure with 50 kVA transformers, with the TOU profile having a higher rate of failure. This was expected since these two charging profiles result in the excessive demand occurring simultaneously in the circuit. With Uncontrolled charging, the start of charging depends on the arrival time. In the TOU strategy, the start of charging is the same for all drivers, resulting in higher failure rate. The Grid Valley Filling charging profile also results in a small failure percentage at 7.2 kW and mixed charging rates with 50 kVA, this is again due to concentrated charging of the vehicles at specific times.

The failure rate decreases as the transformers are replaced with 75 kVA transformers; however, some transformers still fail in the scenarios with TOU charging profile at 7.2 kW and mixed charging, further suggesting that TOU charging profile is not a suitable strategy with regards to the distribution system.

Table 18 Percent of Transformers exceeding the HST limit

Charging Profile	Charging Level (kW)	Percent of Transformers Exceeding HST of 200°C	
		50 kVA	75 kVA
Uncontrolled	3.3	52.37	0
	7.2	84.17	0
	Mixed	67.27	0
TOU	3.3	91.57	0
	7.2	100	62.00
	Mixed	95.92	31.40
Grid Valley Filling	7.2	1.64	0
	Mixed	1.06	0

9.1.7.2.3 Transformer Aging

In the previous section, the HST was determined and the transformers likely to fail under each scenario identified. The HST is then used to calculate the aging acceleration factor (AAF)

and subsequently the equivalent aging factor (EAF) and loss of life percent for a period of 24 hours. The EAF results for the scenario with Uncontrolled charging at 7.2 kW with a 75 kVA transformer, are shown in Figure 34-B. The summary of the results for all scenarios is shown in Table 19. Note that for scenarios resulting in transformer failure, the data in the table corresponds only to transformers that do not fail (the percent of transformers failing in each scenarios is shown in Table 18).

Table 19 Equivalent aging factor for a period of 24 hours (corresponding only to transformers that do not fail)

Charging Profile	Charging Level (kW)	50 kVA			75 kVA		
		Min	Avg	Max	Min	Avg	Max
Baseload	NA	-	17.2747	-	-	0.2796	-
Uncontrolled	3.3	20.7338	52.2008	93.5889	0.3384	0.8035	3.4403
	7.2	18.3938	49.7296	95.0892	0.3090	1.2954	13.7031
	Mixed	20.7338	51.7277	93.3408	0.3381	1.0449	13.0923
TOU	3.3	20.8548	32.4661	63.8518	0.3285	0.5385	0.7633
	7.2	NA	NA	NA	0.8144	11.9926	37.3946
	Mixed	21.3782	31.9941	62.9448	0.3351	3.6066	37.3946
Grid Valley Filling	3.3	17.2837	17.9620	26.7779	0.2805	0.2938	0.3746
	7.2	17.2824	19.1061	39.7619	0.2803	0.3088	0.7551
	Mixed	17.2835	18.5358	36.7366	0.2804	0.3031	2.9188
Grid Valley Filling with Timeslot Rejection	3.3	17.2775	17.2828	17.2887	0.2808	0.2906	0.3032
	7.2	17.2772	17.2805	17.2854	0.2814	0.2904	0.3114
	Mixed	17.2770	17.2817	17.2887	0.2818	0.2905	0.3036
Grid Valley Filling with Modified Timeslot Rejection	3.3	17.2775	17.2877	17.3454	0.2808	0.2906	0.3032
	7.2	17.2773	17.2871	17.3380	0.2814	0.2904	0.3114
	Mixed	17.2770	17.2875	17.3454	0.2818	0.2905	0.3036
Forced Cool-Down Period Method	3.3	17.2270	17.3213	18.5008	0.2808	0.2904	0.3028
	7.2	17.2776	17.2960	17.2969	0.2811	0.2895	0.3032
	Mixed	17.2776	17.3094	18.5008	0.2818	0.2902	0.3041

The overall take away from Table 19 is that a 50 kVA transformer needs to be replaced frequently for the load profiles studied as indicated by high EAFs. This was expected since, for the Baseload, the average loading of the 50 kVA transformer is 102 percent. The distribution transformers have an average load of 15-40% of the rating (the average load factor calculated in

[62] is 26.6% with 70% of the transformers having a load factor of 19-34%, while the average load factor determined in [63] is equal to 30%). As a result, the 50 kVA transformer is under-designed for the Baseload alone. However, it is interesting to note that implementing the majority of the *controlled* charging strategies presented here, reduces the chances of transformer failure with the addition of plug-in electric vehicles' load even for a poorly designed transformer. Among these scenarios Grid Valley Filling with Timeslot Rejection, Grid Valley Filling with Modified Timeslot Rejection, and Forced Cool-Down Period method result in better EAF outcomes in the order mentioned.

For the 75 kVA transformer, Grid Valley Filling with Timeslot Rejection and Modified Timeslot Rejection are almost identical since the load profiles for these scenarios differ only in order of a few kW and only for a handful of transformers. For these transformers, the Forced Cool-Down Period method results in lowest loss of life. These transformers are operating at lower temperatures and as a result the one-hour cool-down time has a greater impact compared to 50 kVA transformers operating at high temperatures (higher than 140°C) where the one hour cool-down might not be sufficient to bring the HST to temperatures below the limit.

9.1.8 Conclusion

Various PEV charging control strategies are analyzed. The Uncontrolled and TOU charging strategies exacerbate overloading when dealing with PEV charging. Roughly 32% and 100% of transformers were subjected to loads above 100 kVA with 7.2 kW charging for the Uncontrolled and TOU charging strategies, respectively. Grid Valley Filling generates a valley filling profile at the grid level, but can further increase transformer overloading. It was found that 73.9% of transformers were subjected to additional overloading above 75 kVA with 7.2 kW

charging. When 50 kVA transformers are used, overloading can still be minimized, but the profile charging will be steered away from the desired valley filling profile.

It was found that the Modified Timeslot Rejection strategy produces a valley filling profile at the grid level while preventing overloading with 75 kVA transformers. All loads caused by BEV charging for the Modified Timeslot Rejection strategy were below 64 kVA with the 7.2 kW charging rate. Simple modifications can be made to the proposed algorithms to take other capacity constraints into consideration. A cooling down period is an example of a modification that has been studied.

Uncontrolled and TOU charging profiles are the two strategies with the most negative impacts on the distribution transformers. In particular, it is likely that substantial distribution circuit upgrade is required to accommodate TOU charging across the grid. Vehicle charging management substantially reduces the chance of transformer failure even for under-designed transformers.

The proposed algorithm could be used prevent transformers from overloading, while achieving a desirable level of valley filling at the grid level simultaneously. In order to implement this algorithm, some limited communication between transformers and BEVs is required. This technology, while feasible, is not readily available in current transformers, and an upgrade of hardware would be required. It should also be noted that the algorithm uses predicted daily Baseloads. Since such predictions are based recent usage data, given the limited scale and the number of users, variability might be high. Thus, more effort is needed on obtaining reasonable predictions for the daily (non-BEV) load.

Acknowledgements

This work was supported by the Graduate Assistance in Areas of National Need (GAANN) Fellowship. We would also like to thank Renee Cinar for providing us with the transformer data used in this paper.

10 Works Cited

[1] G. Razeghi, L. Zhang, T. Brown, S. Samuelsen, Impacts of plug-in hybrid electric vehicles on a residential transformer using stochastic and empirical analysis, J. Power Sources. 252 (2014) 277–285. https://doi.org/10.1016/j.jpowsour.2013.11.089.

[2] O. US EPA, Inventory of U.S. Greenhouse Gas Emissions and Sinks, US EPA. (2017). https://www.epa.gov/ghgemissions/inventory-us-greenhouse-gas-emissions-and-sinks (accessed May 10, 2019).

[3] J.H. Williams, A. DeBenedictis, R. Ghanadan, A. Mahone, J. Moore, W.R. Morrow, S. Price, M.S. Torn, The Technology Path to Deep Greenhouse Gas Emissions Cuts by 2050: The Pivotal Role of Electricity, Science. 335 (2012) 53–59. https://doi.org/10.1126/science.1208365.

[4] O. Egbue, S. Long, Barriers to widespread adoption of electric vehicles: An analysis of consumer attitudes and perceptions, Energy Policy. 48 (2012) 717–729. https://doi.org/10.1016/j.enpol.2012.06.009.

[5] S. Li, L. Tong, J. Xing, Y. Zhou, The Market for Electric Vehicles: Indirect Network Effects and Policy Design, J. Assoc. Environ. Resour. Econ. 4 (2017) 89–133. https://doi.org/10.1086/689702.

[6] N. Caperello, K.S. Kurani, J. TyreeHageman, Do You Mind if I Plug-in My Car? How etiquette shapes PEV drivers' vehicle charging behavior, Transp. Res. Part Policy Pract. 54 (2013) 155–163. https://doi.org/10.1016/j.tra.2013.07.016.

[7] Alternative Fuels Data Center: Maps and Data - U.S. Plug-in Electric Vehicle Sales by Model, (n.d.). https://afdc.energy.gov/data/ (accessed May 10, 2019).

[8] E. Ramos Muñoz, G. Razeghi, L. Zhang, F. Jabbari, Electric vehicle charging algorithms for coordination of the grid and distribution transformer levels, Energy. 113 (2016) 930–942. https://doi.org/10.1016/j.energy.2016.07.122.

[9] L. Zhang, T. Brown, G.S. Samuelsen, Fuel reduction and electricity consumption impact of different charging scenarios for plug-in hybrid electric vehicles, J. Power Sources. 196 (2011) 6559–6566. https://doi.org/10.1016/j.jpowsour.2011.03.003.

[10] B. Tarroja, J.D. Eichman, L. Zhang, T.M. Brown, S. Samuelsen, The effectiveness of plug-in hybrid electric vehicles and renewable power in support of holistic environmental goals: Part 1 – Evaluation of aggregate energy and greenhouse gas performance, J. Power Sources. 257 (2014) 461–470. https://doi.org/10.1016/j.jpowsour.2013.09.147.

[11] P. Denholm, W. Short, An evaluation of utility system impacts and benefits of optimally dispatched plug-in hybrid electric vehicles, Revised., National Renewable Energy Laboratory, Golden, Colo, 2006. http://purl.access.gpo.gov/GPO/LPS88462 (accessed January 7, 2016).

[12] L. Gan, U. Topcu, S.H. Low, Stochastic distributed protocol for electric vehicle charging with discrete charging rate, in: 2012 IEEE Power Energy Soc. Gen. Meet., 2012: pp. 1–8. https://doi.org/10.1109/PESGM.2012.6344847.

[13] Y. Tang, J. Zhong, M. Bollen, Aggregated optimal charging and vehicle-to-grid control for electric vehicles under large electric vehicle population, Transm. Distrib. IET Gener. 10 (2016) 2012–2018. https://doi.org/10.1049/iet-gtd.2015.0133.

[14] Z. Ma, D. Callaway, I. Hiskens, Decentralized charging control for large populations of plug-in electric vehicles, in: 2010 49th IEEE Conf. Decis. Control CDC, 2010: pp. 206–212. https://doi.org/10.1109/CDC.2010.5717547.

[15] Z. Ma, I. Hiskens, D. Callaway, A Decentralized MPC Strategy for Charging Large Populations of Plug-in Electric Vehicles, IFAC Proc. Vol. 44 (2011) 10493–10498. https://doi.org/10.3182/20110828-6-IT-1002.03334.
[16] L. Gan, U. Topcu, S. Low, Optimal decentralized protocol for electric vehicle charging, in: 2011 50th IEEE Conf. Decis. Control Eur. Control Conf. CDC-ECC, 2011: pp. 5798–5804. https://doi.org/10.1109/CDC.2011.6161220.
[17] L. Zhang, T. Brown, S. Samuelsen, Evaluation of charging infrastructure requirements and operating costs for plug-in electric vehicles, J. Power Sources. 240 (2013) 515–524. https://doi.org/10.1016/j.jpowsour.2013.04.048.
[18] B. Tarroja, L. Zhang, V. Wifvat, B. Shaffer, S. Samuelsen, Assessing the stationary energy storage equivalency of vehicle-to-grid charging battery electric vehicles, Energy. 106 (2016) 673–690. https://doi.org/10.1016/j.energy.2016.03.094.
[19] L. Zhang, F. Jabbari, T. Brown, S. Samuelsen, Coordinating plug-in electric vehicle charging with electric grid: Valley filling and target load following, J. Power Sources. 267 (2014) 584–597. https://doi.org/10.1016/j.jpowsour.2014.04.078.
[20] H. Zhang, Z. Hu, Z. Xu, Y. Song, Optimal Planning of PEV Charging Station With Single Output Multiple Cables Charging Spots, IEEE Trans. Smart Grid. 8 (2017) 2119–2128. https://doi.org/10.1109/TSG.2016.2517026.
[21] R.J. Flores, B.P. Shaffer, J. Brouwer, Electricity costs for an electric vehicle fueling station with Level 3 charging, Appl. Energy. 169 (2016) 813–830. https://doi.org/10.1016/j.apenergy.2016.02.071.
[22] S. Saxena, J. MacDonald, S. Moura, Charging ahead on the transition to electric vehicles with standard 120V wall outlets, Appl. Energy. 157 (2015) 720–728. https://doi.org/10.1016/j.apenergy.2015.05.005.
[23] S. Bellekom, R. Benders, S. Pelgröm, H. Moll, Electric cars and wind energy: Two problems, one solution? A study to combine wind energy and electric cars in 2020 in The Netherlands, Energy. 45 (2012) 859–866. https://doi.org/10.1016/j.energy.2012.07.003.
[24] M.Ş. Kuran, A.C. Viana, L. Iannone, D. Kofman, G. Mermoud, J.P. Vasseur, A Smart Parking Lot Management System for Scheduling the Recharging of Electric Vehicles, IEEE Trans. Smart Grid. 6 (2015) 2942–2953. https://doi.org/10.1109/TSG.2015.2403287.
[25] C. Hutson, G.K. Venayagamoorthy, K.A. Corzine, Intelligent Scheduling of Hybrid and Electric Vehicle Storage Capacity in a Parking Lot for Profit Maximization in Grid Power Transactions, in: 2008 IEEE Energy 2030 Conf., 2008: pp. 1–8. https://doi.org/10.1109/ENERGY.2008.4781051.
[26] W. Su, M.-Y. Chow, Computational intelligence-based energy management for a large-scale PHEV/PEV enabled municipal parking deck, Appl. Energy. 96 (2012) 171–182. https://doi.org/10.1016/j.apenergy.2011.11.088.
[27] R.M. Shukla, S. Sengupta, A.N. Patra, Smart plug-in electric vehicle charging to reduce electric load variation at a parking place, in: 2018 IEEE 8th Annu. Comput. Commun. Workshop Conf. CCWC, 2018: pp. 632–638. https://doi.org/10.1109/CCWC.2018.8301710.
[28] S. Faddel, A.T. Al-Awami, M.A. Abido, Fuzzy Optimization for the Operation of Electric Vehicle Parking Lots, Electr. Power Syst. Res. 145 (2017) 166–174. https://doi.org/10.1016/j.epsr.2017.01.008.
[29] J.S. Krupa, D.M. Rizzo, M.J. Eppstein, D. Brad Lanute, D.E. Gaalema, K. Lakkaraju, C.E. Warrender, Analysis of a consumer survey on plug-in hybrid electric vehicles, Transp. Res. Part Policy Pract. 64 (2014) 14–31. https://doi.org/10.1016/j.tra.2014.02.019.

[30] H.A. Bonges III, A.C. Lusk, Addressing electric vehicle (EV) sales and range anxiety through parking layout, policy and regulation, Transp. Res. Part Policy Pract. 83 (2016) 63–73. https://doi.org/10.1016/j.tra.2015.09.011.
[31] 2017 National Household Travel Survey, U.S. Department of Transportation, Federal Highway Administration, n.d. http://nhts.ornl.gov.
[32] Time-Of-Use, SCE.Com. (n.d.). https://www.sce.com/wps/portal/home/business/rates/time-of-use (accessed February 27, 2018).
[33] Time-Of-Use Residential Rate Plans, SCE.Com. (n.d.). http://www.sce.com/residential/rates/Time-Of-Use-Residential-Rate-Plans (accessed April 8, 2019).
[34] F. Lambert, Tesla launches a new 'Workplace Charging' program to supply free charging stations to businesses, Electrek. (2018). https://electrek.co/2018/02/22/tesla-workplace-charging-program/ (accessed February 27, 2018).
[35] J. Kleinberg, É. Tardos, Algorithm Design, 1 edition, Pearson, Boston, 2005.
[36] A. Ohnsman, Amazon's Multibillion-Dollar Bet On Electric Delivery Vans Is Game-Changer For Startup Rivian, Forbes. (n.d.). https://www.forbes.com/sites/alanohnsman/2019/09/19/amazons-multibillion-dollar-bet-on-electric-delivery-vans-is-game-changer-for-startup-rivian/ (accessed October 17, 2019).
[37] UPS And NYSERDA To Convert UPS Diesel Delivery Trucks In NYC To Electric, Press. (n.d.). https://pressroom.ups.com/pressroom/ContentDetailsViewer.page?ConceptType=PressReleases&id=1510239934903-452 (accessed October 17, 2019).
[38] M. Liu, P.K. Phanivong, Y. Shi, D.S. Callaway, Decentralized Charging Control of Electric Vehicles in Residential Distribution Networks, IEEE Trans. Control Syst. Technol. 27 (2019) 266–281. https://doi.org/10.1109/TCST.2017.2771307.
[39] Demand Response, SCE.Com. (n.d.). https://www.sce.com/wps/portal/home/business/savings-incentives/demand-response (accessed February 22, 2018).
[40] S. Shao, M. Pipattanasomporn, S. Rahman, Challenges of PHEV penetration to the residential distribution network, in: IEEE Power Energy Soc. Gen. Meet. 2009 PES 09, 2009: pp. 1–8. https://doi.org/10.1109/PES.2009.5275806.
[41] K. Clement-Nyns, E. Haesen, J. Driesen, The Impact of Charging Plug-In Hybrid Electric Vehicles on a Residential Distribution Grid, IEEE Trans. Power Syst. 25 (2010) 371–380. https://doi.org/10.1109/TPWRS.2009.2036481.
[42] A. Kavousi-Fard, A. Khodaei, Efficient integration of plug-in electric vehicles via reconfigurable microgrids, Energy. 111 (2016) 653–663. https://doi.org/10.1016/j.energy.2016.06.018.
[43] I. Graabak, Q. Wu, L. Warland, Z. Liu, Optimal planning of the Nordic transmission system with 100% electric vehicle penetration of passenger cars by 2050, Energy. 107 (2016) 648–660. https://doi.org/10.1016/j.energy.2016.04.060.
[44] K. Hedegaard, H. Ravn, N. Juul, P. Meibom, Effects of electric vehicles on power systems in Northern Europe, Energy. 48 (2012) 356–368. https://doi.org/10.1016/j.energy.2012.06.012.
[45] S. Sekhar, S. Wavhal, A. Budhane, V. Ramasundaram, A. Ashtikar, Integration of Solar and Wind Energy into Smart Grid- An Overview, 5 (2015) 4.

[46] A. Kusiak, A. Verma, X. Wei, Wind Turbine Capacity Frontier From SCADA, (n.d.) 4.
[47] S. Shokrzadeh, E. Bibeau, Sustainable integration of intermittent renewable energy and electrified light-duty transportation through repurposing batteries of plug-in electric vehicles, Energy. 106 (2016) 701–711. https://doi.org/10.1016/j.energy.2016.03.016.
[48] L. Gan, U. Topcu, S.H. Low, Optimal decentralized protocol for electric vehicle charging, IEEE Trans. Power Syst. 28 (2013) 940–951. https://doi.org/10.1109/TPWRS.2012.2210288.
[49] P. Richardson, D. Flynn, A. Keane, Local Versus Centralized Charging Strategies for Electric Vehicles in Low Voltage Distribution Systems, IEEE Trans. Smart Grid. 3 (2012) 1020–1028. https://doi.org/10.1109/TSG.2012.2185523.
[50] A. Kavousi-Fard, A. Abbasi, M.-A. Rostami, A. Khosravi, Optimal distribution feeder reconfiguration for increasing the penetration of plug-in electric vehicles and minimizing network costs, Energy. 93, Part 2 (2015) 1693–1703. https://doi.org/10.1016/j.energy.2015.10.055.
[51] M. Carrión, R. Zárate-Miñano, Operation of renewable-dominated power systems with a significant penetration of plug-in electric vehicles, Energy. 90, Part 1 (2015) 827–835. https://doi.org/10.1016/j.energy.2015.07.111.
[52] W.-J. Ma, V. Gupta, U. Topcu, On distributed charging control of electric vehicles with power network capacity constraints, in: Am. Control Conf. ACC 2014, 2014: pp. 4306–4311. https://doi.org/10.1109/ACC.2014.6859139.
[53] John Wayne-Orange County, CA | 57° | Light Rain Mist, Weather Undergr. (n.d.). http://www.wunderground.com/us/ca/john-wayne-orange-county (accessed January 5, 2016).
[54] NHTS Data Center, (n.d.). http://nhts.ornl.gov/download.shtml (accessed January 19, 2016).
[55] 2013 Conditions and Performance - Policy | Federal Highway Administration, (n.d.). https://www.fhwa.dot.gov/policy/2013cpr/chap1.cfm (accessed October 18, 2019).
[56] ChargePoint, (n.d.). http://www.chargepoint.com/evs (accessed August 17, 2015).
[57] Time-Of-Use Residential Rate Plans, SCE.Com. (n.d.). https://www.sce.com/wps/portal/home/residential/rates/residential-plan/ (accessed August 17, 2015).
[58] M.K. Pradhan, T.S. Ramu, On the estimation of elapsed life of oil-immersed power transformers, IEEE Trans. Power Deliv. 20 (2005) 1962–1969. https://doi.org/10.1109/TPWRD.2005.848663.
[59] D. Peterchuck, A. Pahwa, Sensitivity of transformer's hottest-spot and equivalent aging to selected parameters, IEEE Trans. Power Deliv. 17 (2002) 996–1001. https://doi.org/10.1109/TPWRD.2002.803708.
[60] IEEE Guide for Loading Mineral-Oil-Immersed Transformers and Step-Voltage Regulators, IEEE Std C5791-2011 Revis. IEEE Std C5791-1995. (2012) 1–123. https://doi.org/10.1109/IEEESTD.2012.6166928.
[61] G.B. Reigh Walling, Distribution Transformer Thermal Behavior and Aging in Local-Delivery Distribution Systems, (2007).
[62] M.W. Gangel, R.F. Propst, Distribution Transformer Load Characteristics, IEEE Trans. Power Appar. Syst. 84 (1965) 671–684. https://doi.org/10.1109/TPAS.1965.4766242.
[63] S.W. Hadley, Impact of Plug-in Hybrid Vehicles on the Electric Grid, 2006. https://doi.org/10.2172/974613.